

Nuevas Técnicas de Cálculo y Física de Precisión en Colisionadores de Alta Energía

Alice Maria Donati



Universidad de Granada

Departamento de Física Teórica y del Cosmos
Universidad de Granada
España

Julio 2015

Editor: Universidad de Granada. Tesis Doctorales

Autora: Alice Maria Donati

SISBN: 978-84-9125-543-7

URI: <http://hdl.handle.net/10481/42675>

New Calculation Techniques and Precision Physics in High Energy Colliders

Alice Maria Donati



Universidad de Granada

Departamento de Física Teórica y del Cosmos
University of Granada
Spain

July 2015

La doctoranda Alice Maria Donati y el director de la tesis Roberto Pittau,
profesor titular de universidad,

GARANTIZAMOS: al firmar esta tesis doctoral, que el trabajo ha sido
realizado por la doctoranda bajo la dirección de los directores de la tesis y
hasta donde nuestro conocimiento alcanza, en la realización del trabajo, se
han respetado los derechos de otros autores y otras autoras a ser citadas,
cuando se han utilizado sus resultados o publicaciones.

Granada, 28 de julio de 2015.

Director de la tesis

Doctoranda

Fdo: Roberto Pittau

Alice Maria Donati

D. Roberto Pittau, profesor titular de Universidad,

CERTIFICA: que la presente tesis doctoral, *NEW CALCULATION TECHNIQUES AND PRECISION PHYSICS IN HIGH ENERGY COLLIDERS*, ha sido realizada por Doña Alice Maria Donati bajo su dirección en el Dpto. de Física Teórica y del Cosmos de la Universidad de Granada, así como que ésta ha realizado una estancia en el extranjero por un periodo superior a tres meses en el *CERN*.

Granada, 28 de julio de 2015

Fdo: Roberto Pittau

Resumen

En esta tesis se ha estudiado, puesto a prueba y desarrollado el esquema de regularización dimensional en cuatro dimensiones FDR [58], un nuevo método para calcular correcciones radiativas en teoría cuántica de campos perturbativa (TCCP).

En el primer capítulo, se dan las motivaciones para esta investigación, mostrando mediante algunos ejemplos fenomenológicos la importancia de hacer cálculos precisos para el programa de física del gran colisionador de hadrones (LHC), especialmente como herramienta para la búsqueda de nueva física. Entre las varias técnicas desarrolladas recientemente para llevar a cabo esta tarea, FDR propone un enfoque novedoso con el objetivo de reemplazar el amplio uso de la regularización dimensional (RD). Antes de describir el método, se introduce el problema de los infinitos en TCCP, mostrando como estos emergen a nivel de integración de bucle o del espacio de las fases: la estrategia tradicional para tratar estos objetos consiste en parametrizar los infinitos con el fin de controlarlos hasta que se cancelen entre sí. Sin embargo, este enfoque requiere un gran esfuerzo analítico para calcular cantidades que no son ni siquiera físicas, dificultando la implementación en un método numérico. FDR elimina este obstáculo a través de la sustracción de los infinitos a nivel de integrando, de forma congruente y algorítmica, proporcionando así un atajo hacia el resultado físico.

En el segundo capítulo, se describe en detalle el conjunto de las nuevas tecnologías utilizadas y desarrolladas en esta tesis, explicando los mecanismos y las ventajas de FDR y proporcionando de tal manera un manual para utilizar el método de forma práctica en cálculos realistas. A diferencia de los enfoques tradicionalmen-

te utilizados para ocuparse de las integrales divergentes, en FDR la sustracción de infinitos ultravioleta (UV) está en la definición misma de una nueva integral de bucle, finita a nivel de integrando. La integral FDR es invariante bajo la traslación del momento de bucle, y respeta las simplificaciones usuales entre numerador y denominador, así que es posible manipular algebraicamente el integrando y reducirlo tensorialmente antes de integrarlo. Los diagramas de Feynman a dos o más bucles, expresados en términos de integrales FDR, son congruentes bajo sub-integración. Las amplitudes calculadas en FDR respetan automáticamente la invariancia gauge y las demás simetrías del lagrangiano. Todas las expresiones son UV-finitas, así que la renormalización estándar, mediante la absorción de los infinitos dentro de los parámetros del Lagrangiano, se evita por completo: solamente una renormalización finita tiene que llevarse a cabo para relacionar los parámetros con cantidades físicas. Este procedimiento, a más de un bucle, resulta simplificado en FDR, porque los infinitos son sustraídos al principio, así que se puede evitar la renormalización orden a orden que es necesaria por ejemplo en RD. El mismo mecanismo que regula los infinitos UV se ocupa también de los infinitos infrarrojos (IR), permitiendo la cancelación que garantiza el teorema de Kinoshita, Lee y Naunberg entre los infinitos de la radiación virtual y real. Gracias a sus cuatro dimensiones y al hecho de que los infinitos IR son expresados en términos de logaritmos (en vez de polos) de una escala pequeña, FDR puede constituir el punto de partida para desarrollar métodos de integración numérica y de sustracción a nivel de integrando para fomentar el cálculo numérico rápido de procesos con muchas patas externas.

Después de haber descrito las características de FDR, el capítulo 3 ilustra el método con unos ejemplos prácticos:

- el cálculo de la amplitud de $H \rightarrow \gamma\gamma$ a un bucle en un gauge arbitrario ha supuesto una comprobación de la invariancia gauge en FDR, y la primera ocasión para trabajar con líneas fermiónicas internas;
- las correcciones gluónicas a la amplitud de $H \rightarrow \gamma\gamma$ en la aproximación de gran masa del quark top ha impulsado la tecnología para calcular integrales de vacío a dos bucles y

ha mostrado las ventajas de FDR con respecto a RD: de hecho, todos los términos espurios del tipo ϵ/ϵ se evitan en FDR, lo cual simplifica el cálculo a varios niveles. Se han utilizado las propiedades del contenido de vacío extraído en la definición de integral FDR para construir un test para validar el cálculo;

- la identidad de Ward en QED para el proceso $H \rightarrow \gamma\gamma$ es verificada a uno y dos bucles a nivel de integrando para ilustrar el mecanismo que permite que FDR respete la invariancia de gauge;
- la sección eficaz para $H \rightarrow gg$ en la teoría efectiva con quark top infinitamente pesado al primer orden perturbativo representa un ejemplo de cálculo en presencia de estado final sin masas, una ocasión para estudiar la combinación de radiación virtual y real con métodos numéricos basados en FDR.

En el último capítulo, se resumen las características de FDR y se proponen algunas nuevas líneas de investigación. La descripción detallada y los ejemplos de trabajo en FDR proporcionados en esta tesis generan confianza en el método, y confiamos en que inspiren su uso en estudios futuros como alternativa a RD. En concreto, preveemos un gran potencial de FDR para la realización de cuentas puramente numéricas al segundo orden perturbativo.

Abstract

In this thesis we have studied, tested, and developed the four dimensional regularization/renormalization (FDR) scheme, a novel approach to the calculation of radiative corrections in perturbative quantum field theory (pQFT), a task that is primarily hindered by the presence of unphysical infinities emerging from loop and phase space integration. Unlike the methods traditionally used to cope with this problem, in FDR the subtraction of the ultraviolet (UV) divergences is built in the definition of a new loop integral, made finite at the integrand level, and without ever modifying the Lagrangian. The method is fully four-dimensional, and it automatically preserves gauge invariance, as we have verified by calculating the one-loop amplitude for $H \rightarrow \gamma\gamma$ in arbitrary gauge. By studying the gluonic corrections to the top-loop induced $H \rightarrow \gamma\gamma$ process, we have also shown that FDR is particularly convenient when applied to two-loop calculations, as it avoids a great deal of the work that in dimensional regularization (DR) is induced by ϵ/ϵ terms. Infrared (IR) singularities in virtual and final state real radiation can also be cured in the same framework; the matching and cancellation of this type of divergence in inclusive observables was also studied, by reviewing the analytic calculation of the next-to-leading-order (NLO) decay rate for $H \rightarrow gg$, and by applying to this same process some FDR-based numerical Monte Carlo (MC) methods.

Contents

1	Introduction	1
1.1	Why precision physics	1
1.2	Infinities in perturbative quantum field theories	8
2	FDR	13
2.1	The FDR Integral	16
2.1.1	Definition of the FDR integral	16
2.1.2	FDR defining expansion	19
2.1.2.1	Two-loop case	20
2.1.3	Shift invariance and uniqueness	23
2.1.4	Independence of the UV cutoff	27
2.1.5	Global prescription	29
2.1.5.1	Extra-integrals	32
2.1.5.2	Extra-integrals at two loops	34
2.1.5.3	Internal fermions	37
2.1.6	Sub-integration consistency	40
2.1.6.1	Extra-extra integrals	43
2.1.6.2	FDR vs FDH	44
2.1.7	Master integrals in FDR	44
2.1.7.1	One-loop integrals	44
2.1.7.2	Two-loop integrals	45
2.1.8	Tensorial reduction	47
2.1.8.1	Tensorial reduction of vacuum integrals	48
2.1.8.2	Passarino-Veltman reduction in FDR	49
2.1.8.3	Integration by parts identities	51
2.1.9	Infrared infinities	54
2.1.9.1	Scaleless integrals	56
2.2	Calculating Loop Amplitudes in FDR	58

2.2.1	Gauge invariance	58
2.2.2	Renormalization	59
2.2.2.1	Avoiding order-by-order renormalization.	61
2.2.3	The FDR scheme	63
2.3	Calculating IR-Safe Observables in FDR	65
2.3.1	Real radiation	65
2.3.2	Naive numerical matching	68
2.3.3	FDR local subtraction	70
2.3.4	A possible scheme beyond NLO	73
3	FDR at work	77
3.1	$H \rightarrow \gamma\gamma$ at one loop in R_ξ -gauge	79
3.1.1	The W loop contribution	83
3.1.2	The fermionic loop contribution	85
3.1.3	Conclusions	86
3.2	$H \rightarrow \gamma\gamma$ at two loops	87
3.2.1	The calculation	87
3.2.2	The building blocks	89
3.2.3	The result	91
3.2.4	Renormalization	92
3.2.5	The Vacuum Content	94
3.2.5.1	Calculating the vacuum content of an integral	97
3.2.5.2	Tensorial reduction of the vacuum content	97
3.2.6	Conclusions	98
3.3	Ward identities for $H \rightarrow \gamma\gamma$ at one and two loops	99
3.3.1	The QED Ward identity	99
3.3.2	The Feynman identity	100
3.3.3	The Ward Identity at one loop	103
3.3.4	The Ward Identity at two loops	105
3.4	$H \rightarrow gg$ at NLO	111
3.4.1	Preliminaries	111
3.4.1.1	Renormalization	112
3.4.1.2	Analytic calculation of the virtual correction	113
3.4.1.3	The three-body massive phase space	114
3.4.2	Analytic calculation of the real correction	115
3.4.2.1	Comparing with DR	116
3.4.3	Naive numerical combination	117
3.4.3.1	Naive purely numerical combination	120

3.4.4	FDR local subtraction	121
3.4.5	Conclusions and outlooks	123
4	Conclusions	125
A	The basic two-loop vacuum integral	129
A.1	The indirect approach	131
A.2	The direct approach	132
B	Two-loop vacuum integrals	134
C	Feynman rules	137
C.1	$H \rightarrow \gamma\gamma$ at one loop in R_ξ -gauge	137
C.2	$H \rightarrow \gamma\gamma$ at two loops	138
C.3	$H \rightarrow gg(g)$ and $H \rightarrow ggg(g)$ at NLO	140
D	Monte Carlo Integration	143
D.1	Single Peak Mapping	144
D.2	Multi-channel approach	145
D.2.1	Optimization of the <i>a-priori</i> weights	145
	Bibliography	156

Chapter 1

Introduction

1.1 Why precision physics

This thesis is about a method for calculating radiative corrections in pQFT. The topic belongs to the broader field of developing the technology necessary to make precision calculations for the LHC. In order to explain why this is relevant, we will first show with some examples that precise predictions are necessary, and then that the technology presently at hand may experience difficulty in reaching the demanded accuracy. Let's take a glance at the context in which this thesis was born and brought about: the Higgs boson was discovered a few years ago [1, 2], no clear signal of new physics has been obtained, and the chances of discovering light new physics have significantly decreased. At the dawn of the high luminosity run of the LHC, our best hopes of finding physics beyond the Standard Model (BSM) may lie in measuring tiny deviations from the Standard Model (SM) background.

Indeed, the huge amount of data collected at the LHC, together with recent progress in the theoretical description of the phenomenology of proton colliders, make a precision programme at the LHC feasible and even desirable. Without waiting for the next generation of lepton colliders, a compromise might be prolific between the natural purpose of the LHC -*searching*- and that of *measuring* with precision.

An example of this “discovery precision physics” is the measurement of the Higgs boson's couplings. New physics associated with the Higgs boson could emerge as a small deviation from the SM: it has been pointed out that some BSM scenarios would affect the Higgs couplings at the few-percent level [3],

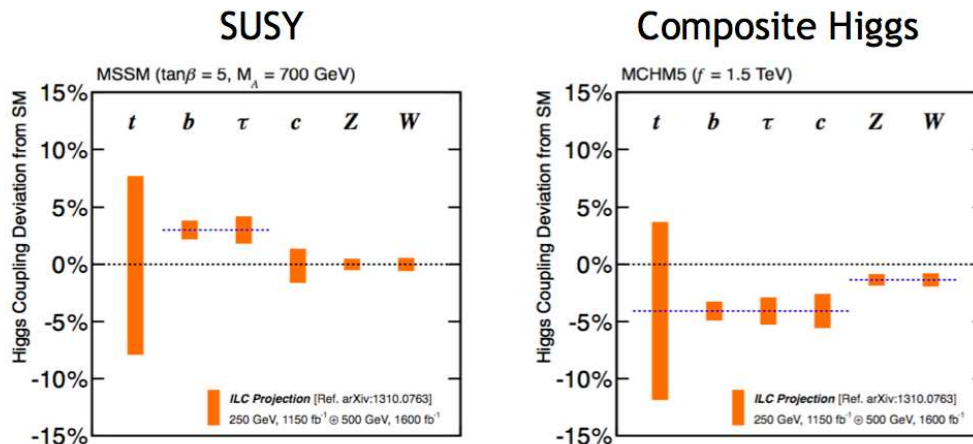


Figure 1.1: ILC projections for some Higgs boson’s couplings normalized to the SM ones, in different models.

making the accurate calculation of these parameters a primary goal. The appearance of different patterns in the values of the Higgs coupling might discriminate among different EWSB models [4], as depicted in fig. 1.1.

Undoubtedly, progress in the experimental and analysis technique is also in order for an effective precision programme at the LHC, in the realm of reducing the systematics; nonetheless, for the moment, for many observables the accuracy of the measurement is comparable or exceeds that of the prediction. It is hence a priority to consistently reduce the theoretical uncertainty to levels that are comparable with the experimental errors.

Some recent examples of the effectiveness of precision calculation as a discovery tool are provided by the next-to-next-to leading order (NNLO) QCD corrections to the inclusive and differential top pair production [5, 6]. Because stops have the same mass as top quarks and they decay to tops with negligible missing energy, their experimental trace cannot be distinguished from that of top quarks; yet their existence would increase the measured top total cross section. The recent calculation on the top pair production, with NNLO QCD corrections, reduced the uncertainty on the predicted cross section to a 4%, allowing us to exclude the existence of light stops in a light neutralino model: no significant excess was found with respect to the SM cross section [5].

In addition, the fully differential cross section of the top pair production,

with NNLO QCD corrections, allowed to relax the top forward-backward asymmetry puzzle: indeed, enhanced with NNLO corrections, the top pair forward-backward asymmetry results shifted by around 27% with respect to the NLO prediction, thereby coming to perfect agreement with the latest measurements at Tevatron [6].

Because the playground is a proton collider, perturbative QCD (pQCD) is the framework within which observables are computed. There are different sources of theoretical uncertainty, alongside the different ingredients of a calculation:

- parton distribution functions (pdf),
- input parameters, such as the coupling constants and the quark masses,
- the partonic cross sections.

Here, we direct our focus on the last item of this list, the computation of partonic cross sections. In pQFT, these objects are obtained as perturbative series in the coupling constants, the error coming essentially from the truncation of such series. In particular, pushing the calculation to further degrees of accuracy involves calculating radiative corrections with more loops and more external particles. Ultimately the problem can be tracked down to dealing with difficult integrals, may they be in the virtual momenta of particles emitted and absorbed in the virtual spectrum, or in the phase space, i.e. over the kinematics of the final state particles. Advancing in the calculation of partonic cross sections hence requires

- progress in the computation of loop integrals and amplitudes;
- being able to integrate higher multiplicity processes, allowing the Kinoshita-Lee-Nauenberg (KLN) cancellation of the IR infinities in a process-independent way.

Thanks to the great advances of the last couple of decades, we stand at a point where NLO calculations for processes with an arbitrary number of particles in the final state are automated or nearly automated [7–20]. The question is now whether this degree of precision is sufficient for the needs of the LHC. We'll now give some motivations and some examples that explain why this is not the case.

The slow convergence of the QCD perturbative series in α_S is perhaps the number one reason for the need of higher order corrections. The majority of

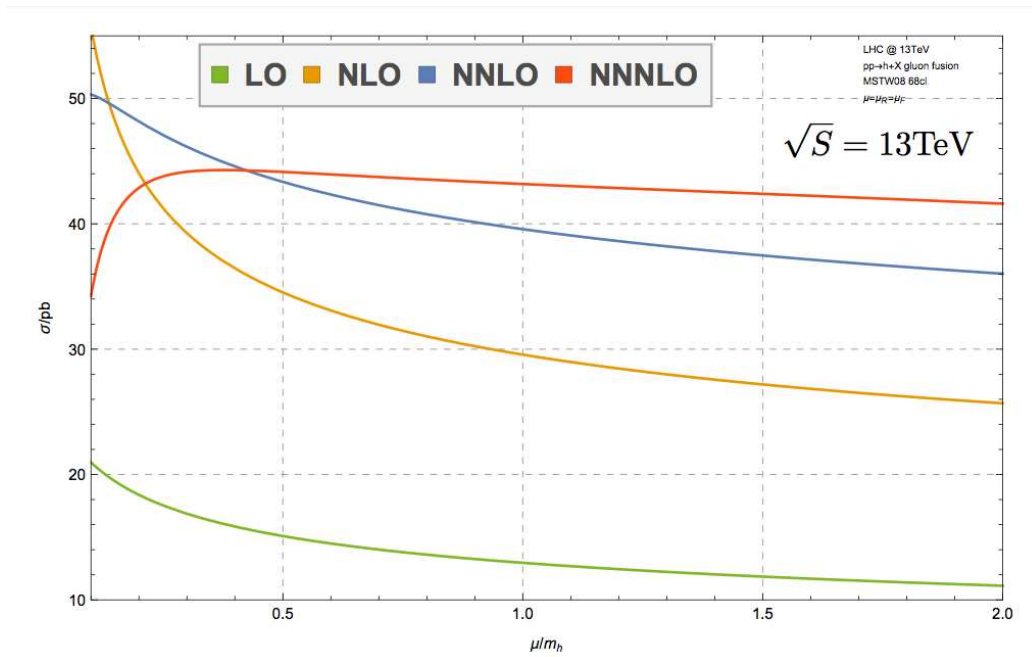


Figure 1.2: Scale variation of the Higgs boson production total cross section, at LO, NLO, NNLO and N³LO [21].

processes at LHC are calculated with NLO accuracy: the uncertainty due to the missing higher orders can be estimated by varying the factorization and renormalization scales, and it is typically of the order of 10% of the predicted cross sections, when going to NNLO; this usually exceeds the experimental error, as well as the theoretical error due to pdfs [22]. Consider the following examples:

- the Higgs boson production total cross section, recently computed up to N³LO [21], exhibits an ingent variation with respect to the scale, as shown in fig. 1.2, which stabilizes only beyond the NNLO level; knowing with precision this observable provides an important consistency check for the SM;
- the cross section of $pp \rightarrow WZ$ presents a tension between data and predictions, as shown in fig. 1.3, where all measured cross sections are bigger that the expected ones [23]; the QCD NNLO corrections could make light on the problem, as suggested by the fact that recent

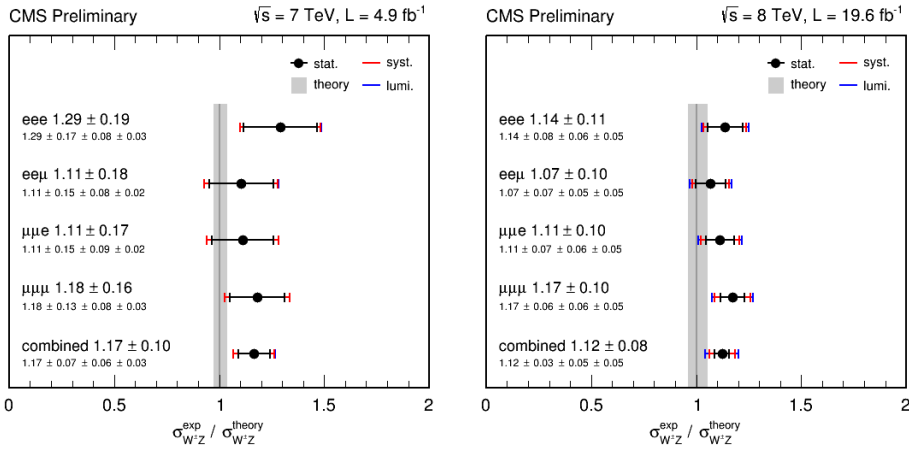


Figure 1.3: Ratio of the measured cross sections to the theoretical prediction for WZ production at $\sqrt{s} = 7$ TeV [23].

calculations for $pp \rightarrow WW$ and $pp \rightarrow ZZ$ [24, 25] have shown an increment of the 10% order as going from the NLO to the NNLO QCD cross sections: a shift of this magnitude would be enough to understand the mismatch observed;

Another important topic is that of parton showers, an essential ingredient in event generators to describe hadronization. The problem resides in the use of parton showers as a shortcut to pQCD calculations that are too hard: with such approach, this technology is used out of its scope and domain of validity of low- Q^2 , inducing systematic errors on the extraction of data itself. To overcome the issue, it is crucial to take steps in the matter of matching/merging parton showers with fixed order results, and to upgrade the event generators in such a way that they will be more and more grounded on exact matrix elements. An example of this is a classic problem of precision physics, i.e. the determination of the W boson mass M_W : in this case, the lack of the mixed QCD and EW corrections to the Drell Yan cross section generates an ambiguity in the determination of M_W at the level of 2-5% [26], unacceptable if we aim at the 1% reached by experimental measurements. Finally, analogously to the way in which the theoretical cross sections affect the measurements, they also have an impact on pdf determination: accurate computation of hard scattering corrections for DIS and hadronic vector

Process	Experimental systematic	Theory error (not pdf)
Drell-Yan	~1%	~2% (NNLO)
Higgs	~10%	~2% (NNNLO)
Higgs+jet	~10%	~7% (NNLO)
W+jet	~10%	~2% (NNLO)
top pair	~4%	~4% (NNLO)
top pair + jet	~14%	~10% (NLO)
VV, ZZ	~8%	~3% (NNLO)
V+2 jets	~10%	5%(NLO)
single top	~10%	~1% (NNLO _{factorizable})

Table 1.1: Current experimental and theoretical uncertainty for some important processes. In these cases, the two errors are comparable, so that removing experimental and theoretical sources of systematics is more important than further improving the perturbative series. This table was taken from indico.cern.ch/event/360104/session/7/contribution/26/material/slides/.

gauge-boson production, at the inclusive and differential level, are an essential ingredient for improving our knowledge on the pdfs [27].

The LHC is calling for a new revolution in calculation techniques, able to break the NNLO frontier. Several new methods have recently established themselves toward the simplification of the multi-loop problem: spinor helicity methods, generalized unitarity, OPP, Openloops, extended use of integration-by-parts (IBP) identities and differential equations, better understanding of the mathematical nature of the amplitude (symbols, generalized polylogarithms, ...) [28–33]. In the context of multi-particle final state, NNLO subtraction schemes have lately made their appearance, such as the antenna method and sector decomposition [20, 34–38].

Several results have been obtained for amplitudes at one, two and even three loops; and the new NNLO subtraction methods have been shown to work in practice on several processes (see table 1.1). Nonetheless, we are still far from mastering a general method, that can be applied to the wide variety of processes typical of the physics at the LHC.

Overall, the arisal of extremely large analytic expressions and the issue of numerical stability are among the main difficulties that are being faced; they are expected to become more critical as we consider more involved processes.

Acknowledged the importance of pursuing technological progress for precision physics at the LHC, and that the interest on the topic is well alive, it is now the time to introduce FDR, not as a competitor of the latest techniques, but as a fresh look at pQFT. Perturbative QFT calculations are plagued by integrals that diverge in the intermediate steps: the traditional way of dealing with such objects consist in parametrizing the infinities, so as to put them under control until the moment they cancel, when the expression we are calculating is physical enough. However, this approach forces a huge analytic effort, because the presence of poles makes it mandatory to have clean analytic expressions of objects that in the end have nothing to do with the physics, hindering a potential numerical path to the point of making it impossible. The aim of FDR is that of sidestepping this obstacle, by subtracting the infinities at the integrand level. Suppose this can be achieved in a consistent and algorithmic way: a whole new space for exploiting numeric integration would open up, supplying a shortcut to the physical answer.

The aim of this thesis is that of providing evidence on the standing hypothesis of the last sentece: we will describe FDR and explain its mechanisms through practical examples, showing that it leads to calculations that are neat and easy to implement.

1.2 Infinities in perturbative QFT

FDR is regularization and a renormalization scheme. Before going into the details of the method, we would like to briefly review where do the infinities arise in pQFT, and how have they usually been dealt with.

The calculation of radiative corrections involves loop integrals, over the momenta of virtual particles, and phase space integrals, over the kinematics of the final state. In the intermediate steps of a calculation, some of these integrals might be divergent, because the connection is temporarily lost between the physics and the mathematical expressions at hand. The need emerges of inventing clever ways of parametrizing the infinities while patiently working through the calculation, trusting that the final result will be finite. After regulating the divergences, the UV ones are then renormalized away, that is they are reabsorbed into the definition of the parameters of the theory. Soft and collinear infinities generated in the phase space integral of final states containing massless particles cancel out when combined with the corresponding virtual contribution; soft infinities arising in the initial state radiation behave similarly, whilst the collinear ones are reabsorbed in the parton densities.

Consider, for example, the following simple one-loop integral,

$$\int d^4q \frac{1}{(q^2 - M^2 + i\varepsilon)^2} \propto \int \frac{d^4q}{q^4}, \quad (1.1)$$

which diverges logarithmically as the integration momentum becomes arbitrarily large. In order to regularize it, let us introduce a parameter on which the integral depends analytically, such that it diverges in the physical limit, but it is well-defined elsewhere.

An obvious option is to put a *cut-off* on the integration range. After performing a Wick rotation and moving to euclidian space, the integral can be expressed as

$$\lim_{\Lambda \rightarrow \infty} i\pi^2 \int_0^\Lambda k^3 dk \frac{1}{(k^2 + M^2)^2}, \quad (1.2)$$

where $k = \sqrt{E_q^2 + |\mathbf{q}|^2}$, with $q = (E_q, \mathbf{q})$. The integral can now be evaluated, and the dependence on the infinite scale Λ will drop in physical amplitudes. The problem with this method is that it breaks Lorentz and shift invariance.

A more sophisticated approach is the regularization proposed by Pauli and Villars [39]. It is based on the idea of arbitrarily introducing another

particle with mass $M' \neq M$, in such a way that divergent integrals always appear in the combination

$$\lim_{M' \rightarrow \infty} \int d^4q \left(\frac{1}{(q^2 - M^2 + i\varepsilon)^2} - \frac{1}{(q^2 - M'^2 + i\varepsilon)^2} \right). \quad (1.3)$$

The two integrands have the same UV behavior, so that the infinities cancel. Integrals like that of eq. (1.3) are shift- and Lorentz-invariant. However, the naive introduction of a fictitious particle is not able to respect gauge invariance in the case of non-abelian theories. Enforcing gauge invariance *a posteriori* is always possible, by imposing the Ward-Slavnov-Taylor identities of the theory considered, but it can be cumbersome and error-prone.

Indeed, avoiding this downside is one of the assets of DR [40], where the loop integral is regarded as a function of the space-time dimension $n = 4 + \epsilon$, divergent only in the limit $n \rightarrow 4$. In practice, the integral becomes

$$\lim_{n \rightarrow 4} \int \frac{d^n q}{\mu^\epsilon} \frac{1}{(q^2 - M^2 + i\varepsilon)^2}, \quad (1.4)$$

where an arbitrary scale μ has been introduced in order to keep the same mass-dimension as that of the original integral. The singularity is parametrized as a pole $1/\epsilon$: in a finite amplitude the global coefficient of such pole vanishes; as for the arbitrary scale μ , it either drops or is traded for a physical scale, via renormalization. DR, even though physically less transparent, is more “natural” with respect to the regularization methods previously introduced: changing the space-time dimension doesn’t break any property of the original integral, which maintains shift and gauge invariance automatically.

One last approach that is worth mentioning in this introduction is the BPHZ scheme of renormalization [41–43]. Take for example

$$I(p) = \int d^4q J(q, p), \quad \text{with} \quad J(q, p) = \frac{1}{(q^2 - M^2)[(q + p)^2 - M^2]} \quad (1.5)$$

where we have dropped the $i\varepsilon$ prescription for simplicity. By Taylor-expanding the integrand with respect to the external momentum around $p = 0$,

$$J(q, p) = J(q, 0) + p^\mu \frac{\partial J}{\partial p^\mu}(q, 0) + \dots \quad (1.6)$$

it is possible to extract a subtraction term able to make the original integral finite. Indeed, each term of the series is more convergent than the one before.

In our case, by subtracting $J(p, 0)$ we already obtain a finite integral, that is

$$I(p)|_{BPHZ} = \int d^4q \left(\frac{1}{(q^2 - M^2)[(q+p)^2 - M^2]} - \frac{1}{(q^2 - M^2)^2} \right), \quad (1.7)$$

without introducing any extra parameter. The idea of the BPHZ scheme is that this subtraction term can be systematically encoded into the Lagrangian as a counterterm; with this procedure it is also possible to treat integrals with no external momenta, like that in eq. (1.1). This approach historically led to the mathematical proof of renormalization, and it is sometimes useful when addressing formal issues on QFT. However, it becomes inefficient in practical calculations, especially in the case of gauge theories, because it can break gauge invariance, and in presence of massless particles.

As a matter of fact, things get more intricate for massless theories. Let's consider once again the integral of eq. (1.1): if $M = 0$, then it diverges logarithmically also when q is arbitrarily small. If an external momentum, such that $p^2 = 0$, appears in the integral,

$$\int d^4q \frac{1}{q^2 [q^2 + 2(q \cdot p)]}, \quad (1.8)$$

then it diverges in the region where q is soft and collinear to p . Roughly speaking, if θ is the angle between \mathbf{q} and \mathbf{p} , the product

$$2(q \cdot p) = 2 |\mathbf{q}| |\mathbf{p}| (1 - \cos \theta) \quad (1.9)$$

is quadratically zero when $|\mathbf{q}| \rightarrow 0$ and $\theta \rightarrow 0$. Some ways of curing this type of singularity consist in keeping the external momenta off-shell, or to assign a fictitious mass to the integration momenta, or to add an IR cut-off.

In DR this problem is automatically fixed, without the need of introducing extra scales, which stands as another well-appreciated property of DR. A UV-finite amplitude can exhibit poles $1/\epsilon$ of IR origin. These have to be matched with the appropriate treatment of the real radiation in order to cancel, at the level of the cross section.

Indeed, it is impossible to distinguish a massless particle that has been emitted and absorbed in the virtual spectrum, from one that has reached the final state but it is not detectable, either because too soft or because it is collinear to another particle. This translates into a classic quantum mechanics problem solved thanks to the KLN [44] and the Bloch-Nordsieck [45]

theorems: two indistinguishable states make up a single well-defined observable. This means that a cross section with complete radiative corrections up to a given order is IR-finite. For example, consider a process with m observed particles in its final state. Its inclusive cross section at NLO is made up of the Born cross section, the virtual correction at one loop, and the tree-level cross section of the same process plus a massless particle emitted softly or collinearly. Schematically,

$$\sigma(pp \rightarrow m \text{ particles} + X) = \sigma_m^{(0)} + \alpha_S \sigma_m^{(1\ell)} + \alpha_S \sigma_{m+1}^{(0)} + \mathcal{O}(\alpha_S^2), \quad (1.10)$$

and it is the combination

$$\sigma_m^{(1\ell)} + \sigma_{m+1}^{(0)} \quad (1.11)$$

to be finite.

This type of approach works for soft particles in the initial and final state, and for collinear particles in the final state only. If the collinear particle is emitted in the initial state, virtual and real processes can be distinguished, because they differ in their centre of mass energy. This case falls out of the hypothesis of the KLN theorem, but thanks to the universality of collinear emission, it can be solved with a procedure similar to renormalization, by absorbing the infinities into the pdfs.

DR has become the standard for QFT calculations, due to its nice properties: indeed,

- it is Lorentz and shift-invariant,
- it preserves gauge invariance and unitarity,
- it is applicable to both the UV and IR regimes.

The main drawback of any DR-based method is that it is not four-dimensional. Although a tautology, this statement has indeed serious consequences: it forces a huge analytic effort in order to keep the poles in ϵ under control, especially beyond the one-loop level where finite terms coming from the ratio ϵ/ϵ pop out in several occasions. This makes it impossible to pursue a numerical strategy, at least for a good part of the calculation.

This is why the literature is rich in attempts to four-dimensional regularization schemes, such as differential renormalization [46], constrained differential renormalization [47, 48], which both work in coordinate space, implicit

renormalization [49,50], symmetry preserving regularization [51] and LR [52], directly applicable in momentum space.

One of the novelties of FDR with respect to these techniques is that it not only abandons DR to be four-dimensional, but it also steps back from the traditional renormalization approach: UV infinities, which are unphysical, are subtracted from the integrals, at the integrand level, and they are not absorbed into the parameters of the theory; the subtraction is encoded in the definition of loop integral, and the Lagrangian is left untouched. Moreover, the same mechanism which cures the UV infinities handles also the IR ones, allowing for the KLN theorem to be satisfied. Although it is a completely different approach with respect to DR, it shares with this method the properties that makes it practical. In the next chapter we describe the method in detail, demonstrating how these claims are realized in practice; and in the ensuing chapter we show FDR at work on some realistic calculations.

Chapter 2

FDR

In this chapter we present the FDR method as a novel way to tackle calculations in QFT. The bulk of new technology that was used and partly invented during this thesis work is described in detail, explaining the mechanisms and the assets of the technique.

In the last chapter we have seen the difficulties that one has to face when attacking a precision calculation. From the different strategies that have been adopted so far, we have learnt what are the ingredients that the ideal method should possess. As far as virtual radiation is concerned, one would like to define a loop integral which is

- finite in the UV region, and identical to normal integration for convergent integrands;
- shift-invariant;
- gauge-invariant (and respectful of all other symmetries of the theory taken in exam);
- independent of the cut-off, but dependent on an arbitrary scale (the renormalization scale μ_R).

The cut-off method fails on shift invariance, while Pauli-Villars and BPHZ are not gauge-invariant in the SM. DR is able to overcome all these problems, establishing itself as the standard technique for multi-loop calculations. However, working in an arbitrary number of dimensions forces a huge analytic effort, and prevents the full use of numerical tools to go around difficult integrals and other cumbersome steps of a calculation. In addition, none of

these methods is independent of the UV cut-off, thus requiring renormalization. Moreover, depending solely on an arbitrary scale is an important feature especially if one wants to use EFTs in the direct quest of new physics.

FDR comes as a solution to this hurdle: by defining a loop integral with all the properties listed above, but in four dimensions and completely finite – i.e. avoiding the parametrization of the infinities –, it provides a method with all the appealing features of DR, yet suitable for numerical hybridation.

Moreover, a good method requires also that

- at least all external particles are described by four-dimensional objects, so that also predictions for supersymmetric (SUSY) models can be computed;
- at two loops and beyond, the integration is consistent with *sub*-integration (i.e. it should be equivalent to calculate the full diagram or to compute the integral of a sub-diagram and insert it back in the full one).

Maintaining the central idea of DR, some of its variants like dimensional reduction (DRed) and four dimensional helicities (FDH) allow for SUSY calculations, because they are defined in such a way that only the loop integral is in n dimensions, while all external tensors are four-dimensional. However, they break the last property, so that extra attention must be paid when one wants to calculate for example QCD processes that involve external fermions.

FDR, obviously in harmony with the first of these requirements, is also constructed with sub-integration consistency.

Finally, a convenient method should be compatible also when massless theories are considered and IR divergences arise, calling for the matching of virtual and real radiation in order to have well-defined observables. FDR is naturally extended so as to cure also this type of divergent behaviour, and thanks to its four-dimensionality and finiteness it can be taken as the starting point to design more clever subtraction methods, allowing for the fast numerical calculation of multi-leg processes.

All this is described in the present chapter, organized as to follow the steps of a realistic calculation, starting from the diagrams, mounting them into the amplitude, and finally integrating the matrix elements in the phase space to obtain the prediction for a physical observable. In the first section we define the FDR integral, and we learn how to compute it. In the second section, we concentrate on gauge invariance and renormalization as fundamental properties of a physical amplitude. Finally, in the last section, we

explain how FDR treats the IR-divergent real radiation, and we propose the sketch of the FDR local subtraction method.

The chapter stands as a manual for practical calculations in FDR, and it prepares the path for the next chapter in which the method is put into practice.

2.1 The FDR Integral

In this section we present the basic building block of FDR, i.e. the *FDR integral*. Indeed, it is via a redefinition of loop integrals that FDR proposes a novel approach to calculations in QFT, four-dimensional and entirely finite. While the definition of the FDR integral is based on a simple idea, its consequences –also at the technical level– are profound, and are worthy of extended discussion. From Section 2.1.1 to Section 2.1.6 the FDR recipe to regulate loop integrals is described in detail, with examples and technical remarks at the one- and two-loop level. In Section 2.1.7, the analytic results of some simple FDR integrals are reported. In Section 2.1.8, it is shown how the usual techniques for tensorial reduction apply to FDR. Finally, in Section 2.1.9 the FDR integral is proven to be well-defined also in the case of massless theories in the presence of IR singularities.

2.1.1 Definition of the FDR integral

As a simple example, let us consider a scalar one-loop integral containing two propagators. Its integrand,

$$\frac{1}{\overline{D}_0 \overline{D}_1} \equiv \frac{1}{(q^2 - M_0^2 + i0) [(q + p_1)^2 - M_1^2 + i0]}, \quad (2.1)$$

can be rewritten as follows:

$$\frac{1}{\overline{D}_0 \overline{D}_1} = \left[\frac{1}{\overline{q}^4} \right] + \frac{d_1}{\overline{q}^4 \overline{D}_1} + \frac{d_0}{\overline{q}^2 \overline{D}_0 \overline{D}_1}, \quad (2.2)$$

where

$$\begin{aligned} \overline{D}_i &= (q + p_i)^2 - M_i^2 + i0 = \overline{q}^2 - d_i, & p_0 &= 0, \\ \overline{q}^2 &= q^2 + i0 \equiv q^2 - \mu^2, & d_i &= M_i^2 - p_i^2 - 2(q \cdot p_i). \end{aligned} \quad (2.3)$$

As usual, q denotes a generic integration momentum; the bar means that the $+i0$ propagator prescription is made explicit and formally identified with a vanishing mass $-\mu^2$: in this way, the factors $1/\overline{q}^2$ appearing in the r.h.s. of eq. (2.2) are made IR-safe.

Since d_1 is at most linear in q and $d_0 = M_0^2$, the only UV-divergent term of the r.h.s. of eq. (2.2) is that in squared brackets (a convention that we

will use throughout the rest of the text body),

$$\left[\frac{1}{\bar{q}^4} \right], \quad (2.4)$$

which is also independent of any physical scale. The idea at the base of FDR is that of disregarding this type of terms, and integrating in four dimensions the remaining UV-finite part alone:

$$\int [d^4q] \frac{1}{\overline{D_0 D_1}} \equiv \lim_{\mu \rightarrow 0} \int d^4q \left(\frac{d_1}{\bar{q}^4 \overline{D_1}} + \frac{d_0}{\bar{q}^2 \overline{D_0 D_1}} \right). \quad (2.5)$$

From now on, the symbol $[d^4q]$ will always denote an FDR integral. Differently with respect to a dimensionally regularized Feynman integral, the limit $\mu \rightarrow 0$ is taken outside integration, so that the induced IR divergences are kept under control. Moreover, due to this limit, only a logarithmic dependence on μ remains that is interpreted as the renormalization scale, as we explain in some detail in the next section.

This definition is naturally extended to any integrand, scalar or tensorial, and to any loop level. The separation of the UV infinities and of the physical finite part, which we dub *FDR defining expansion* of the integrand, can be systematically brought about thanks to the *partial fraction identities*. For example,

$$\frac{1}{\overline{D_i}} = \frac{1}{\bar{q}^2} + \frac{d_i}{\bar{q}^2 \overline{D_i}} \quad (2.6)$$

is the only identity that one needs to *FDR expand* one-loop integrands. In section 2.1.2 some examples are listed and the complementary information needed to carry out this procedure beyond one-loop.

The UV-divergent and scale-free terms that are extracted with the FDR defining expansion are referred to as *vacuum configurations*. They can be scalar or tensorial. For example, at one loop,

$$\left[\frac{1}{\bar{q}^2} \right], \quad \left[\frac{1}{\bar{q}^4} \right], \quad \left[\frac{q^\alpha q^\beta}{\bar{q}^4} \right], \quad \left[\frac{q^\alpha q^\beta}{\bar{q}^6} \right], \quad \left[\frac{q^\alpha q^\beta q^\gamma q^\delta}{\bar{q}^8} \right], \quad \dots \quad (2.7)$$

It is important to realize that divergent tensor structures are fully subtracted from the original integrand as well. It can be shown that FDR tensors are

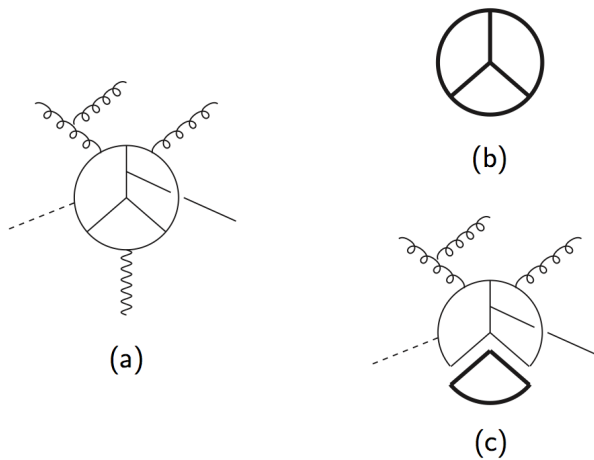


Figure 2.1: Here is represented a generic Feynman diagram (a) in order to illustrate pictorially the meaning of the FDR integral: as loop momenta become very large, all internal scales become negligible in comparison, and the diagram resembles a vacuum bubble. This is true when all loop momenta are infinite (b), but also when only some of them probe the UV region (c), which means that in FDR both global and sub-vacua are subtracted.

equivalent to DR tensors at one loop, but differences start at two loops and beyond [53].

Calling J the original integrand of an ℓ -loop function, one can always separate the vacuum configurations and the physical finite part; schematically,

$$J(q_1, \dots, q_\ell) = J_{\text{INF}}(q_1, \dots, q_\ell) + J_{\text{F},\ell}(q_1, \dots, q_\ell), \quad (2.8)$$

The FDR integral over J is then *defined* as the integral in four dimensions of the finite part only, that is

$$\int [d^4 q_1] \dots [d^4 q_\ell] J(q_1, \dots, q_\ell) \equiv \lim_{\mu \rightarrow 0} \int d^4 q_1 \dots d^4 q_\ell J_{\text{F},\ell}(q_1, \dots, q_\ell). \quad (2.9)$$

The interpretation is the following: when the loop momenta become very large, all the physical scales involved in a Green function (masses, external momenta) are negligible in comparison, so that the diagram effectively behaves as a vacuum bubble, which is unphysical, and should not be accounted for in the calculation (see fig. 2.1).

Notice that FDR and normal integration coincide in a convergent integral, since no divergent part J_{INF} can be extracted from its integrand.

It is handy at times to express the FDR integral as a difference of two otherwise-regulated integrals, one over the original integrand and the other one over the vacuum configurations. By choosing DR as a regularization scheme, with space-time dimension $n = 4 + \epsilon$, we can write that

$$\begin{aligned} & \int [d^4 q_1] \dots [d^4 q_\ell] J(q_1, \dots, q_\ell) = \\ & = \lim_{\mu \rightarrow 0} \left(\int \frac{d^n q_1 \dots d^n q_\ell}{\mu_R^{\ell \epsilon}} J(q_1, \dots, q_\ell) - \int \frac{d^n q_1 \dots d^n q_\ell}{\mu_R^{\ell \epsilon}} J_{\text{INF}}(q_1, \dots, q_\ell) \right). \end{aligned} \quad (2.10)$$

By introducing another scale μ' , FDR itself could also be used to regularize the integrals in the r.h.s. of last equation.

Eq. (2.10) also demonstrates that whenever IR-finite loop integrals are known in DR, their FDR counterparts can also be computed.

2.1.2 FDR defining expansion

The definition of the FDR integral relies on the possibility of consistently separating the UV infinities from the physical part of an integrand. This procedure, dubbed *FDR defining expansion*, is carried out by using the partial fraction identities, such as eq. (2.6), which must be iteratively applied to the integrand at hand until all divergences are collected into terms independent of the kinematics. An example of FDR expansion at one loop is provided by eq. (2.2). The same mechanism works unchanged when powers of the loop momentum appear in the numerator. For example,

$$\begin{aligned} \frac{q^\alpha q^\beta}{\overline{D_0} \overline{D_1}} &= \left[\frac{q^\alpha q^\beta}{\overline{q^4}} \right] + (d_0 + M_1^2 - p_1^2) \left[\frac{q^\alpha q^\beta}{\overline{q^6}} \right] \\ &\quad - 2p_{1\gamma} \left[\frac{q^\alpha q^\beta q^\gamma}{\overline{q^6}} \right] + 4p_1^\gamma p_1^\delta \left[\frac{q^\alpha q^\beta q^\gamma q^\delta}{\overline{q^8}} \right] \\ &\quad + q^\alpha q^\beta \left(\frac{4(q \cdot p_1)^2 d_1}{\overline{q^8} \overline{D_{p_1}}} + (M_1^2 - p_1^2) \frac{d_0 + d_1 - 2(q \cdot p_1)}{\overline{q^6} \overline{D_{p_1}}} \right. \\ &\quad \left. - 2d_0 \frac{(q \cdot p_1)}{\overline{q^6} \overline{D_{p_1}}} + \frac{d_0^2}{\overline{q^4} \overline{D_{p_0}} \overline{D_{p_1}}} \right). \end{aligned} \quad (2.11)$$

Power-counting is the only piece of technology that one needs, apart from partial fractioning, in order to be able to FDR expand any one-loop integrand. In the following we collect some useful additional information that comes handy when dealing with two-loop integrals.

2.1.2.1 Two-loop case

In these thesis the only two-loop integrals that we consider are vacuum integrals, i.e. free of any momentum scale, in the form

$$[\alpha m_1 | \beta m_2 | \gamma m_{12}] = \int [d^4 q_1][d^4 q_2] \frac{1}{\overline{D}_1^\alpha \overline{D}_2^\beta \overline{D}_{12}^\gamma}, \quad (2.12)$$

where we have introduced the compact notation $[\alpha m_1 | \beta m_2 | \gamma m_{12}]$, and the conventions

$$\overline{D}_1 = \vec{q}_1^2 - m_1^2, \quad \overline{D}_2 = \vec{q}_2^2 - m_2^2, \quad \overline{D}_{12} = \vec{q}_{12}^2 - m_{12}^2, \quad q_{12} = q_1 + q_2. \quad (2.13)$$

The only physical scales on which integrals of this type depend are masses. This simple case is all we need in order to work out the cross section for the $H \rightarrow \gamma\gamma$ decay at two loop in the limit of large top mass, as performed in Section 3.2.

Two-loop power counting and partial fractioning

The UV power counting at two loops is made by computing the parameter

$$p = \min \left\{ 2(\alpha + \beta), 2(\alpha + \gamma), 2(\beta + \gamma), (\alpha + \beta + \gamma) \right\}. \quad (2.14)$$

The integral is UV-divergent whenever $p \leq 4$. What is more, if $(\alpha + \beta + \gamma) \leq 4$ too, the integral exhibits a real two-loop divergence; otherwise, it is a sub-divergence that can be expressed as a one-loop divergent integral multiplied by a convergent object. Correspondingly, the two-loop vacuum configurations are classified into *global vacua* and *sub-vacua*. The first are two-loop integrands at most logarithmically divergent, such as

$$\left[\frac{1}{\vec{q}_1^2 \vec{q}_2^2 \vec{q}_{12}^2} \right], \quad \left[\frac{1}{\vec{q}_1^4 \vec{q}_2^2 \vec{q}_{12}^2} \right], \quad \left[\frac{q_1^\alpha q_1^\beta}{\vec{q}_1^6 \vec{q}_2^2 \vec{q}_{12}^2} \right], \quad \left[\frac{q_1^\alpha q_1^\beta}{\vec{q}_1^4 \vec{q}_2^4 \vec{q}_{12}^2} \right], \quad \dots \quad (2.15)$$

whilst sub-vacua are one-loop vacuum configurations, like those of eq. (2.7), which multiply some finite one-loop structure. In FDR terms of this type are fully subtracted, with profound consequences (see Section 2.1.7 and Section 2.2.2.1).

On top of the partial fraction identity of eq. (2.6), some additional identities, such as

$$\frac{1}{\bar{q}_{12}^2} = \frac{1}{\bar{q}_2^2} - \frac{q_1^2 + 2(q_1 \cdot q_2)}{\bar{q}_2^2 \bar{q}_{12}^2}, \quad \frac{1}{\bar{q}_2^2} = \frac{1}{\bar{q}_1^2} - \frac{q_{12}^2 - 2(q_1 \cdot q_{12})}{\bar{q}_1^2 \bar{q}_2^2}. \quad (2.16)$$

are required in order to extract the sub-divergences.

Examples

1. Expansion for $\int [d^4 q_1][d^4 q_2] \frac{1}{\bar{D}_1 \bar{D}_2 \bar{D}_{12}}$:

$$\begin{aligned} \frac{1}{\bar{D}_1 \bar{D}_2 \bar{D}_{12}} &= \left[\frac{1}{\bar{q}_1^2 \bar{q}_2^2 \bar{q}_{12}^2} \right] + m_1^2 \left[\frac{1}{\bar{q}_1^4 \bar{q}_2^2 \bar{q}_{12}^2} \right] + m_2^2 \left[\frac{1}{\bar{q}_1^2 \bar{q}_2^4 \bar{q}_{12}^2} \right] + m_{12}^2 \left[\frac{1}{\bar{q}_1^2 \bar{q}_2^2 \bar{q}_{12}^4} \right] \\ &+ \frac{m_1^4}{(\bar{D}_1 \bar{q}_1^4)} \left[\frac{1}{\bar{q}_2^4} \right] + \frac{m_2^4}{(\bar{D}_2 \bar{q}_2^4)} \left[\frac{1}{\bar{q}_1^4} \right] + \frac{m_{12}^4}{(\bar{D}_{12} \bar{q}_{12}^4)} \left[\frac{1}{\bar{q}_1^4} \right] \\ &- m_1^4 \frac{q_1^2 + 2(q_1 \cdot q_2)}{(\bar{D}_1 \bar{q}_1^4) \bar{q}_2^4 \bar{q}_{12}^2} - m_2^4 \frac{q_2^2 + 2(q_1 \cdot q_2)}{\bar{q}_1^4 (\bar{D}_2 \bar{q}_2^4) \bar{q}_{12}^2} \\ &- m_{12}^4 \frac{q_{12}^2 - 2(q_1 \cdot q_{12})}{\bar{q}_1^4 \bar{q}_2^2 (\bar{D}_{12} \bar{q}_{12}^4)} + \frac{m_1^2 m_2^2}{(\bar{D}_1 \bar{q}_1^2) (\bar{D}_2 \bar{q}_2^2) \bar{q}_{12}^2} \\ &+ \frac{m_1^2 m_{12}^2}{(\bar{D}_1 \bar{q}_1^2) \bar{q}_2^2 (\bar{D}_{12} \bar{q}_{12}^2)} + \frac{m_2^2 m_{12}^2}{\bar{q}_1^2 (\bar{D}_2 \bar{q}_2^2) (\bar{D}_{12} \bar{q}_{12}^2)} \\ &+ \frac{m_1^2 m_2^2 m_{12}^2}{(\bar{D}_1 \bar{q}_1^2) (\bar{D}_2 \bar{q}_2^2) (\bar{D}_{12} \bar{q}_{12}^2)}. \end{aligned} \quad (2.17)$$

2. Expansion for $\int [d^4 q_1][d^4 q_2] \frac{1}{\bar{D}_1^2 \bar{D}_2 \bar{D}_{12}}$:

$$\begin{aligned}
\frac{1}{\overline{D}_1^2 \overline{D}_2 \overline{D}_{12}} &= \left[\frac{1}{\overline{q}_1^4 \overline{q}_2^2 \overline{q}_{12}^2} \right] + \left(\frac{2m_1^2}{\overline{q}_1^4 \overline{D}_1} + \frac{m_1^4}{\overline{q}_1^4 \overline{D}_1^2} \right) \left[\frac{1}{\overline{q}_2^4} \right] + \\
&- 2m_1^2 \frac{q_1^2 + 2(q_1 \cdot q_2)}{(\overline{q}_1^4 \overline{D}_1) \overline{q}_2^4 \overline{q}_{12}^2} - m_1^4 \frac{q_1^2 + 2(q_1 \cdot q_2)}{(\overline{q}_1^4 \overline{D}_1^2) \overline{q}_2^4 \overline{q}_{12}^2} + \\
&+ \frac{m_2^2}{(\overline{q}_1^2 \overline{D}_1)(\overline{q}_2^2 \overline{D}_2) \overline{q}_{12}^2} + \frac{m_1^2 m_2^2}{(\overline{q}_1^2 \overline{D}_1^2)(\overline{q}_2^2 \overline{D}_2) \overline{q}_{12}^2} + \\
&+ \frac{m_{12}^2}{(\overline{q}_1^2 \overline{D}_1) \overline{q}_2^2 (\overline{q}_{12}^2 \overline{D}_{12})} + \frac{m_1^2 m_{12}^2}{(\overline{q}_1^2 \overline{D}_1^2) \overline{q}_2^2 (\overline{q}_{12}^2 \overline{D}_{12})} + \\
&+ \frac{m_2^2 m_{12}^2}{(\overline{q}_1^2 \overline{D}_1)(\overline{q}_2^2 \overline{D}_2)(\overline{q}_{12}^2 \overline{D}_{12})} + \frac{m_1^2 m_2^2 m_{12}^2}{(\overline{q}_1^2 \overline{D}_1^2)(\overline{q}_2^2 \overline{D}_2)(\overline{q}_{12}^2 \overline{D}_{12})}
\end{aligned} \tag{2.18}$$

3. Expansion for $\int [d^4 q_1][d^4 q_2] \frac{q_1^\alpha q_1^\beta}{\overline{D}_1^3 \overline{D}_2 \overline{D}_{12}}$:

$$\begin{aligned}
\frac{q_1^\alpha q_1^\beta}{\overline{D}_1^3 \overline{D}_2 \overline{D}_{12}} &= \left[\frac{q_1^\alpha q_1^\beta}{\overline{q}_1^6 \overline{q}_2^2 \overline{q}_{12}^2} \right] + \left(\frac{q_1^\alpha q_1^\beta}{\overline{D}_1^3} - \left[\frac{q_1^\alpha q_1^\beta}{\overline{q}_1^6} \right] \right) \left(\left[\frac{1}{\overline{q}_2^4} \right] - \frac{q_1^2 + 2(q_1 \cdot q_2)}{\overline{q}_2^4 \overline{q}_{12}^2} \right) \\
&+ \frac{q_1^\alpha q_1^\beta}{\overline{D}_1^3 \overline{q}_2^2 \overline{D}_{12}} \left(\frac{m_2^2}{\overline{D}_2} + \frac{m_{12}^2}{\overline{q}_{12}^2} \right).
\end{aligned} \tag{2.19}$$

4. Expansion for $\int [d^4 q_1][d^4 q_2] \frac{1}{\overline{D}_1^2 \overline{D}_2 \overline{q}_{12}^2}$:

$$\begin{aligned}
\frac{1}{\overline{D}_1^2 \overline{D}_2 \overline{q}_{12}^2} &= \left[\frac{1}{\overline{q}_1^4 \overline{q}_2^2 \overline{q}_{12}^2} \right] + \left(\frac{m_1^2}{\overline{D}_1 \overline{q}_1^4} + \frac{m_1^2}{\overline{D}_1^2 \overline{q}_1^2} \right) \left(\left[\frac{1}{\overline{q}_2^4} \right] - \frac{q_1^2 + 2(q_1 \cdot q_2)}{\overline{q}_2^4 \overline{q}_{12}^2} \right) \\
&+ \frac{m_2^2}{\overline{D}_1^2 (\overline{D}_2 \overline{q}_2^2) \overline{q}_{12}^2}.
\end{aligned} \tag{2.20}$$

5. Expansion for $\int [d^4 q_1][d^4 q_2] \frac{q_1^\alpha q_1^\beta}{\overline{D}_1^2 \overline{D}_2 \overline{q}_{12}^2}$:

$$\begin{aligned}
\frac{q_1^\alpha q_1^\beta}{\overline{D}_1^2 \overline{D}_2^2 \overline{q}_{12}^2} &= \left(\frac{m_2^2}{\overline{D}_2 \overline{q}_2^4} + \frac{m_2^2}{\overline{D}_2^2 \overline{q}_2^2} \right) \left(\left[\frac{q_1^\alpha q_1^\beta}{\overline{q}_1^6} \right] - \frac{(q_2^2 + 2(q_1 \cdot q_2)) q_1^\alpha q_1^\beta}{\overline{q}_1^6 \overline{q}_{12}^2} \right) \\
&+ \left[\frac{q_1^\alpha q_1^\beta}{\overline{q}_1^4 \overline{q}_2^4 \overline{q}_{12}^2} \right] + \left(\frac{1}{\overline{D}_1^2} - \frac{1}{\overline{q}_1^4} \right) \frac{q_1^\alpha q_1^\beta}{\overline{D}_2^2 \overline{q}_{12}^2} \quad (2.21)
\end{aligned}$$

6. Expansion for $\int [d^4 q_1][d^4 q_2] \frac{q_{12}^\alpha q_{12}^\beta}{\overline{D}_1^2 \overline{D}_2^2 \overline{q}_{12}^2}$:

$$\begin{aligned}
\frac{q_{12}^\alpha q_{12}^\beta}{\overline{D}_1^2 \overline{D}_2^2 \overline{q}_{12}^2} &= \left[\frac{q_{12}^\alpha q_{12}^\beta}{\overline{q}_{12}^6} \right] \left(\left(\frac{m_1^2}{\overline{D}_1 \overline{q}_1^4} + \frac{m_1^2}{\overline{D}_1^2 \overline{q}_1^2} \right) + \left(\frac{m_2^2}{\overline{D}_2 \overline{q}_2^4} + \frac{m_2^2}{\overline{D}_2^2 \overline{q}_2^2} \right) \right) \\
&+ \left[\frac{q_{12}^\alpha q_{12}^\beta}{\overline{q}_1^4 \overline{q}_2^4 \overline{q}_{12}^2} \right] + \frac{q_{12}^\alpha q_{12}^\beta}{\overline{q}_{12}^2} \left(\left(\frac{1}{\overline{D}_1^2} - \frac{1}{\overline{q}_1^4} \right) \left(\frac{1}{\overline{D}_2^2} - \frac{1}{\overline{q}_2^4} \right) + \right. \\
&\left. \left(\frac{1}{\overline{q}_1^4} - \frac{1}{\overline{q}_{12}^4} \right) \left(\frac{1}{\overline{D}_2^2} - \frac{1}{\overline{q}_2^4} \right) + \left(\frac{1}{\overline{q}_2^4} - \frac{1}{\overline{q}_{12}^4} \right) \left(\frac{1}{\overline{D}_1^2} - \frac{1}{\overline{q}_1^4} \right) \right) \quad (2.22)
\end{aligned}$$

2.1.3 Shift invariance and uniqueness

FDR integrals are invariant under the shift of any integration variable. This can be easily proven by using the fact that they can be thought as finite differences of shift invariant DR-regulated divergent integrals as in eq. (2.10). A direct proof of shift invariance at one and two loops is presented in the next section.

Before going into these details, it is worth mentioning that a direct consequence of shift invariance is the uniqueness of the FDR integral as defined in eq. (2.9). In fact, the subtracted integrands in $J_{INF}(q_1, \dots, q_\ell)$ are unambiguously determined by the UV content of the original integrand, the only possible ambiguity being shifts of the loop momenta in $J(q_1, \dots, q_\ell)$, which, thanks to shift invariance, produce the same FDR integral.

Proof of shift invariance

We demonstrate that, for positive integers α , β , γ and δ ,

$$\int [d^4 q] \frac{1}{\overline{D}^\alpha(0)} = \int [d^4 q] \frac{1}{\overline{D}^\alpha(p)} \quad (2.23)$$

where $\overline{D}(0)$ is the usual denominator of the propagator, and $\overline{D}(p)$ is the shifted one, that is

$$\overline{D}(0) = q^2 - m^2 - \mu^2, \quad \overline{D}(p) = (q + p)^2 - m^2 - \mu^2; \quad (2.24)$$

and, at two loops,

$$\int \frac{[d^4 q_1][d^4 q_2]}{\overline{D}_1^\beta(0) \overline{D}_2^\gamma(0) \overline{D}_{12}^\delta(0)} = \int \frac{[d^4 q_1][d^4 q_2]}{\overline{D}_1^\beta(p_1) \overline{D}_2^\gamma(p_2) \overline{D}_{12}^\delta(p_{12})} \quad (2.25)$$

where

$$\overline{D}_i(0) = q_i^2 - m_i^2 - \mu^2, \quad \overline{D}_i(p_i) = (q_i + p_i)^2 - m_i^2 - \mu^2. \quad (2.26)$$

Since polynomially divergent integrals vanish, the divergent parts of any one- or two-loop FDR integral can be written – after expanding in the external momenta – in terms of the four cases

$$\alpha = 1, \quad \alpha = 2, \quad \beta = \gamma = \delta = 1, \quad \text{and} \quad \beta = \gamma = 1 \text{ with } \delta > 1. \quad (2.27)$$

In all the other cases eqs. (2.23) and (2.25) coincide with finite integrals, for which shift invariance trivially holds.

We start proving eq. (2.23) with $\alpha = 1$. One writes the FDR expansions of the two sides of the equation as

$$\begin{aligned} \frac{1}{\overline{D}(0)} &= \left[\frac{1}{\overline{q}^2} \right] + \left[\frac{m^2}{\overline{q}^4} \right] + J_{F,1}(q), \\ \frac{1}{\overline{s}(p)} &= \left[\frac{1}{\overline{q}^2} \right] + \left[\frac{d(p)}{\overline{q}^4} \right] + 4 \left[\frac{(q \cdot p)^2}{\overline{q}^6} \right] + J'_{F,1}(q). \end{aligned} \quad (2.28)$$

where $d(p) = m^2 - p^2 - 2(q \cdot p)$ and $J_{F,1}, J'_{F,1}$ are the finite parts. Then

$$\begin{aligned} \int [d^4 q] \frac{1}{\overline{D}(0)} &= \lim_{\mu \rightarrow 0} \left(\int d^n q \frac{1}{\overline{D}(0)} - \int d^n q \frac{m^2}{\overline{q}^4} - \int d^n q \frac{1}{\overline{q}^2} \right) \\ &= \lim_{\mu \rightarrow 0} \left(\int d^n q \frac{1}{\overline{D}(p)} - \int d^n q \frac{m^2}{\overline{q}^4} - \int d^n q \frac{1}{(q+p)^2 - \mu^2} \right), \end{aligned} \quad (2.29)$$

where the shift invariance of the dimensionally regulated integrals over $1/\overline{D}$ and $1/\overline{q}^2$ has been used. By now expanding the last integrand one obtains

$$\frac{1}{(q+p)^2 - \mu^2} - \frac{1}{\overline{q}^2} = -\frac{p^2 + 2(q \cdot p)}{\overline{q}^4} + 4\frac{(q \cdot p)^2}{\overline{q}^6} + \mathcal{O}(p^3). \quad (2.30)$$

Since the l.h.s. of eq. (2.30) vanishes upon integration at any order in p , the same happens for the combination

$$-\frac{p^2 + 2(q \cdot p)}{\overline{q}^4} + 4\frac{(q \cdot p)^2}{\overline{q}^6}. \quad (2.31)$$

The last integral in eq. (2.29) can then be rewritten as

$$\int d^n q \frac{1}{(q+p)^2 - \mu^2} = \int d^n q \left(\frac{1}{\overline{q}^2} - \frac{p^2 + 2(q \cdot p)}{\overline{q}^4} + 4\frac{(q \cdot p)^2}{\overline{q}^6} \right), \quad (2.32)$$

so that

$$\int [d^4 q] \frac{1}{\overline{D}(0)} = \lim_{\mu \rightarrow 0} \int d^4 q J'_{F,1}(q) = \int [d^4 q] \frac{1}{\overline{D}(p)}, \quad (2.33)$$

which proves eq. (2.23) with $\alpha = 1$. The case $\alpha = 2$ is proven by taking the derivative of eq. (2.33) with respect to m^2 .

We now deal with the case $\beta = \gamma = \delta = 1$ of eq. (2.25). The FDR expansion of the l.h.s. of eq. (2.25) is given by eq. (2.17). As for the r.h.s., having introduced the notation

$$\overline{s}_i = (q_i + p_i)^2 - m_i^2 - \mu^2 \quad \text{and} \quad d_i = m_i^2 - p_i^2 - 2(q_i \cdot p_i), \quad (2.34)$$

the expansion reads

$$\begin{aligned}
\frac{1}{\bar{s}_1 \bar{s}_2 \bar{s}_{12}} &= \left[\frac{1}{\bar{q}_1^2 \bar{q}_2^2 \bar{q}_{12}^2} \right] + \left[\frac{d_1}{\bar{q}_1^4 \bar{q}_2^2 \bar{q}_{12}^2} \right] + \left[\frac{d_2}{\bar{q}_1^2 \bar{q}_2^4 \bar{q}_{12}^2} \right] + \left[\frac{d_{12}}{\bar{q}_1^2 \bar{q}_2^2 \bar{q}_{12}^4} \right] \\
&+ 4 \left[\frac{(q_1 \cdot p_1)^2}{\bar{q}_1^6 \bar{q}_2^2 \bar{q}_{12}^2} \right] + 4 \left[\frac{(q_2 \cdot p_2)^2}{\bar{q}_1^2 \bar{q}_2^6 \bar{q}_{12}^2} \right] + 4 \left[\frac{(q_{12} \cdot p_{12})^2}{\bar{q}_1^2 \bar{q}_2^2 \bar{q}_{12}^6} \right] \\
&+ 4 \left[\frac{(q_1 \cdot p_1)(q_2 \cdot p_2)}{\bar{q}_1^4 \bar{q}_2^4 \bar{q}_{12}^2} \right] + 4 \left[\frac{(q_1 \cdot p_1)(q_{12} \cdot p_{12})}{\bar{q}_1^4 \bar{q}_2^2 \bar{q}_{12}^4} \right] \\
&+ 4 \left[\frac{(q_2 \cdot p_2)(q_{12} \cdot p_{12})}{\bar{q}_1^2 \bar{q}_2^4 \bar{q}_{12}^4} \right] + \left(\frac{d_1^2}{\bar{q}_1^4 \bar{s}_1} - 4 \frac{(q_1 \cdot p_1)^2}{\bar{q}_1^6} \right) \left[\frac{1}{\bar{q}_2^4} \right] \\
&+ \left(\frac{d_2^2}{\bar{q}_2^4 \bar{s}_2} - 4 \frac{(q_2 \cdot p_2)^2}{\bar{q}_2^6} \right) \left[\frac{1}{\bar{q}_1^4} \right] + \left(\frac{d_{12}^2}{\bar{q}_{12}^4 \bar{s}_{12}} - 4 \frac{(q_{12} \cdot p_{12})^2}{\bar{q}_{12}^6} \right) \left[\frac{1}{\bar{q}_1^4} \right] \\
&+ J'_{F,2}(q_1, q_2).
\end{aligned} \tag{2.35}$$

Then, by rewriting

$$\frac{m_i^4}{\bar{D}_i(0)\bar{q}_i^4} = \frac{1}{\bar{D}_i(0)} - \frac{1}{\bar{q}_i^2} - \frac{m_i^2}{\bar{q}_i^4} \tag{2.36}$$

and shifting all the $\bar{D}_i(0)$ and the quadratically divergent integrals, eq. (2.17) produces

$$\begin{aligned}
\int \frac{[d^4 q_1][d^4 q_2]}{\bar{D}_1(0)\bar{D}_2(0)\bar{D}_{12}(0)} &= \lim_{\mu \rightarrow 0} \int d^n q_1 d^n q_2 \left(\frac{1}{\bar{s}_1 \bar{s}_2 \bar{s}_{12}} \right. \\
&\quad - \frac{1}{(s_1 - m_1^2)(s_2 - m_2^2)(s_{12} - m_{12}^2)} \\
&\quad - m_1^2 \left[\frac{1}{\bar{q}_1^4 \bar{q}_2^2 \bar{q}_{12}^2} \right] - m_2^2 \left[\frac{1}{\bar{q}_1^2 \bar{q}_2^4 \bar{q}_{12}^2} \right] - m_{12}^2 \left[\frac{1}{\bar{q}_1^2 \bar{q}_2^2 \bar{q}_{12}^4} \right] \\
&\quad - \left(\frac{1}{\bar{s}_1} - \frac{1}{(q_1 + p_1)^2 - \mu^2} - \frac{m_1^2}{\bar{q}_1^4} \right) \left[\frac{1}{\bar{q}_2^4} \right] \\
&\quad - \left(\frac{1}{\bar{s}_2} - \frac{1}{(q_2 + p_2)^2 - \mu^2} - \frac{m_2^2}{\bar{q}_2^4} \right) \left[\frac{1}{\bar{q}_1^4} \right] \\
&\quad \left. - \left(\frac{1}{\bar{s}_{12}} - \frac{1}{(q_{12} + p_{12})^2 - \mu^2} - \frac{m_{12}^2}{\bar{q}_{12}^4} \right) \left[\frac{1}{\bar{q}_1^4} \right] \right).
\end{aligned} \tag{2.37}$$

An expansion up to $\mathcal{O}(p_1^2)$, $\mathcal{O}(p_2^2)$ and $\mathcal{O}(p_1 p_2)$ of the second line and of the terms

$$\frac{1}{((q_i + p_i)^2 - \mu^2)}$$

in the last three lines produces extra integrands which – by the same argument used at one-loop – vanish upon integration. The addition of such terms reconstructs $J'_{F,2}(q_1, q_2)$ as given in eq. (2.35), so that

$$\begin{aligned} \int \frac{[d^4 q_1][d^4 q_2]}{\overline{D}_1(0)\overline{D}_2(0)\overline{D}_{12}(0)} &= \lim_{\mu \rightarrow 0} \int d^4 q_1 d^4 q_2 J'_{F,2}(q_1, q_2) \\ &= \int \frac{[d^4 q_1][d^4 q_2]}{\overline{D}_1(p_1)\overline{D}_2(p_2)\overline{D}_{12}(p_{12})}. \end{aligned} \quad (2.38)$$

Finally, deriving with respect to m_{12}^2 demonstrates the last case, i.e. eq. (2.25) with $\beta = \gamma = 1$ and $\delta \geq 1$.

With more loops the proof follows the samereasoning: the mismatch between the FDR expansion of shifted and unshifted integrands is cured by vanishing integrals obtained by expanding the polynomially divergent integrals in $J_{\text{INF}}(q_1, \dots, q_\ell)$ at the relevant order in p , as in eq. (2.30).

2.1.4 Independence of the UV cutoff

Let's start from eq. (2.8). As a result of the subtraction of the vacuum configurations, non-integrable powers of $1/\overline{q}^2$ are developed in $J_{F,i}(q_1, \dots, q_\ell)$. Such IR poles get regulated by the μ^2 propagator prescription. Thus, the original UV cutoff is traded for an IR one: μ . We now show that the dependence on μ is at most logarithmic, and that this IR cut-off can always be exchanged for an arbitrary scale μ_R , which can be interpreted as the renormalization scale.

Suppose for the moment that the original integrand is not IR-divergent, and consider again eq. (2.10), which we report here for legibility:

$$\begin{aligned} &\int [d^4 q_1] \dots [d^4 q_\ell] J(q_1, \dots, q_\ell) = \\ &= \lim_{\mu \rightarrow 0} \left(\int \frac{d^n q_1 \dots d^n q_\ell}{\mu_R^{\ell \epsilon}} J(q_1, \dots, q_\ell) - \int \frac{d^n q_1 \dots d^n q_\ell}{\mu_R^{\ell \epsilon}} J_{\text{INF}}(q_1, \dots, q_\ell) \right). \end{aligned} \quad (2.39)$$

Since the first term in its r.h.s. is the original dimensionally regulated integral, it does not depend on μ in the limit $\mu \rightarrow 0$. On the other hand,

polynomially divergent integrands in J_{INF} cannot contribute either, because they generate polynomials in μ which instantly vanish in the limit $\mu \rightarrow 0$. Therefore, the μ dependence in the l.h.s. is entirely due to powers of $\ln(\mu/\mu_R)$ created by the subtraction of the logarithmically divergent integrals of J_{INF} . If one redefines the FDR integral without the subtraction of such logarithms, no dependence on μ is produced. This is equivalent to the operation of adding back all $\ln(\mu/\mu_R)$ s to the l.h.s. of eq. (2.10). Then, the limit $\mu \rightarrow 0$ can be taken, μ becomes μ_R and no cutoff is left. In other words, when subtracting the vacuum configurations from J we have unwillingly dropped – together with the UV divergent part – an IR-divergent term, responsible for the appearance of a spurious $\ln(\mu/\mu_R)$ in $J_{F,\ell}$: by returning this object to the physical part, we effectively exchange μ for μ_R .

This reasoning is still valid when IR singularities are also around. Indeed, IR and UV divergences can be systematically separated, upon the introduction of an extra scale M_{IR} , by means of the relation

$$\begin{aligned} \frac{1}{(q+p)^2} &= \frac{1}{q^2 - M_{IR}^2} - \left(\frac{1}{q^2 - M_{IR}^2} - \frac{1}{(q+p)^2} \right) \\ &= \frac{1}{q^2 - M_{IR}^2} - \frac{M_{IR}^2 + 2(q \cdot p)}{(q^2 - M_{IR}^2)(q+p)^2}. \end{aligned} \quad (2.40)$$

Moreover, at one-loop, UV and IR infinities simultaneously occur only in scaleless integrals, which, like in DR, vanish in FDR, as explained in 2.1.9.

The identification $\ln \mu = \ln \mu_R$ after the limit $\mu \rightarrow 0$ is understood in all FDR integrals appearing in this chapter and the following. By adding this tailpiece to its definition, the FDR integral is made independent of any cut-off. As one would expect, it depends logarithmically on an arbitrary scale, at the same perturbative order of the calculation one is performing. This dependence is dropped - or rather pulled back to a higher order - once the parameters of the Lagrangian are fixed in terms of some observables, i.e. after undertaking a *finite renormalization* (see Section 2.2.2).

Example

Let us explicitly work out a simple example in order to make this point more clear. Given that $\overline{D} = \overline{q}^2 - M^2$, consider the integrand

$$\frac{1}{\overline{D}^2} = \left[\frac{1}{\overline{q}^4} \right] + \frac{M^2}{\overline{q}^4 \overline{D}} + \frac{M^4}{\overline{q}^2 \overline{D}^2}. \quad (2.41)$$

Knowing that

$$\int \frac{d^n q}{\mu_R^\epsilon} \frac{1}{(q^2 - m^2)^2} = -i\pi^2 \left(\ln \frac{m^2}{\mu_R^2} + \frac{2}{\epsilon} + \Delta \right), \quad (2.42)$$

where $\Delta = \gamma_E + \ln \pi$, the r.h.s. of eq. (2.10), before the limit, reads:

$$\int \frac{d^n q}{\mu_R^\epsilon} \frac{1}{\overline{D}^2} - \int \frac{d^n q}{\mu_R^\epsilon} \left[\frac{1}{\overline{q}^4} \right] = -i\pi^2 \left(\ln \frac{M^2 + \mu^2}{\mu_R^2} + \ln \frac{\mu^2}{\mu_R^2} \right). \quad (2.43)$$

The poles and universal constants exactly cancel; the second logarithm, however, is the remnant of the spurious IR separation that we have induced.

We obtain the same result if we directly integrate in four dimensions the finite part of eq. (2.41):

$$\int d^4 q \left(\frac{M^2}{\overline{q}^4 \overline{D}} + \frac{M^4}{\overline{q}^2 \overline{D}^2} \right) = -i\pi^2 \ln \frac{M^2 + \mu^2}{\mu^2}. \quad (2.44)$$

By subtracting to this the $\ln(\mu/\mu_R)$ of eq. (2.43), or equivalently by replacing $\ln \mu \rightarrow \ln \mu_R$, we can take the limit $\mu \rightarrow 0$:

$$\begin{aligned} \int [d^4 q] \frac{1}{\overline{D}^2} &= \lim_{\mu \rightarrow 0} \left\{ \int d^4 q \left(\frac{M^2}{\overline{q}^4 \overline{D}} + \frac{M^4}{\overline{q}^2 \overline{D}^2} \right) + i\pi^2 \ln \frac{\mu^2}{\mu_R^2} \right\} \\ &= -i\pi^2 \ln \frac{M^2}{\mu_R^2}. \end{aligned} \quad (2.45)$$

This is what we call FDR integral.

2.1.5 Global prescription

A crucial point in the definition of the FDR integral is the $i0$ prescription of the propagator, which is made explicit and identified with a small mass $-\mu^2$. Usually, the $i0$ of the Feynman propagator is dropped within the integrand and effectively overlooked, because - since a propagator represents an off-shell virtual particle - the limit

$$\frac{1}{\overline{D}} = \frac{1}{q^2 - M^2 + i0} \rightarrow \frac{1}{q^2 - M^2} \quad (2.46)$$

is well-defined. Instead, in FDR $i0 = -\mu^2$ is maintained because it cures the IR divergences produced by the FDR expansion: the limit $\mu \rightarrow 0$ is moved outside the integration with all the profound consequences explained in Section 2.1.4.

The prescription is interpreted as a deformation of the squared loop momenta, which implies that a μ^2 must be consistently subtracted from any q^2 appearing in the amplitude, not only those in a propagator: *in FDR, any q^2 generated by the Feynman rules must be promoted to $\bar{q}^2 = q^2 - \mu^2$.* This operation is not always trivial; special attention must be paid when dealing with fermionic lines, as explained in Section 2.1.5.3.

This rule, replacing $q^2 \rightarrow \bar{q}^2$ everywhere, is dubbed *global prescription*; it ensures that the usual simplifications between numerator and denominator take place, which in turn plays a key role in preserving the symmetries of the amplitude (see Section ??). Take for example,

$$\int [d^4q] \frac{\bar{q}^2}{\overline{D_0} \overline{D_1} \overline{D_2}} = \int [d^4q] \left(\frac{1}{\overline{D_1} \overline{D_2}} + \frac{d_0}{\overline{D_0} \overline{D_1} \overline{D_2}} \right). \quad (2.47)$$

Given an UV-divergent FDR integral, simplifying a reducible numerator before integrating (the r.h.s. of the last equation) produces the same result that one would obtain by directly working out the original integral (the l.h.s.). This is true if the integrands in eq. (2.47) give the same result upon FDR integration, that is if they generate the same remainder after removing the divergent vacuum configurations. The three denominators in the l.h.s. of eq. (2.47) can be rewritten as

$$\frac{1}{\overline{D_0} \overline{D_1} \overline{D_2}} = \left[\frac{1}{\bar{q}^6} \right] + \frac{d_2}{\bar{q}^6 \overline{D_2}} + \frac{d_1}{\bar{q}^4 \overline{D_1} \overline{D_2}} + \frac{d_0}{\bar{q}^2 \overline{D_0} \overline{D_1} \overline{D_2}}, \quad (2.48)$$

while only the first term in the r.h.s. needs an expansion (since the second one is finite):

$$\frac{1}{\overline{D_1} \overline{D_2}} = \left[\frac{1}{\bar{q}^4} \right] + \frac{d_2}{\bar{q}^4 \overline{D_2}} + \frac{d_1}{\bar{q}^2 \overline{D_1} \overline{D_2}}. \quad (2.49)$$

Inserting these back into eq. (2.47), one obtains

$$\begin{aligned} \int [d^4 q] \frac{\bar{q}^2}{\bar{D}_0 \bar{D}_1 \bar{D}_2} &= \int [d^4 q] \left(\frac{1}{\bar{D}_1 \bar{D}_2} + \frac{d_0}{\bar{D}_0 \bar{D}_1 \bar{D}_2} \right) \\ &= \lim_{\mu \rightarrow 0} \int d^4 q \left\{ \frac{d_2}{\bar{q}^4 \bar{D}_2} + \frac{d_1}{\bar{q}^2 \bar{D}_1 \bar{D}_2} + \frac{d_0}{\bar{D}_0 \bar{D}_1 \bar{D}_2} \right\} \end{aligned} \quad (2.50)$$

which means that we can identify

$$\frac{\bar{q}^2}{\bar{D}_0 \bar{D}_1 \bar{D}_2} = \left(\frac{1}{\bar{D}_1 \bar{D}_2} + \frac{d_0}{\bar{D}_0 \bar{D}_1 \bar{D}_2} \right), \quad (2.51)$$

at the integrand level. It is important to realize that eq. (2.48) reproduces the last integral in eq. (2.50) *only if* the original q^2 appearing above the three denominators in the l.h.s. of eq. (2.47) is also promoted to \bar{q}^2 . Otherwise it would give

$$\lim_{\mu \rightarrow 0} \int d^4 q \left\{ \frac{q^2 d_2}{\bar{q}^6 \bar{D}_2} + \frac{q^2 d_1}{\bar{q}^4 \bar{D}_1 \bar{D}_2} + \frac{q^2 d_0}{\bar{q}^2 \bar{D}_0 \bar{D}_1 \bar{D}_2} \right\} \quad (2.52)$$

which differs by

$$\int [d^4 q] \frac{\mu^2}{\bar{D}_0 \bar{D}_1 \bar{D}_2} \neq 0. \quad (2.53)$$

Integrals of this type, referred to as *extra-integrals*, give a finite contribution. In Section 2.1.5.1 it is also explained how to calculate them, and several examples are presented.

What is more, having defined the extra-integrals, it is possible to express an FDR tensorial integral in terms of scalars and a constant. For example, considering vacuum integrals with $\bar{D} = \bar{q}^2 - M^2$ for simplicity,

$$\int [d^4 q] \frac{q^\alpha q^\beta}{\bar{D}^3} = \frac{g^{\alpha\beta}}{4} \left(\int [d^4 q] \frac{1}{\bar{D}^2} + M^3 \int [d^4 q] \frac{1}{\bar{D}^3} + \int [d^4 q] \frac{\mu^2}{\bar{D}^3} \right). \quad (2.54)$$

If the integrand is simplified to a sum of irreducible terms first, extra-integrals can only come up when performing the tensorial reduction (see some examples of how to implement this procedure in FDR in Section 2.1.8).

In practice, the global prescription means that all the usual algebraic manipulations at the level of the integrand can be performed within an FDR integral. As a consequence, one needs to worry about the FDR definition only when calculating the master integrals.

2.1.5.1 Extra-integrals

Extra-integrals, like that of eq. (2.53), are FDR integrals with powers of μ^2 in the numerator, but that do not vanish in the limit $\mu \rightarrow 0$.

Let us consider a simplified version of eq. (2.47), in which external momenta are zero and the masses are all the same, i.e.

$$\int [d^4q] \frac{\bar{q}^2}{D^3} = \int [d^4q] \frac{1}{D^2} + \int [d^4q] \frac{M^2}{D^3}. \quad (2.55)$$

By contradiction, suppose extra-integrals were null. Then,

$$\int [d^4q] \frac{q^2}{D^3} + c = \int [d^4q] \frac{1}{D^2} + \int [d^4q] \frac{M^2}{D^3}, \quad (2.56)$$

with $c = 0$. The FDR integrals appearing in the last equation can be easily calculated (see eq. (2.107)), either directly or as a difference of DR integrals, thereby obtaining

$$\int [d^4q] \frac{q^2}{D^3} = \int [d^4q] \frac{1}{D^2} = -i\pi^2 \ln \frac{M^2}{\mu^2}, \quad \int [d^4q] \frac{1}{D^3} = -\frac{i\pi^2}{2M^2}. \quad (2.57)$$

This clearly proves that $c \neq 0$ and that

$$\int [d^4q] \frac{\mu^2}{D^3} = \frac{i\pi^2}{2}. \quad (2.58)$$

This also gives us a hint on how to proceed in order to compute the extra-integrals.

Calculating extra-integrals

In general, whenever addressing the problem of calculating an FDR integral, the first step is to determine the FDR defining expansion of its integrand, which in turn depends on the power-counting. In this context, a μ^r in the numerator plays the role of a tensorial structure of rank r , so that the FDR defining expansion of an extra-integral is that of the integrand obtained by replacing $\mu \rightarrow q$. Take for example

$$\frac{\mu^2}{D^3} \leftrightarrow \frac{q^\alpha q^\beta}{D^3}. \quad (2.59)$$

The FDR defining expansion then reads

$$\frac{\mu^2}{D^3} = \left[\frac{\mu^2}{\bar{q}^6} \right] + \mu^2 \left(\frac{M^2}{\bar{q}^6 D} + \frac{M^2}{\bar{q}^4 D^2} + \frac{M^2}{\bar{q}^2 D^3} \right). \quad (2.60)$$

At this point we can either directly calculate the four-dimensional integral of the finite part, or we can use eq. (2.10), which proves to be exceptionally convenient in the case of extra-integrals:

$$\int [d^4 q] \frac{\mu^2}{D^3} = \lim_{\mu \rightarrow 0} \left(\int d^n q \frac{\mu^2}{D^3} - \int d^n q \left[\frac{\mu^2}{\bar{q}^6} \right] \right). \quad (2.61)$$

Because is finite the first integral in the r.h.s. vanishes in the limit $\mu \rightarrow 0$; on the other hand, the second integral is proportional to $1/\mu^2$, and gives a constant when multiplied by μ^2 ; namely,

$$\int [d^4 q] \frac{\mu^2}{D^3} = - \lim_{\mu \rightarrow 0} \mu^2 \int d^n q \frac{1}{\bar{q}^6} = \frac{i\pi^2}{2}. \quad (2.62)$$

Following this logic, it is understood that we only need to know the vacuum configurations of an extra-integral in order to calculate it: indeed, the extra-integral of eq. (2.53) gives exactly the same result as that of eq. (2.107). This makes it a relatively easy task also at a higher loop level. In the next paragraph we make some explicit examples at two loops, in order to clarify a few technical caveats.

Finally, notice that at one loop FDR extra-integrals have an exact counterpart in DR. Playing around with the example considered before, consider the tensorial reduction of eq. (2.54) in DR:

$$\begin{aligned} \int \frac{d^n q q^\alpha q^\beta}{\mu_R^\epsilon D^3} &= \frac{g^{\alpha\beta}}{n} \left(\int \frac{d^n q}{\mu_R^\epsilon} \frac{1}{D^2} + M^3 \int \frac{d^n q}{\mu_R^\epsilon} \frac{1}{D^3} \right) \\ &= \frac{g^{\alpha\beta}}{4} \left(\int \frac{d^n q}{\mu_R^\epsilon} \frac{1}{D^2} + M^3 \int \frac{d^n q}{\mu_R^\epsilon} \frac{1}{D^3} + \frac{\epsilon}{4} \int \frac{d^n q}{\mu_R^\epsilon} \frac{1}{D^2} + \mathcal{O}(\epsilon^2) \right). \end{aligned} \quad (2.63)$$

Indeed,

$$\frac{\epsilon}{4} \int \frac{d^n q}{\mu_R^\epsilon} \frac{1}{D^2} = \frac{i\pi^2}{2} + \mathcal{O}(\epsilon^2) \leftrightarrow \int [d^4 q] \frac{\mu^2}{D^3}. \quad (2.64)$$

In general, one can prove that

$$\int \frac{d^n q}{\mu_R^\epsilon} \frac{(-\tilde{q}^2)^k}{D_0^{(n)} D_1^{(n)} \dots} = \int [d^4 q] \frac{(\mu^2)^k}{\overline{D}_0 \overline{D}_1 \dots}, \quad (2.65)$$

where $\tilde{q}^2 = (q^{(n)})^2 - q^2$ is the ϵ -dimensional part of an n -vector, and the superscript (n) denotes an object living in n dimensions.

2.1.5.2 Extra-integrals at two loops

Consider, as an example of extra-integral at two loops,

$$\int [d^4 q_1][d^4 q_2] \frac{\mu^2|_1}{\overline{D}_1^2 \overline{D}_2^2 \overline{D}_{12}} \quad (2.66)$$

where we have used again the conventions of eq. (2.13), i.e.

$$\overline{D}_1 = \tilde{q}_1^2 - m_1^2, \quad \overline{D}_2 = \tilde{q}_2^2 - m_2^2, \quad \overline{D}_{12} = \tilde{q}_{12}^2 - m_{12}^2, \quad q_{12} = q_1 + q_2, \quad (2.67)$$

plus

$$\tilde{q}_i^2 = q_i^2 - \mu^2|_i. \quad (2.68)$$

In this context, as a matter of fact, the index i in $\mu^2|_i$ denotes the expansion to be used: although only one kind of μ^2 exists

$$\int [d^4 q_1][d^4 q_2] \frac{\mu^2|_1}{\overline{D}_1^2 \overline{D}_2^2 \overline{D}_{12}}, \quad \int [d^4 q_1][d^4 q_2] \frac{\mu^2|_2}{\overline{D}_1^2 \overline{D}_2^2 \overline{D}_{12}} \quad \text{and} \quad \int [d^4 q_1][d^4 q_2] \frac{\mu^2|_{12}}{\overline{D}_1^2 \overline{D}_2^2 \overline{D}_{12}} \quad (2.69)$$

are in general different, because they are defined by expanding

$$\frac{q_1^2}{\overline{D}_1^2 \overline{D}_2^2 \overline{D}_{12}}, \quad \frac{q_2^2}{\overline{D}_1^2 \overline{D}_2^2 \overline{D}_{12}} \quad \text{and} \quad \frac{q_{12}^2}{\overline{D}_1^2 \overline{D}_2^2 \overline{D}_{12}}, \quad (2.70)$$

respectively. In the limiting case $m_{12} = 0$, the FDR defining expansions for the first and for the last integrand are reported in Section 2.1.2, in eq. (2.21) and eq. (2.22), and they are indeed different.

Having different $\mu|_i$ in the numerator implies that they are sensitive to changes of variables. For example, if $q_1 \rightarrow q_1 - q_2$ and $q_2 \rightarrow -q_2$,

$$\int [d^4 q_1][d^4 q_2] \frac{\mu^2|_{12}}{\overline{D}_1^2 \overline{D}_2^2 \overline{D}_{12}} \rightarrow \int [d^4 q_1][d^4 q_2] \frac{\mu^2|_1}{\overline{D}_1 \overline{D}_2^2 \overline{D}_{12}^2}. \quad (2.71)$$

Factorizable two-loop integrals provide easy cases studies. For example, it is easily understood that

$$\int [d^4 q_1] \frac{\mu_1^2}{\overline{D}_1^\alpha} \times \int [d^4 q_1] \frac{1}{\overline{D}_2^\beta} \neq \int [d^4 q_1] \frac{1}{\overline{D}_1^\alpha} \times \int [d^4 q_1] \frac{\mu_2^2}{\overline{D}_2^\beta}, \quad (2.72)$$

unless $\alpha = \beta$ or both $\alpha, \beta \geq 3$. Moreover, even though in general $\mu_{12}^2 \neq \mu_1^2 + \mu_2^2$,

$$\begin{aligned} \int [d^4 q_1][d^4 q_2] \frac{\mu_{12}^2}{\overline{D}_1^\alpha \overline{D}_2^\beta} &= \int [d^4 q_1] \frac{\mu_1^2}{\overline{D}_1^\alpha} \times \int [d^4 q_2] \frac{1}{\overline{D}_2^\beta} \\ &+ \int [d^4 q_1] \frac{1}{\overline{D}_1^\alpha} \times \int [d^4 q_2] \frac{\mu_2^2}{\overline{D}_2^\beta}. \end{aligned} \quad (2.73)$$

where we have used the fact that a rank-1 vacuum integral vanishes. Analogously,

$$\begin{aligned} \int [d^4 q_1][d^4 q_2] \frac{\mu_{12}^4}{\overline{D}_1^\alpha \overline{D}_2^\beta} &= \int [d^4 q_1][d^4 q_2] \frac{\mu_1^4 + \mu_2^4 + 2\mu_1^2 \mu_2^2}{\overline{D}_1^\alpha \overline{D}_2^\beta} \\ &+ \int [d^4 q_1][d^4 q_2] \frac{(\overline{q}_1^2 + \mu_1^2)(\overline{q}_2^2 + \mu_2^2)}{\overline{D}_1^\alpha \overline{D}_2^\beta}. \end{aligned} \quad (2.74)$$

Calculating extra-integrals at two loops

Just like the one-loop case, we can calculate the extra-integrals by considering the finite part of the relevant denominator expansion or *indirectly*, by taking the difference between the original integrand and its vacuum configurations. This second way is usually more convenient, because the original integral does not contribute in the limit $\mu \rightarrow 0$, and we only need to be able to calculate the vacuum content.

There are two global vacua that behave as $1/\mu^2$, such that when multiplied by μ^2 they return a finite contribution (like $1/\overline{q}^6$ at one loop); namely,

$$\int d^n q_1 d^n q_2 \left[\frac{q_1^2 + 2(q_1 \cdot q_2)}{\overline{q}_1^6 \overline{q}_2^4 \overline{q}_{12}^2} \right] \propto \frac{1}{\mu^2}, \quad \int d^n q_1 d^n q_2 \left[\frac{1}{\overline{q}_1^4 \overline{q}_2^4 \overline{q}_{12}^2} \right] \propto \frac{1}{\mu^2}, \quad (2.75)$$

They can be calculated by using the results collected in Section 2.1.7. They

yield

$$\begin{aligned}\mu^2 \int [d^4 q_1][d^4 q_2] \frac{q_1^2 + 2(q_1 \cdot q_2)}{\bar{q}_1^6 \bar{q}_2^4 \bar{q}_{12}^2} &= -\frac{2\pi^4}{3} f - \frac{\pi^4}{2}, \\ \mu^2 \int [d^4 q_1][d^4 q_2] \frac{1}{\bar{q}_1^4 \bar{q}_2^4 \bar{q}_{12}^2} &= -\frac{2\pi^4}{3} f.\end{aligned}\quad (2.76)$$

with f reported in eq. (A.5) of Appendix A.

For example,

$$\begin{aligned}\int [d^4 q_1][d^4 q_2] \frac{\mu^2|_1}{\bar{D}_1^2 \bar{D}_2^2 \bar{q}_{12}^2} &= -\lim_{\mu \rightarrow 0} \mu^2 \left\{ \int d^4 q_1 d^4 q_2 \frac{1}{\bar{q}_1^4 \bar{q}_2^4 \bar{q}_{12}^2} \right. \\ &\quad \left. - i\pi^2 \ln \frac{m_2^2}{\mu^2} \int d^4 q \frac{1}{\bar{q}^6} \right\},\end{aligned}\quad (2.77)$$

which is different with respect to

$$\begin{aligned}\int [d^4 q_1][d^4 q_2] \frac{\mu^2|_{12}}{\bar{D}_1^2 \bar{D}_2^2 \bar{q}_{12}^2} &= -\lim_{\mu \rightarrow 0} \mu^2 \left\{ \int d^4 q_1 d^4 q_2 \frac{1}{\bar{q}_1^4 \bar{q}_2^4 \bar{q}_{12}^2} \right. \\ &\quad \left. - i\pi^2 \left(\ln \frac{m_1^2}{\mu^2} + \ln \frac{m_2^2}{\mu^2} \right) \int d^4 q \frac{1}{\bar{q}^6} \right\}.\end{aligned}\quad (2.78)$$

As expected, in the r.h.s. $\mu|_i^2 = \mu^2$. Notice that a local vacuum as well as a global one contribute: we understand that n -loop extra-integrals are expressed in terms of scalar integrals with less than n loops and constants.

As a last example, consider

$$\int [d^4 q_1][d^4 q_2] \frac{\mu^2|_1}{\bar{D}_1^3 \bar{D}_2 \bar{D}_{12}} = \lim_{\mu \rightarrow 0} \mu^2 \int d^4 q_1 d^4 q_2 \frac{q_1^2 + 2(q_1 \cdot q_2)}{\bar{q}_1^6 \bar{q}_2^4 \bar{q}_{12}^2}, \quad (2.79)$$

where the first of eq. (2.76) was used. All two-loop extra-integrals relevant for the calculations of Chapter 3 can be derived from the last three equations.

FDR and DR

Finally, it is worth saying that at two loops a simple correspondence such that of eq. (2.65), between *extra*-integrals and ϵ -dimensional objects in DR, does not exist.

To show this, let us compare FDR with FDH, a variant of DR. This method [54], equivalent to DRed at one loop, keeps all integration loops in n dimensions, while observed external particles are four-dimensional, so as to preserve supersymmetry. Unobserved internal lines are defined in such a way that the contraction

$$q_\alpha q_\beta g^{\alpha\beta} = (q^{(n)})^2 = (q^{(4)})^2 + \tilde{q}^2 \quad (2.80)$$

gives rise to an n dimensional object when q is an integration momentum, that can be split into a four-dimensional $((q^{(4)})^2)$ and an ϵ -dimensional (\tilde{q}^2) component. If \tilde{q}^2 is identified with $-\mu^2$, there is a formal equivalence – at the integrand level – between the procedures used by FDR and FDH to determine the *extra*-integrals [55,56]. At one loop, this correspondence is complete, as in eq. (2.65). However, at two loops, differences start when integrating, because in FDH, like in any other conventional subtraction scheme, sub-divergences must be compensated by counterterms added at a previous renormalization stage. As a consequence, *extra*-integrals at two loops give different results, when computed in FDR and FDH. For example, if $m_1 = m_2 = m_{12} = m$

$$\int [d^4 q_1][d^4 q_2] \frac{\mu_1^2}{D_1 D_2 D_{12}} = \pi^4 \left(\frac{2}{3} f + \frac{1}{2} \ln \frac{m^2}{\mu^2} \right), \quad (2.81)$$

with f defined in eq. A.5, while

$$\int d^n q_1 d^n q_2 \frac{-\tilde{q}_1^2}{D_1 D_2 D_{12}} = \pi^4 \left(\frac{1}{2\epsilon} - \frac{3}{8} + \frac{1}{2} \left(\ln \frac{m^2}{\mu^2} + \Delta \right) + \mathcal{O}(\epsilon) \right), \quad (2.82)$$

with $\Delta = \gamma_E + \ln \pi$ and $\mu = \mu_R$ in both equations.

2.1.5.3 Internal fermions

When a diagram contains fermion lines, loop momenta appear contracted with Dirac matrices. After performing all summations over free internal indices, the global prescription dictates that also a \not{q} should be *barred*

$$\not{q} \rightarrow \bar{\not{q}} = \not{q} \pm \mu, \quad (2.83)$$

where the sign is chosen accordingly to the position of the \not{q} within the fermionic string. In the one-loop case, one chooses arbitrarily the sign of μ within the first $\bar{\not{q}}$; the sign of the subsequent one is opposite if an even number

of γ -matrices occur between the two \not{q} 's, and it is the same otherwise; that is

$$(\dots \bar{\not{q}} \gamma^{\alpha_1} \dots \gamma^{\alpha_n} \not{q} \dots) = (\dots (\not{q} \pm \mu) \gamma^{\alpha_1} \dots \gamma^{\alpha_n} (\not{q} \mp (-)^n \mu) \dots). \quad (2.84)$$

This rule is sufficient in the presence of one fermion line only, which is the case in all explicit calculations presented in Chapter 3. With two or more lines, and no summation indices among them, each fermion string can be separately treated as described. If sums occur, after applying the above algorithm, extra μ^2 terms need to be extracted according to the following procedure:

$$\begin{aligned} \text{Tr} [\dots \not{q} \Gamma^{(n)} \gamma_\alpha] \text{Tr} [\dots \not{q} \Gamma^{(m)} \gamma^\alpha] &\rightarrow \text{Tr} [\dots \not{q} \Gamma^{(n)} \gamma_\alpha] \text{Tr} [\dots \not{q} \Gamma^{(m)} \gamma^\alpha] \\ &\quad - (-1)^{(n+m)} \mu^2 \text{Tr} [\dots \Gamma^{(n)}] \text{Tr} [\dots \Gamma^{(m)}] \end{aligned} \quad (2.85)$$

where $\Gamma^{(k)}$ represents a string of k gamma matrices. Eq. (2.85) is proven by noticing that n (m) anticommutations are needed to bring \not{q} near γ_α (γ^α) and can easily be checked by taking the traces and substituting $q^2 \rightarrow \bar{q}^2$.

For example,

$$\text{Tr} [(\not{q} + m) \gamma^\alpha (\not{q} + \not{p}_1 + m) (\not{q} + \not{p}_2 + m) \gamma^\beta], \quad (2.86)$$

and its FDR regulated version reads

$$\text{Tr} [(\not{q} + m) \gamma^\alpha (\not{q} + \not{p}_1 + m) (\not{q} + \not{p}_2 + m) \gamma^\beta] + m \mu^2 \text{Tr} [\gamma^\alpha \gamma^\beta]. \quad (2.87)$$

By following these rules, the same results are obtained as if we were computing the trace first and replacing $q^2 \rightarrow \bar{q}^2$ afterwards. In both cases, the reducible numerators are reconstructed properly and can be simplified with the denominator.

Sometimes, when calculating certain amplitudes, it is convenient to replace $\not{q} \rightarrow \bar{\not{q}}$ in the first place, because it allows a trivial proof of the Ward identity at the integrand level (Section 3.3). In practical calculations, however, it is often convenient to fully simplify reducible numerators before computing the loop integrals. In that way, only irreducible tensors appear and extra integrals are just produced by tensor decomposition, as in eq. (2.54). This is the strategy that we adopt in the calculations presented in Chapter 3.

Internal fermions at two loops

The corresponding procedure at two loops is better explained with an example. Consider the trace

$$J^{\alpha\beta} = Tr [\not{q}_1 \gamma^\alpha \not{q}_2 \gamma^\beta \not{q}_1 \not{q}_2] , \quad (2.88)$$

where q_1 and q_2 are the integration momenta. Its FDR counterpart reads

$$\begin{aligned} \bar{J}^{\alpha\beta} = & J^{\alpha\beta} + \mu^2|_1 Tr [\gamma^\alpha \not{q}_2 \gamma^\beta \not{q}_2] - \mu^2|_2 Tr [\not{q}_1 \gamma^\alpha \gamma^\beta \not{q}_1] - 2\tilde{\mu}_{12}^2 Tr [\gamma^\alpha \not{q}_2 \gamma^\beta \not{q}_1] \\ & + Tr [\gamma^\alpha \gamma^\beta] \left(\mu^2|_1 \mu^2|_2 - 2\tilde{\mu}_{12}^4 + 2(q_1 \cdot q_2) \tilde{\mu}_{12}^2 \right) , \end{aligned} \quad (2.89)$$

with

$$\tilde{\mu}_{12}^2 = \frac{1}{2} \left(\mu^2|_{12} - \mu^2|_1 - \mu^2|_2 \right) . \quad (2.90)$$

Eq. (2.89) is obtained from eq. (2.88) by using –one after the other– the one-loop replacements $\not{q}_1 \rightarrow \bar{\not{q}}_1$ and $\not{q}_2 \rightarrow \bar{\not{q}}_2$, which generate the terms proportional to $\mu^2|_1$ and $\mu^2|_2$. The $\tilde{\mu}_{12}^2$ parts originate, instead, from the replacement

$$(q_1 \cdot q_2) = \frac{1}{2} \left(q_{12}^2 - q_1^2 - q_2^2 \right) \rightarrow \frac{1}{2} \left(\bar{q}_{12}^2 - \bar{q}_1^2 - \bar{q}_2^2 \right) , \quad (2.91)$$

and are obtained by simultaneously barring \not{q}_1 and \not{q}_2 in eq. (2.88) (with the same one-loop rule for the sign of $\mu|_i$ inside each \not{q}_i) and subtracting the $\mu^2|_i$ terms already determined. What is left is, by construction, proportional to powers of $\mu|_1 \mu|_2 \equiv \tilde{\mu}_{12}^2$ and gives the remaining terms in eq. (2.89). Once again, taking the trace of $\bar{J}^{\alpha\beta}$ is equivalent to the replacements

$$q_1^2 \rightarrow \bar{q}_1^2, \quad q_2^2 \rightarrow \bar{q}_2^2, \quad (q_1 \cdot q_2) \rightarrow \frac{1}{2} \left(\bar{q}_{12}^2 - \bar{q}_1^2 - \bar{q}_2^2 \right) , \quad (2.92)$$

after computing the original trace $J^{\alpha\beta}$. Thus, the generated $\mu|_i$'s ensure the right simplifications between numerator and denominator.

The chirality matrix γ_5

If chirality matrices are also involved, a gauge invariant treatment [57] requires their anticommutation at the beginning (or the end) of open strings before replacing $\not{q} \rightarrow \bar{\not{q}}$. In the case of closed loops, γ_5 should be put next to the vertex corresponding to a potential non-conserved current. This reproduces the correct coefficient of the triangular anomaly, as observed in [58].

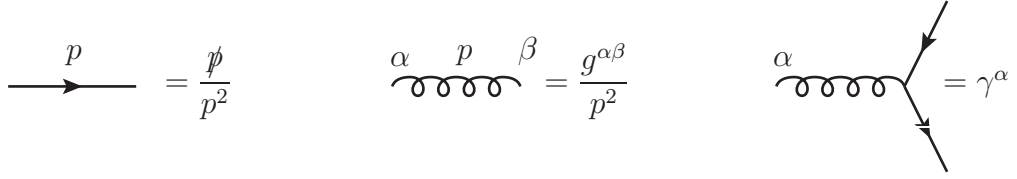


Figure 2.2: Simplified Feynman rules used in the examples of this section.

2.1.6 Sub-integration consistency

A crucial property of multi-loop calculus is the sub-integration consistency, i.e. that calculating the full diagram or inserting the integral of a sub-diagram into the original one must give the same result. In order to fulfill this requirement, the rules of global prescription must be complemented with another set of rules that goes under the name of *sub-prescription*. This topic is not relevant for the calculations performed in this thesis, however it is an essential ingredient of FDR, developed in [59].

With the help of a simple example, we explain why global prescription is not enough to guarantee sub-integration consistency, and we construct a solution to this issue. Consider

$$= \int [d^4 q_1][d^4 q_2] \frac{N(q_1, q_2)}{\bar{q}_1^2 \bar{q}_2^2 \bar{D}_1 \bar{D}_2 \bar{D}_{12}} \quad (2.93)$$

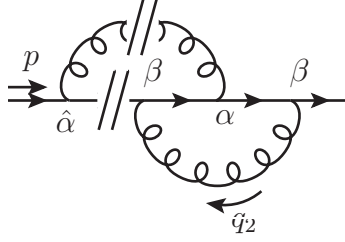
with $\bar{D}_i = (q_i + p)^2 - \mu^2 - M^2$, where we have used the simplified Feynman rules of fig. 2.2, in order to only concentrate on the interesting pieces of the calculation, and

$$N(q_1, q_2) = \gamma_\beta(\not{q}_2 + \not{p})\gamma_\alpha(\not{q}_{12} + \not{p})\gamma^\beta(\not{q}_1 + \not{p})\gamma^\alpha. \quad (2.94)$$

No promotion $q_i^2 \rightarrow \bar{q}_i^2$ has been performed yet in the numerator. We now want to show that, if we perform the global prescription on $N(q_1, q_2)$ and

integrate the resulting two-loop FDR integral, we do not obtain the same result that we would get if we were to consider the two one-loop sub-diagrams separately first.

Let us concentrate on the sub-integration in q_2 . The diagram in eq. (2.93) can be “cut” so as to emphasize the sub-diagram with loop momentum q_2 ,



where we have indicated with $\hat{\alpha}$ the Lorentz index that does not belong to the sub-diagram. Let's extract from $N(q_1, q_2)$ the terms in which two \not{q}_2 appear, i.e. the part which is modified by the promotion $q_2^2 \rightarrow \bar{q}_2^2$, that is

$$N_2(q_2) = \gamma_\beta \not{q}_2 \gamma_\alpha \not{q}_2 \gamma^\beta (\not{q}_1 + \not{p}) \gamma^{\hat{\alpha}}, \quad (2.95)$$

where $\gamma^{\hat{\alpha}}$ refers to the vertex external to the sub-diagram, but the usual identities hold, e.g. $\gamma_\alpha \gamma^{\hat{\alpha}} = 4$. By performing some algebra we can rewrite N_2 in such a way that all \not{q}_2 sit next to each other in the string of Dirac matrices:

$$N_2(q_2) = -8q_2 \cdot (q_1 + p) \hat{\not{q}}_2 + 4(\not{q}_1 + \not{p}) (\hat{\not{q}}_2 \not{q}_2 - \not{q}_2 \hat{\not{q}}_2) \quad (2.96)$$

where, following the usual notation, $\hat{\not{q}}_2 = q_2^\alpha \gamma_\alpha$. A standard global prescription, since it makes no distinction between \not{q}_2 and $\hat{\not{q}}_2$, doesn't generate any new term, i.e.

$$N_2(q_2) \rightarrow \bar{N}_2(q_2) = N_2(q_2). \quad (2.97)$$

Now, let's consider $N_2(q_2)$ as the numerator of an independent one-loop integral, i.e.

$$\int [d^4 q_2] \frac{N_2(q_2)}{\bar{q}_2^2 \bar{D}_2 \bar{D}_{12}}, \quad (2.98)$$

where q_1 is now interpreted as an external momentum. The one-loop global prescription (i.e. the sub-prescription in this context) dictates that

$$\begin{aligned} N_2(q_2) \rightarrow \hat{N}_2(q_2) &= \left[\gamma_\beta (\not{q}_2 + \hat{\mu}|_2) \gamma_\alpha (\not{q}_2 + \hat{\mu}|_2) \gamma^\beta \right] (\not{q}_1 + \not{p}) \gamma^{\hat{\alpha}} \\ &= N_2(q_2) + \hat{\mu}|_2^2 4(\not{q}_1 + \not{p}). \end{aligned} \quad (2.99)$$

where we have effectively ignored the presence of γ^α , as it does not belong to the sub-diagram. The mismatch between the results obtained via standard global prescription and by imposing sub-integration consistency is a new type of FDR integral called *extra-extra-integral*,

$$I = 4 \int [d^4 q_1] \frac{\not{q}_1 + \not{p}}{\bar{q}_1^2 \bar{D}_1} \int [d^4 q_2] \frac{\hat{\mu}|_2^2}{\bar{q}_2^2 \bar{D}_2 \bar{D}_{12}}. \quad (2.100)$$

The hat over $\hat{\mu}|_2^2$ reminds that it was extracted by considering the sub-diagram with loop momentum q_2 on its own; correspondingly, the FDR expansion should be performed as if it belonged to a one-loop integral, as explained in Section 2.1.6.1. The same extra-extra integral I we would have obtained from eq. (2.96) if we had distinguished \not{q}_2 and $\hat{\not{q}}_2$, by promoting $q_2^2 \rightarrow q^2 - \hat{\mu}|_2^2$ only in $\not{q}_2 \not{q}_2$ and not in $\hat{\not{q}}_2 \not{q}_2$.

To summarize, the correct result is obtained by subtracting the extra-extra integrals coming from the global prescription on N_2 , zero in this case, i.e.

$$-(\bar{N}_2 - N_2),$$

and adding back the extra-extra-integrals coming from the sub-prescription,

$$+(\hat{N}_2 - N_2).$$

Because the diagram is symmetric under the exchange $q_1 \leftrightarrow q_2$, exactly the same contribution is obtained from the sub-diagram with loop momentum q_1 . Therefore, eq. (2.93) must be replaced by

$$\int [d^4 q_1][d^4 q_2] \frac{\bar{N}(q_1, q_2)}{\bar{q}_1^2 \bar{q}_2^2 \bar{D}_1 \bar{D}_2 \bar{D}_{12}} + 2I. \quad (2.101)$$

Finally notice that if $N_2(q_2)$ didn't generate a divergent one-loop integral, that of eq. (2.1.6), we would have that both $\bar{N}_2 = \hat{N}_2 = N_2$. This case, somehow trivial, is that of the gluonic corrections to $H \rightarrow \gamma\gamma$ which we calculate in Section 3.2.

Let's generalize what learnt with this example. After carrying out the *global prescription*, which might generate *extra integrals*, one must also perform the *sub-prescription* on each sub-diagram, which in turn might generate

extra-extra integrals. Schematically, at two loops, the numerator is modified according to

$$N(q_1, q_2) \rightarrow \underbrace{\overline{N}(q_1, q_2; \mu|_1^2, \mu|_2^2)}_{\text{global prescription}} + \sum_{i=1}^2 \underbrace{\left(\widehat{N}_i(q_i; \hat{\mu}|_i^2) - \overline{N}_i(q_i; \hat{\mu}|_i^2) \right)}_{\text{sub-prescription}} \quad (2.102)$$

where \overline{N}_i is obtained by promoting all q_i^2 in N_i , while in \widehat{N}_i we only promote the q_i^2 obtained by contracting indices that are internal to that specific sub-diagram; it is thus mandatory to know the topology of the diagram in order to calculate its FDR integrals. For both \overline{N}_i and \widehat{N}_i the promotion is

$$q_i^2 \rightarrow q_i^2 - \hat{\mu}|_i^2 \neq \overline{q}_i^2, \quad (2.103)$$

so that the mismatch $\widehat{N}_i - \overline{N}_i$ is always an extra-extra integral; as mentioned above, this means that the FDR defining expansion to be brought about in order to calculate it is that of a one-loop integral, as explained in Section 2.1.6.1.

The formula of eq. (2.102) applies to all two-loop calculations, and we expect that a generalization to higher loop diagrams will lead to an iterative version of the same formula. Indeed, sub-integration consistency is a fundamental property that must be always encoded in the definition of a multi-loop integral. Contingently, no sub-prescription was necessary in the calculations of Chapter 3.

2.1.6.1 Extra-extra integrals

Extra-extra integrals, appearing only in multi-loop calculations, are one-loop extra-integrals multiplied by a loop integral, like that of eq. (2.100). Pursuing this example, the sub-integral in q_2 must be computed as if it was a one-loop integral by itself, i.e.

$$\int [d^4 q_2] \frac{\hat{\mu}|_2^2}{\overline{q}_2^2 \overline{D}_2 \overline{D}_{12}} = - \int [d^4 q_2] \frac{\hat{\mu}|_2^2}{\overline{q}_2^6} = \frac{i\pi^2}{2} \quad (2.104)$$

where we have used the technique for calculating extra-integrals explained in Section 2.1.5.1, i.e. by taking minus the vacuum part. Inserting it back into eq. (2.100), we obtain that

$$I = 4 \int [d^4 q_1] \frac{\not{q}_1 + \not{p}}{\overline{q}_1^2 \overline{D}_1} \int [d^4 q_2] \frac{\hat{\mu}|_2^2}{\overline{q}_2^2 \overline{D}_2 \overline{D}_{12}} = 2i\pi^2 \int [d^4 q_1] \frac{\not{q}_1 + \not{p}}{\overline{q}_1^2 \overline{D}_1}, \quad (2.105)$$

which is a normal FDR integral.

Extra-extra integrals are not extra integrals: if we were to replace $\hat{\mu}|_2^2$ with $\mu|_2^2$ in I , we would obtain a different result, because we would use a different FDR expansion.

2.1.6.2 FDR vs FDH

FDH [60, 61] is a variant of DR in which all objects external to a loop integral are four-dimensional, in particular $\gamma_\mu \gamma^\mu = 4$. Recently [62] it has been shown that this method, effective in purely gluonic QCD, breaks unitarity in presence of external quarks. Without the sub-prescription, FDR would fall in the same mistake, hence suggesting that the illness affecting FDH could be cured by the same remedy, as an alternative to the mechanisms proposed so far [63, 64].

2.1.7 Master integrals in FDR

There is nothing peculiar in the calculation of FDR integrals after the defining expansion is performed and vacuum configurations are dropped. All available techniques for integral manipulations are applicable, e.g. the Passarino-Veltman reduction (Section 2.1.8.2) or integration-by-parts identities (Section 2.1.8.3). Moreover master integrals known in a different scheme can be translated into FDR with the small additional effort amounting to the calculation of the vacuum configurations. Finally since everything is four dimensional it is worth noticing that FDR opens up the option of numerical integration over loop momenta.

In this section, we collect some observations about the analytic calculation of FDR integrals, and we report the explicit result of some simple FDR integrals, at one and two loops, in order to have some ready-at-hand examples to use in the rest of the chapter, and to collect the building blocks that are needed in the calculations of Chapter 3.

2.1.7.1 One-loop integrals

At one loop there exists a one-to-one relationship between integrals calculated in FDR and DR, realized by the replacement

$$\ln \mu \rightarrow \ln \mu - \frac{1}{\epsilon} - \frac{\Delta}{2}, \quad \Delta \equiv \gamma_E + \ln \pi. \quad (2.106)$$

As we will see in more detail in Section 2.2.2, this means that an amplitude calculated in FDR is equivalent to the same amplitude calculated in DRed within the $\overline{\text{MS}}$ scheme of renormalization.

The last equation is easily understood by looking at eq. (2.10). In the one-loop version, it is trivially show that $J(q)$ and $J_{INF}(q)$ have the same pole structure and the same universal constants. In addition, DRed considers all external objects to be four-dimensional, so that in both schemes $g^{\alpha\beta}g_{\alpha\beta} = \gamma^\alpha\gamma_\alpha = 4$.

For example,

$$\int \frac{d^n q}{\mu^\epsilon} \frac{1}{(q^2 - M^2)^2} = -i\pi^2 \left(\ln \frac{M^2}{\mu^2} + \frac{2}{\epsilon} + \Delta \right) \leftrightarrow \int [d^4 q] \frac{1}{\overline{D}^2} = -i\pi^2 \ln \frac{M^2}{\mu^2}.$$

Notice that, in order to translate a DR one-loop integral to FDR, we don't need to know the full exact result in DR, only its Laurent expansion up to $\mathcal{O}(\epsilon^0)$.

Every one-loop integral free of momentum scales, i.e. a *vacuum integral*, can be derived from the basic integral of $1/\overline{D}$ with $\overline{D} = \overline{q}^2 - M^2$, by means of integration by parts; that is

$$\int [d^4 q] \frac{1}{\overline{D}^{n+1}} = \frac{1}{\Gamma(n+1)} \frac{d^n}{d(M^2)^n} \left(\int [d^4 q] \frac{1}{\overline{D}} \right), \quad (2.107)$$

where

$$\int [d^4 q] \frac{1}{\overline{D}} = -i\pi^2 M^2 \left(\ln \frac{M^2}{\mu^2} - 1 \right). \quad (2.108)$$

Integrals of this type will be frequently used as examples in the following.

2.1.7.2 Two-loop integrals

We refer to the notation introduced in Section 2.1.2.1. Recall that only vacuum integrals are considered at two loops, as they are the relevant ones for the purposes of this thesis. Apart from integrals of the type of eq. (2.12), also factorizable two-loop integrals may contribute, i.e. products of two one-loop integrals, for which we use the notation

$$[\alpha m_1 | \beta m_2] = \int \frac{[d^4 q_1]}{(\overline{q}_1^2 - m_1)^\alpha} \times \int \frac{[d^4 q_2]}{(\overline{q}_2^2 - m_2)^\beta}. \quad (2.109)$$

Thanks to the fact that local vacua are fully subtracted in FDR, a factorizable integral is just the product of the FDR integrals of its factors. This is a general statement, valid to all orders: *(n - 1)-loop integrals can be directly used in calculations at n loops.*

On the contrary, in DR, if any of the two integrals of eq. (2.109) were UV-divergent, we would have to Laurent-expand the other one up to $\mathcal{O}(\epsilon)$ in order to comprise terms arising from the product ϵ/ϵ . This is not always trivial: often an involved integral is more easily calculated by exploiting the limit $\epsilon \rightarrow 0$ before integration; by doing so however the $\mathcal{O}(\epsilon)$ information would be lost and the result could not be used in a DR calculation at higher orders.

As an explicit example, consider

$$\int [d^4q] \frac{1}{\overline{D}^2} \times \int [d^4q] \frac{1}{\overline{D}^3} = \left(-i\pi^2 \ln \frac{M^2}{\mu^2} \right) \times \left(\frac{i\pi^2}{2M^2} \right) = -\frac{\pi^4}{2M^2} \ln \frac{M^2}{\mu^2}. \quad (2.110)$$

with $\overline{D} = \overline{q}^2 - M^2$. The same calculation in DR yields

$$\int \frac{d^n q_1 d^n q_2}{\mu^{2\epsilon}} \frac{1}{(q_1^2 - M^2)^2 (q_2^2 - M^2)^3} = -\frac{\pi^4}{M^2} \left(\ln \frac{M^2}{\mu^2} + \frac{1}{\epsilon} + \Delta \right). \quad (2.111)$$

where we have used

$$\int \frac{d^n q}{\mu^\epsilon} \frac{1}{(q^2 - M^2)^3} = \frac{i\pi^2}{2M^2} \left[1 + \frac{\epsilon}{2} \left(\ln \frac{M^2}{\mu^2} + \Delta \right) \right]. \quad (2.112)$$

Notice that the coefficients of $\ln(M^2/\mu^2)$ in eq. (2.110) and eq. (2.111) is not the same. Indeed, beyond one loop, the one-to-one correspondence between DR and FDR is broken. This is because in DR one is forced to retain unphysical finite parts, originated by ϵ/ϵ terms, that eventually cancel out in full result, just like the poles do. In this sense, we can say that FDR provides a shortcut to the physical answer, by automatically avoiding the spurious terms ϵ/ϵ .

Vacuum integrals at two loops

All vacuum integrals at two loops can be obtained by deriving with respect to the mass parameters one basic integral, i.e.

$$[\alpha m_1 | \beta m_2 | m_{12}] = \frac{1}{\Gamma(\alpha)\Gamma(\beta)} \frac{d^{\alpha-2} d^{\beta-1}}{d(m_1^2)^{\alpha-2} d(m_2^2)^{\beta-1}} [2m_1 | m_2 | m_{12}]. \quad (2.113)$$

One can prove that

$$[2m_1 | m_2 | m_{12}] = \pi^4 \left\{ \ln \frac{m_1^2}{\mu^2} - \frac{1}{2} \ln^2 \frac{m_1^2}{\mu^2} - f(a, b) + f \right\}, \quad (2.114)$$

where,

$$a = \frac{m_2^2}{m_1^2}, \quad b = \frac{m_{12}^2}{m_1^2}, \quad (2.115)$$

$f(a, b)$ is independent of μ and symmetric under the exchange of its arguments, and $f = f(1, 1)$ is a constant. Eq. (2.114) is derived in Appendix A, where also the function $f(a, b)$ is defined. In short, after determining the FDR defining expansion of the integrand, for example by deriving eq. (2.17) with respect to m_1 , one can either directly integrate the finite part, or use the known DR results in eq. (2.10). For completeness, we report here the expression for $[2m_1 | m_2 | m_{12}]$ calculated in DR [65]:

$$[2m_1 | m_2 | m_{12}] \Big|_{DR} = \pi^4 \left\{ -\frac{1}{\epsilon^2} - \left(\frac{1}{\epsilon} + \log \frac{m_1^2}{\mu^2} + \Delta \right)^2 + \frac{1}{\epsilon} + \log \frac{m_1^2}{\mu^2} + \Delta - \frac{1}{2} - \frac{\pi^2}{12} - f(a, b) \right\}. \quad (2.116)$$

Notice once again that at two loops the one-to-one correspondence between DR and FDR is lost and it is no longer true that FDR integrals are obtained from DR ones after subtracting poles and universal constants.

2.1.8 Tensorial reduction

As we have seen with the simple example of eq. (2.54), tensorial reduction might cause the appearance of extra-integrals. This happens, for example, whenever a pair $q^\alpha q^\beta$ in the numerator is contracted into q^2 , and then replaced by $\bar{q}^2 + \mu^2$. Notice that if this contraction happens within the integrand, for example because of a Feynman rule, q^2 is promoted to \bar{q}^2 with no subsequent appearance of extra μ^2 , by means of the global prescription. Tensorial reduction, on the contrary, always exploits the properties of the *integral* rather than those of the *integrand*s: it takes place after all the operations that define the FDR integral.

All reduction methods that were developed for DR can be used in FDR. The presence of the extra-integrals insures that also the constants arising from a tensorial reduction are fully reconstructed.

At one-loop, a commonly used technique is the Passarino-Veltman (PV) reduction [7], which we present in some detail in the next section. Other methods can be used as well, such as the OPP approach [16]. The basic observation is that any algebraic manipulation of the integrand is legal in FDR, the only subtlety being the replacement $q^2 = \bar{q}^2 + \mu^2$ in the numerator, which may generate a rational part ($R2$ in the OPP language). However, thanks to the correspondence in eq. (2.65), this contribution can be reinserted back -in an OPP like reduction of the FDR integrals- by using the same set of effective Feynman rules computed in DR [66,67], or with the technique described in [68].

At two-loops there is no one established method to perform a full tensorial reduction. In the practical calculation presented in Section 3.2, only vacuum integrals at two loops appear; we discuss how to treat this limiting case in the next section. Moreover, many techniques for determining master-integrals at two loops are based on IBP identities in n dimensions: in [69] it was shown that it is possible, within FDR, to construct a four-dimensional version of these identities, thereby opening the possibility of extending and probably simplifying some of the existing algorithms.

2.1.8.1 Tensorial reduction of vacuum integrals

In absence of external momenta, odd ranked tensors vanish, so that the structures generating extra-integrals are, up to rank 4,

$$\begin{aligned} q_i^\mu q_j^\nu &\rightarrow \frac{(q_i \cdot q_j)}{4} g^{\mu\nu}, \\ q^\mu q^\nu q^\rho q^\sigma &\rightarrow \frac{q^4}{24} g^{\mu\nu\rho\sigma} \quad \text{at one loop,} \\ q_m^\mu q_n^\nu q_r^\rho q_s^\sigma &\rightarrow \frac{1}{72} \left(A_{mnr s}^{\mu\nu\rho\sigma} + A_{mrns}^{\mu\rho\nu\sigma} + A_{msnr}^{\mu\sigma\nu\rho} \right) \quad \text{at two loops,} \end{aligned} \quad (2.117)$$

where $g^{\mu\nu\rho\sigma}$ is the totally symmetric rank-4 tensor, and

$$\begin{aligned} A_{mnr s}^{\mu\nu\rho\sigma} = &\left(5(q_m \cdot q_n)(q_r \cdot q_s) - (q_m \cdot q_r)(q_n \cdot q_s) \right. \\ &\left. - (q_m \cdot q_s)(q_n \cdot q_r) \right) g^{\mu\nu} g^{\rho\sigma}. \end{aligned} \quad (2.118)$$

Denominators can then be reconstructed by rewriting

$$\begin{aligned} q_1^2 &= \bar{q}_1^2 + \mu^2|_1, & q_2^2 &= \bar{q}_2^2 + \mu^2|_2, \\ 2(q_1 \cdot q_2) &= \bar{q}_{12}^2 - \bar{q}_1^2 - \bar{q}_2^2 + \mu^2|_{12} - \mu^2|_1 - \mu^2|_2. \end{aligned} \quad (2.119)$$

During this tensor decomposition, the $\mu^2|_1$, $\mu^2|_2$, $\mu^2|_{12}$ terms are kept only when they generate a non zero contribution. This means that they should be power-counted as the corresponding squared loop momenta, and contribute only if the integral is divergent, as explained in Section 2.1.5.1.

2.1.8.2 Passarino-Veltman reduction in FDR

The main asset of the PV reduction method [7] is that it provides a gauge-invariant decomposition of the amplitude: after the reduction, the full amplitude is expressed in terms of scalar integrals depending on physical thresholds only -multiplied by gauge independent coefficients- plus a rational part.

In this section we review the PV reduction method within FDR. For simplicity, we explicitly work out the decomposition of a rank-2 bubble. In the very same way higher-rank tensors with more denominators can be decomposed, although, for brevity, we do not report any other result.

The integral

$$B^{\mu\nu} = \int [d^4q] \frac{q^\mu q^\nu}{D_0 D_1}, \quad (2.120)$$

can be decomposed in terms of rank-2 symmetric tensors depending on $p \equiv p_1$:

$$B^{\mu\nu} = B_{00} g^{\mu\nu} + B_{11} p^\mu p^\nu, \quad (2.121)$$

where each scalar coefficient B_{ii} depends on M_0^2 , M_1^2 and p^2 . By contracting both sides with $g_{\mu\nu}$ and $p_\mu p_\nu$, we obtain a system of equations from which B_{00} and B_{11} can be extracted:

$$\begin{cases} g_{\mu\nu} B^{\mu\nu} = 4B_{00} + p^2 B_{11} \\ p_\mu p_\nu B^{\mu\nu} = p^2 (B_{00} + p^2 B_{11}) \end{cases}. \quad (2.122)$$

With the usual algebraic manipulations we can express the left hand sides of eq. (2.122) in terms of scalar integrals with 1 or 2 internal legs. Special care should be paid when contracting $B^{\mu\nu}$ with the metric tensor; indeed,

$$g_{\mu\nu} B^{\mu\nu} = \int [d^4q] \frac{q^2}{D_0 D_1} = \int [d^4q] \frac{\bar{q}^2 + \mu^2}{D_0 D_1}. \quad (2.123)$$

\bar{q}^2 takes part in the usual simplifications between numerator and denominator,

$$g_{\mu\nu} B^{\mu\nu} = A_0(M_1^2) + M_0^2 B_0(p^2; M_0^2, M_1^2) + \int [d^4q] \frac{\mu^2}{\bar{D}_0 \bar{D}_1}, \quad (2.124)$$

while a μ^2 is left out. A_0 and B_0 are respectively the scalar tadpole and scalar bubble,

$$A_0(M_1^2) = \int [d^4q] \frac{1}{\bar{D}_1}, \quad B_0(p^2; M_0^2, M_1^2) = \int [d^4q] \frac{1}{\bar{D}_0 \bar{D}_1}. \quad (2.125)$$

Following the logic of Section 2.1.5.1, the last integral in eq. (2.124) is calculated by determining its vacuum configurations,

$$\left[\frac{\mu^2}{\bar{D}_0 \bar{D}_1} \right]_V = \mu^2 \left(\frac{1}{\bar{q}^4} + \frac{d_0 + d_1}{\bar{q}^6} + 4 \frac{(q \cdot p)^2}{\bar{q}^8} \right), \quad (2.126)$$

yielding

$$\begin{aligned} \int [d^4q] \frac{\mu^2}{\bar{D}_0 \bar{D}_1} &= - \lim_{\mu \rightarrow 0} \int d^4q \mu^2 \left\{ \frac{d_0 + d_1}{\bar{q}^6} + 4 \frac{(q \cdot p)^2}{\bar{q}^8} \right\} \\ &= \frac{i\pi^2}{2} \left(M_0^2 + M_1^2 - \frac{p^2}{3} \right). \end{aligned} \quad (2.127)$$

By solving the system in eq. (2.122), we finally obtain

$$\begin{aligned} B_{00} &= -\frac{i\pi^2}{6} \left(\frac{p^2}{3} - \Delta_+ \right) + \frac{A_0(M_0^2)[p^2 - \Delta_-] + A_0(M_1^2)[p^2 + \Delta_-]}{12 p^2} \\ &\quad - \frac{B_0(p^2; M_0^2, M_1^2)[p^4 - 2p^2 \Delta_+ + \Delta_-^2]}{12 p^2}, \\ B_{11} &= \frac{i\pi^2}{6 p^2} \left(\frac{p^2}{3} - \Delta_+ \right) + \frac{-A_0(M_0^2)[p^2 - \Delta_-] + A_0(M_1^2)[2p^2 - \Delta_-]}{3 p^4} \\ &\quad + \frac{B_0(p^2; M_0^2, M_1^2)[(p^2 - \Delta_-)^2 - p^2 M_0^2]}{3 p^4}, \end{aligned} \quad (2.128)$$

where

$$\Delta_{\pm} = M_1^2 \pm M_0^2. \quad (2.129)$$

This result is consistent with that obtained with the standard PV reduction in DR.

There is a one-to-one relationship between any PV equation in FDR and DR, which means that an algorithm that was made up in one method is easily extended to the other.

Up to rank three, the transition rules are here summarized:

$$\begin{aligned}
\epsilon B_{00} &\leftrightarrow - \int [d^4q] \frac{\mu^2}{\overline{D_0 D_1}}, \\
\epsilon p^2 B_{00i} &\leftrightarrow - \int [d^4q] \frac{\mu^2 (q \cdot p_1)}{\overline{D_0 D_1}}, \\
\epsilon C_{00} &\leftrightarrow - \int [d^4q] \frac{\mu^2}{\overline{D_0 D_1 D_2}}, \\
\epsilon \sum_{i=1}^2 (k_i \cdot k_a) C_{00i} &\leftrightarrow - \int [d^4q] \frac{\mu^2 (q \cdot k_a)}{\overline{D_0 D_1 D_2}}, \tag{2.130}
\end{aligned}$$

where

$$\begin{aligned}
B^{\alpha\beta\gamma} &= g^{\{\alpha\beta p_1^\gamma\}} B_{001} + p_1^\alpha p_1^\beta p_1^\gamma B_{111} \\
C^{\alpha\beta} &= g^{\alpha\beta} C_{00} + \sum_{i,j=1}^2 k_i^\alpha k_j^\beta C_{ij} \\
C^{\alpha\beta\gamma} &= \sum_{i=1}^2 g^{\{\alpha\beta k_i^\gamma\}} C_{00i} + \sum_{i,j,l=1}^2 k_i^\alpha k_j^\beta k_l^\gamma C_{ijl}, \\
\text{with } k_a &= \sum_{i=1}^a p_i, \quad \text{and } g^{\{\alpha\beta k_i^\gamma\}} = g^{\alpha\beta} k_i^\gamma + g^{\alpha\gamma} k_i^\beta + g^{\beta\gamma} k_i^\alpha. \tag{2.131}
\end{aligned}$$

As far as boxes up to rank-3 are concerned, no transition rule is necessary as they are UV-convergent integrals, and their expressions are not dependent on any regularization scheme.

2.1.8.3 Integration by parts identities

Many techniques for determining the master-integrals at two loops are based on IBP identities in n dimensions. In [69] it was shown that it is possible, within FDR, to construct a four-dimensional version of these identities,

thereby opening the possibility of extending and probably simplifying the existing algorithms.

In DR, IBP identities are based on the fact that shift-invariant integration is the reverse of differentiation, and that surface terms never contribute when an integral is evaluated in n dimensions. Given a function $J^\alpha(q_1, \dots, q_\ell)$, where α is a Lorentz index, one has that

$$0 = \int d^n q_1 \dots d^n q_\ell \frac{\partial}{\partial q_i^\alpha} J^\alpha(q_1, \dots, q_\ell) = \sum_{r=1}^s \int d^n q_1 \dots d^n q_\ell J_r^\alpha(n; q_1, \dots, q_\ell), \quad (2.132)$$

where the second identity simply accounts for the fact that the derivative of J^α returns a sum of terms. i.e.

$$\frac{\partial}{\partial q_i^\alpha} J^\alpha(q_1, \dots, q_\ell) = \sum_{r=1}^s J_r^\alpha(n; q_1, \dots, q_\ell), \quad (2.133)$$

with $\partial q_i^\alpha / \partial q_i^\alpha = n$. Eq. (2.132) establishes a relationship between the integrals of the different $J_r^\alpha(n; q_1, \dots, q_\ell)$, which can be exploited in their evaluation.

In FDR, integration is not the inverse of differentiation, and $\partial q_i^\alpha / \partial q_i^\alpha = 4$. For these reasons, none of the equalities of eq. (2.132) can be translated straightforwardly. Still, it can be shown that

$$0 = \int [d^4 q_1] \dots [d^4 q_\ell] \frac{\partial}{\partial q_i^\alpha} J^\alpha(q_1, \dots, q_\ell) = \sum_{r=1}^s \int [d^4 q_1] \dots [d^4 q_\ell] J_r^\alpha(4; q_1, \dots, q_\ell). \quad (2.134)$$

The first equality can be inherited by the four-dimensional integral of the finite part of J^α . Indeed, $J^\alpha(q_1, \dots, q_\ell) = J_{INF}^\alpha(q_1, \dots, q_\ell) + J_F^\alpha(q_1, \dots, q_\ell)$ so that

$$\int [d^4 q_1] \dots [d^4 q_\ell] \frac{\partial}{\partial q_i^\alpha} J^\alpha(q_1, \dots, q_\ell) \equiv \lim_{\mu \rightarrow 0} \int d^4 q_1 \dots d^4 q_\ell \frac{\partial}{\partial q_i^\alpha} J_F^\alpha(q_1, \dots, q_\ell) = 0 \quad (2.135)$$

because it is the integral of a total derivative in four dimensions. The proof of the second equality of eq. (2.134) is less trivial; in the following we illustrate how it works on a simple one-loop example.

Consider

$$J^\alpha(q) = \frac{q^\alpha}{D_0 D_1}$$

whose derivative, in n dimensions, reads

$$\frac{\partial}{\partial q^\alpha} \frac{q^\alpha}{D_0 D_1} = \frac{n}{D_0 D_1} - 2 \frac{q^2}{D_0^2 D_1} - 2 \frac{q^2 + (q \cdot p)}{D_0 D_1^2}. \quad (2.136)$$

Then, the IBP identity in DR is given by

$$0 = n \int d^n q \frac{1}{D_0 D_1} - 2 \int d^n q \frac{q^2}{D_0^2 D_1} - 2 \int d^n q \frac{q^2 + (q \cdot p)}{D_0 D_1^2}. \quad (2.137)$$

In FDR, one always starts from the defining expansion; in this case

$$\frac{q^\alpha}{\overline{D}_0 \overline{D}_1} = \left[\frac{q^\alpha}{\overline{q}^4} \right] + q^\alpha \left(\frac{d_1}{\overline{q}^4 \overline{D}_1} + \frac{M^2}{\overline{q}^2 \overline{D}_0 \overline{D}_1} \right), \quad (2.138)$$

where $d_1 = M^2 - p^2 - 2(q \cdot p)$. According to the reasoning of eq. (2.135), the FDR integral of the total derivative of $q^\alpha / (\overline{D}_0 \overline{D}_1)$ vanishes. We now concentrate on the second equality of eq. (2.134), i.e. we want to prove that

$$\int [d^4 q] \frac{\partial}{\partial q^\alpha} \frac{q^\alpha}{\overline{D}_0 \overline{D}_1} = \int [d^4 q] \frac{4}{\overline{D}_0 \overline{D}_1} - \int [d^4 q] \frac{2q^2}{\overline{D}_0^2 \overline{D}_1} - 2 \int [d^4 q] \frac{q^2 + (q \cdot p)}{\overline{D}_0 \overline{D}_1^2}, \quad (2.139)$$

where we have used eq. (2.136) with $n = 4$. Ultimately, this is true because of the distributive property of the FDR integral, which in turn is a direct consequence of shift invariance and the global prescription: it is legal, in FDR, to manipulate the integrand before evaluating the integral. Let's take the time to unveil this mechanism explicitly for this case.

Instead of taking the four-dimensional integral of the finite part, let's write the FDR integral as a difference of DR integrals, as in eq. (2.10), that is

$$0 = \int [d^4 q] \frac{\partial}{\partial q^\alpha} \frac{q^\alpha}{\overline{D}_0 \overline{D}_1} \equiv \lim_{\mu \rightarrow 0} \left(\int d^n q \frac{\partial}{\partial q^\alpha} \frac{q^\alpha}{D_0 D_1} - \int d^n q \frac{\partial}{\partial q^\alpha} \left[\frac{q^\alpha}{\overline{D}_0 \overline{D}_1} \right] \right) \quad (2.140)$$

By doing so, if we insert the n -dimensional derivatives, i.e. eq. (2.136) and

$$\frac{\partial}{\partial q^\alpha} \left[\frac{q^\alpha}{\overline{D}_0 \overline{D}_1} \right] = \left[\frac{n}{\overline{q}^4} \right] - \left[\frac{4q^2}{\overline{q}^6} \right], \quad (2.141)$$

we can rewrite the r.h.s. of eq. (2.140) as

$$\lim_{\mu \rightarrow 0} \int d^n q \left(\frac{n}{D_0 D_1} - 2 \frac{q^2}{D_0^2 D_1} - 2 \frac{q^2 + (q \cdot p)}{D_0 D_1^2} - \left[\frac{n}{\overline{q}^4} \right] + \left[\frac{4q^2}{\overline{q}^6} \right] \right). \quad (2.142)$$

From this expression it is possible to reconstruct the r.h.s of eq. (2.139), because the last two terms in squared brackets can be interpreted as the vacuum configurations of the first three terms. Indeed,

$$\lim_{\mu \rightarrow 0} \int d^n q \left\{ \left(\frac{n}{D_0 D_1} - \left[\frac{n}{\bar{q}^4} \right] \right) - \left(\frac{2q^2}{D_0^2 D_1} - \left[\frac{2q^2}{\bar{q}^6} \right] \right) - \left(\frac{2q^2}{D_0 D_1^2} - \left[\frac{2q^2}{\bar{q}^6} \right] \right) - 2 \frac{(q \cdot p)}{D_0 D_1^2} \right\} = \int [d^4 q] \frac{4}{\bar{D}_0 \bar{D}_1} - \int [d^4 q] \frac{2q^2}{\bar{D}_0^2 \bar{D}_1} - 2 \int [d^4 q] \frac{q^2 + (q \cdot p)}{\bar{D}_0 \bar{D}_1^2} \quad (2.143)$$

where we have put $n = 4$ because the difference of $n/(\bar{D}_0 \bar{D}_1)$ and its vacuum is finite. Together with eq. (2.140), this verifies the IBP identity in FDR, i.e. that

$$0 = \int [d^4 q] \frac{4}{\bar{D}_0 \bar{D}_1} - \int [d^4 q] \frac{2q^2}{\bar{D}_0^2 \bar{D}_1} - 2 \int [d^4 q] \frac{q^2 + (q \cdot p)}{\bar{D}_0 \bar{D}_1^2}. \quad (2.144)$$

Following the same logic, in [69], it is shown that this is always possible, thereby proving explicitly eq. (2.134).

2.1.9 Infrared infinities

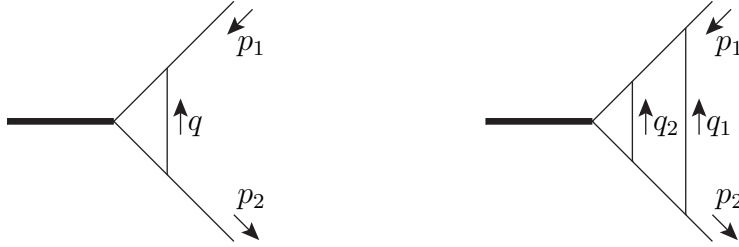


Figure 2.3: Examples of massless one-loop and two-loop scalar integrals. Thin lines represent massless scalar propagators and $p_1^2 = p_2^2 = 0$.

The definition in eq. (2.9) can be maintained also in the presence of IR singularities. For instance, the FDR versions of the massless scalar one- and

two-loop integrals in figure 2.3 read

$$\int [d^4 q] J^{(1)}(q, \mu^2) = \lim_{\mu \rightarrow 0} \int d^4 q J^{(1)}(q, \mu^2) \quad \text{and}$$

$$\int [d^4 q_1][d^4 q_2] J^{(2)}(q_1, q_2, \mu^2) = \lim_{\mu \rightarrow 0} \int d^4 q_1 d^4 q_2 J^{(2)}(q_1, q_2, \mu^2), \quad (2.145)$$

respectively, with

$$J^{(1)}(q, \mu^2) = \frac{1}{\overline{D}_0(q)\overline{D}_{p_1}(q)\overline{D}_{p_2}(q)},$$

$$J^{(2)}(q_1, q_2, \mu^2) = J^{(1)}(q_1, \mu^2) \frac{1}{\overline{D}_0(q_2)\overline{D}_{p_1}(q_{12})\overline{D}_{p_2}(q_{12})},$$

$$\overline{D}_{p_i}(q_j) = \overline{q}_j^2 + 2(q_j \cdot p_i). \quad (2.146)$$

There was no need of FDR expanding because $J^{(1)}$ and $J^{(2)}$ produce UV convergent integrals. Note that the on-shell conditions $p_1^2 = p_2^2 = 0$ are used at the integrand level. Thus, infrared virtual divergences get regulated by the μ^2 -deformed propagators which generates powers of logarithms of μ^2 , upon integration.

For example, the first integral in eq. (2.145) gives

$$C(s) = \int [d^4 q] J^{(1)}(q, \mu^2)$$

$$= \lim_{\mu \rightarrow 0} \frac{i\pi^2}{2s} \ln^2 \left(\frac{\sqrt{1-4\mu_0} + 1}{\sqrt{1-4\mu_0} - 1} \right) = \frac{i\pi^2}{s} \left[\frac{\ln^2(\mu_0) - \pi^2}{2} + i\pi \ln(\mu_0) \right], \quad (2.147)$$

where $s = -2(p_1 \cdot p_2)$, and we have defined

$$\mu_0 = \frac{\mu^2}{s}. \quad (2.148)$$

Of course, the μ in $\ln \mu_0$ is not traded for the renormalization scale, but it remains as an actual IR cut-off. In an inclusive observable, the dependence on μ of the virtual radiation is eventually fully matched by that of the real radiation so that the final result is independent of any cut-off(see Section 2.3), or absorbed into the definition of the pdfs in the case of initial state collinear singularities.

In principle, a different μ^2 can be used to regulate UV divergences (μ_{UV}^2) and IR ones (μ_{IR}^2). However, a common μ^2 simplifies the calculation. Since IR infinities are more easily understood in terms of $\mu_{\text{IR}}^2 > 0$, it is convenient to take $\mu_{\text{UV}}^2 = \mu_{\text{IR}}^2 = \mu^2 > 0$.

2.1.9.1 Scaleless integrals

A particularly interesting situation is when the integral is also UV divergent. In this case it is easy to see that UV divergent scale-less ℓ -loop FDR integrals vanish, as in DR. In fact, the only allowed external variable is a momentum p such that $p^2 = 0$, whose fate is to appear in the numerator of $J_{\text{F},\ell}(q_1, \dots, q_\ell)$ in eq. (2.8) to improve the UV convergence of the original integrand. Therefore, $J_{\text{F},\ell}(q_1, \dots, q_\ell)$ is entirely made of integrands proportional to positive powers of $(q_i \cdot p)$, that vanish, by Lorentz invariance, after integration. The simplest case is the fully massless one-loop 2-point scalar function

$$B^{\text{FDR}}(p^2 = 0; 0, 0) = \int [d^4 q] \frac{1}{\bar{q}^2((q+p)^2 - \mu^2)}. \quad (2.149)$$

The FDR expansion of its integrand reads

$$\frac{1}{\bar{q}^2 \bar{D}_p} = \left[\frac{1}{\bar{q}^4} \right] - 2 \frac{(q \cdot p)}{\bar{q}^4 \bar{D}_p}, \quad (2.150)$$

so that

$$B^{\text{FDR}}(p^2 = 0; 0, 0) = -2 \lim_{\mu \rightarrow 0} \int d^4 q \frac{(q \cdot p)}{\bar{q}^4 \bar{D}_p} = 0. \quad (2.151)$$

The same result is obtained by a direct computation

$$B^{\text{FDR}}(p^2; 0, 0) = -i\pi^2 \lim_{\mu \rightarrow 0} \int_0^1 dx (\ln(\mu^2 - p^2 x(1-x)) - \ln(\mu^2)), \quad (2.152)$$

from which it is manifest that, in the limit $p^2 \rightarrow 0$, a cancellation occurs between two logarithms of UV and IR origin, respectively.

It is instructive to study the same case in DR, where

$$B^{\text{DR}}(p^2; 0, 0) = \int \frac{d^n q}{\mu^\epsilon} \frac{1}{q^2(q+p)^2}. \quad (2.153)$$

Now $B^{\text{DR}}(0, 0, 0)$ vanishes because IR and UV poles in ϵ compensate. In fact, by introducing an arbitrary separation scale M , the two divergences can be split

$$\begin{aligned} \frac{1}{(q+p)^2} &= \frac{1}{q^2 - M^2} - \left(\frac{1}{q^2 - M^2} - \frac{1}{(q+p)^2} \right) \\ &= \frac{1}{q^2 - M^2} - \frac{M^2 + 2(q \cdot p)}{(q^2 - M^2)(q+p)^2}. \end{aligned} \quad (2.154)$$

Then the integrals

$$\begin{aligned} I_{\text{UV}} &= \int \frac{d^n q}{\mu^\epsilon} \frac{1}{q^2(q^2 - M^2)} = i\pi^2 \left(1 - \ln \frac{M^2}{\mu^2} - \frac{2}{\epsilon} - \Delta \right), \\ I_{\text{IR}} &= \int \frac{d^n q}{\mu^\epsilon} \frac{M^2 + 2(q \cdot p)}{q^2(q^2 - M^2)(q+p)^2} = I_{\text{UV}}, \end{aligned} \quad (2.155)$$

where $\Delta = \gamma_E + \ln \pi$, cancel each other. However, this argument has a potential problem, because it requires the cancellation of two analytic continuations, I_{UV} and I_{IR} , originally defined in domains that *do not overlap* [70] ($\epsilon|_{\text{IR}} < 0$ and $\epsilon|_{\text{UV}} > 0$): since no value of ϵ exists where they are defined simultaneously, it is not obvious whether their difference represents the original function $B^{\text{DR}}(0; 0, 0)$. A possible mathematically consistent solution can be formulated in terms of modified Gaussian integrals in the n -dimensional Euclidean space [70]. In contrast, the FDR derivation in eq. (2.151) is straightforward.

In summary, IR divergent loop integrals are defined by taking the limit $\mu \rightarrow 0$ outside integration, after subtracting – when necessary – UV divergent integrands. In order to preserve the cancellation of the IR logarithms in physical quantities, this definition should be accompanied by a consistent treatment of the infinities appearing in the real emission, which we discuss in Section 2.3.

2.2 Calculating Loop Amplitudes in FDR

Having defined the FDR loop integral, we now move the focus of our discussion from the diagram level to the amplitude. In this section, we do not introduce new technology – rather we take the time to think about the consequences of the procedures deligned in the previous section when put into practice.

First of all, we explain how an amplitude calculated in FDR preserves all the symmetries of the original Lagrangian, including local ones. The mechanism insuring this property is encoded in the very definition of the FDR integral together with global prescription, and there is no need to inforce it *a posteriori* like in other four-dimensional methods.

We dedicate the subsequent section to renormalization: indeed, FDR amplitudes are finite by construction. A finite renormalization remains to be done in order to relate the parameters of the Lagrangian to physical observables; as a side remark, this also means that if a parameter does not appear in the final result, nothing has to be done. This procedure, alternative to the counterterm approach to renormalization, leaves the Lagrangian untouched. At two loops, where the equivalence between FDR and DRed integrals is broken, order-by-order renormalization is altogether avoided. Once more, FDR provides a shortcut to the physical answer.

Finally, in the last section, we remark that, although deeply different with respect to any standard approach, FDR still represents a renormalization scheme, which means that translation rules between FDR and other methods can be established. This turns out to be useful when realistic calculations have to made, particularly in QCD, where quantities at the parton level need to be matched with pdfs and running parameters, typically computed in DR.

2.2.1 Gauge invariance

The FDR integral respects by construction all the symmetries of the QFT taken into consideration, including local ones if existing. We limit our discussion to the latters, since gauge invariance provides a stricter constraint with respect to global symmetries.

The fact that FDR preserves gauge invariance is crucial to make it a competitive calculation framework. Indeed, most four-dimensional methods do not respect gauge invariance, this being enforced at the end of the calculation as an extra constraint. However, DR and FDR alike do not break gauge

invariance, which means, for example, that it can be used as a test for the results obtained.

The argument insuring that FDR respects gauge invariance is to be found in the existence of graphical proofs of the Ward-Slavnov-Taylor identities [71], in which the correct relations among Green’s functions are demonstrated – at any loop order – directly at the level of Feynman diagrams. Such proofs are valid under two circumstances:

- divergent loop integrals should be defined in a way that shifting the integration momenta is possible as if they were convergent ones [72];
- simplifications between numerators and denominators should be preserved.

Indeed, quoting Martinus Veltman [73], “*Gauge invariance implies a tight interplay between the numerator of an integrand and its denominator. Changing either of the two will generally destroy gauge invariance . . .*”.

In the previous section, we have seen in detail how the FDR integral respects these two characteristics: in Section 2.1.3 shift invariance was proven; in Section 2.1.5, the global prescription of FDR was explained as the mechanism that guarantees the usual simplifications between numerator and denominator, at the integrand level.

As a last remark, we should emphasize that an FDR amplitude is entirely gauge-invariant, the cut-constructible parts (i.e. those containing the kinematical dependence) as well as the rational part. On the latter a potential ambiguity may remain if we think of FDR in comparison to DR, because in the one case vacuum configurations are subtracted *before* integrating, while in the other poles in ϵ are taken away *after* the integration. However, global prescription together with extra-integrals defined as in Section 2.1.5.1 provide a powerful mechanism able to warrant gauge invariance.

This was explicitly verified with the calculation of the diphoton production from Higgs boson’s decay at one-loop performed in arbitrary R_ξ gauge [74], which we report in Section ???. Moreover, in Section 3.3, the Ward identities at one and two loops for the same process $H \rightarrow \gamma\gamma$ are verified at the integrand level, thus elucidating some of the features of FDR.

2.2.2 Renormalization

In the acronym FDR, the last letter stands for “regularization” and also for “renormalization”. Indeed, the FDR integral is defined in such a way

that all UV infinities are decoupled from the physics and subtracted at the integrand level. All quantities calculated in FDR are finite, without the need of any additional procedure. The only cost of this subtraction was the introduction of an arbitrary scale, $\mu = \mu_R$ as explained in Section 2.1.4, on which the integrals depend logarithmically.

All p physical amplitudes are independent of μ_R , that is after a *global finite renormalization* is undertaken. This is the procedure with which the parameters of the QFT are fixed in terms of physical observables, at the same perturbative order the calculation is performed.

Symbolically, consider a QFT described by the Lagrangian

$$\mathcal{L}(\alpha_1, \dots, \alpha_p), \quad (2.156)$$

which depends on p parameters. In order to calculate the observable $\mathcal{O}_{p+1}^{(\ell)}$, we first need p measurements

$$\mathcal{O}_1^{exp}, \dots, \mathcal{O}_p^{exp}$$

in terms of which the parameters $\alpha_1, \dots, \alpha_p$ are to be expressed, that is

$$\mathcal{O}_i^{(\ell)}(\alpha_1, \dots, \alpha_p) = \mathcal{O}_i^{exp} \Rightarrow \alpha_i = \alpha_i^{(\ell)}\left(\mathcal{O}_1^{exp}, \dots, \mathcal{O}_p^{exp}\right) \equiv \bar{\alpha}_i \quad i = 1, \dots, p. \quad (2.157)$$

In this way, a new prediction is made,

$$\bar{\mathcal{O}}_{p+1}^{(\ell)} = \mathcal{O}_{p+1}^{(\ell)}(\bar{\alpha}_1, \dots, \bar{\alpha}_p), \quad \text{with} \quad \frac{\partial \bar{\mathcal{O}}_{p+1}^{(\ell)}}{\partial \mu_R} = 0, \quad (2.158)$$

and the renormalization scale is dropped, or rather traded for the physical scale at which the observables were measured. Notice that the original Lagrangian is completely untouched.

At one loop, the FDR scheme is equivalent to $\overline{\text{DRed}}$, i.e. $\overline{\text{DRed}}$ with $\overline{\text{MS}}$: exactly the same pieces are subtracted, respectively at the integrand level and after integration. From another viewpoint, this is analogous to observing that the vacuum configurations are equivalent to the counterterms that one would add to the Lagrangian in order to renormalize it at one loop. The FDR integral provides a short-cut to the bunch of operations that are needed in a traditional computation.

As we have seen in Section 2.1.7, the one-to-one correspondence between one-loop integrals in FDR and DR is broken at higher loop levels. The profound consequences that this has on renormalization are explained in the next section.

2.2.2.1 Avoiding order-by-order renormalization.

The proof that DR preserves gauge invariance relies on the possibility of introducing local counterterms in the Lagrangian \mathcal{L} . On the contrary, FDR makes no reference to \mathcal{L} . In this section we use the simple two-loop QED example of the photon self energy [75] to comment on the conceptual differences between the two approaches.

Consider a DR calculation of the one-loop photon self-energy

$$\begin{array}{c} p \\ \nearrow \\ \text{---}\text{---}\text{---} \\ \alpha \quad \text{---}\text{---}\text{---} \\ \searrow \\ \beta \end{array} = i T_{\alpha\beta} \Pi(p^2), \quad T_{\alpha\beta} = g_{\alpha\beta} p^2 - p_\alpha p_\beta,$$

with

$$\begin{aligned} T_{\alpha\beta} &= g_{\alpha\beta} p^2 - p_\alpha p_\beta, \\ \Pi(p^2) &= \frac{1}{\epsilon} \Pi_{-1} + \Pi_0 + \epsilon \Pi_1, \\ \Pi_0 &= \frac{e^2}{2\pi^2} \int_0^1 dx x(1-x) \ln \frac{m^2 - p^2 x(1-x)}{\mu^2}. \end{aligned} \quad (2.159)$$

Then, at two-loops and up to terms $\mathcal{O}(\epsilon^0)$,

$$\begin{array}{c} \text{---}\text{---}\text{---} \\ \text{---}\text{---}\text{---} \\ \text{---}\text{---}\text{---} \end{array} = i T_{\alpha\beta} \Pi^2(p^2) = i T_{\alpha\beta} \left(\frac{\Pi_{-1}^2}{\epsilon^2} + \frac{2\Pi_{-1}\Pi_0}{\epsilon} + \Pi_0^2 + 2\Pi_{-1}\Pi_1 \right).$$

At the one-loop level, the renormalized result in $\overline{\text{MS}}$ is simply obtained by removing the pole and truncating the expansion at $\mathcal{O}(\epsilon^0)$, which yields $\Pi_0(p^2)$. If one were to do the same thing at two loops, i.e. merely dropping the poles, the last expression would give

$$\Pi_0^2 + 2\Pi_{-1}\Pi_1,$$

which is not the correct result.

This is because at two loops the structure of infinities is richer. Like the pole in the one-loop case, the double pole exhibits a coefficient that is at most proportional to a polynomial in the relevant scale, e.g. p^2 ; on the other hand, the coefficient to the single pole can contain logarithms of the

relevant scale: indeed, in the present case, it contains the Π_0 of eq. (2.159). According to this difference, divergences are labelled *local* (polynomial) or *non-local* (logarithmic) respectively.

In the one-loop case, only local infinities appear, which in $\overline{\text{MS}}$ are absorbed into simple counterterms. This is equivalent to dropping them all together, as prescribed by FDR. With more loops, however, the differences between the two approaches begin. Indeed, the logarithms of the non-local singularities cannot be absorbed into a simple counterterm. As is well known, the correct procedure to undertake in DR is to renormalize order by order, i.e. to add one-loop counterterms in \mathcal{L} such that

$$\text{wavy line with loop} + \text{wavy line with dot} = iT_{\alpha\beta} \Pi_0 + \mathcal{O}(\epsilon).$$

The one-loop counterterms exactly compensate the dependence of the non-local divergences. Thus

$$\text{two loops} + \text{loop with dot} + \text{dot with loop} + \text{two dots} = iT_{\alpha\beta} \Pi_0^2 + \mathcal{O}(\epsilon).$$

This procedure also makes sure that the finite part preserves gauge invariance and unitarity.

In FDR, *all* divergences are subtracted at the level of the definition of the loop integration, so that the product of two one-loop diagrams is simply the product of the two finite parts, with no need of introducing extra interactions in \mathcal{L} . Thus, one directly obtains

$$\text{two loops} = iT_{\alpha\beta} \Pi_{\text{FDR}}^2(p^2),$$

with $\Pi_{\text{FDR}}(p^2) = \Pi_0$. This difference can be also understood from the $DR \leftrightarrow FDR$ naive correspondence

$$\begin{aligned} \epsilon &\leftrightarrow \mu \\ \frac{1}{\epsilon} &\leftrightarrow \ln \mu, \end{aligned} \tag{2.160}$$

which gives $\lim_{\epsilon \rightarrow 0} \epsilon/\epsilon = 1$, while $\lim_{\mu \rightarrow 0} \mu \ln \mu = 0$.

To conclude, it is manifest that spurious ϵ/ϵ terms such as $\Pi_{-1}\Pi_1$ – which need to be kept under control in DR by the order-by-order renormalization – never appear in FDR. The result of an FDR calculation typically depends on the parameters contained in \mathcal{L} , and a (finite) global renormalization is needed only to link them to experimental measurements at the desired perturbative accuracy. In particular – and in contrast with DR – no renormalization is necessary when no parameter appears in the final result, which is the situation of the calculation presented in Section 3.2.

2.2.3 The FDR scheme

FDR provides a completely new approach to calculations in QFT. Nonetheless, it is effectively *a renormalization scheme*, which means that results obtained in FDR can be mapped in expressions calculated in different schemes, via some transition rules. In particular, one wants to be able to translate FDR results in DR, which is the standard framework used to compute running parameters and parton densities. This is especially important in QCD, where the parton cross sections need to be matched with the running of α_S and the pdfs in order to obtain realistic predictions.

At one loop, we have seen that there exist a simple transition rule, from FDR to DR expressions,

$$\ln \mu \rightarrow \ln \mu - \frac{1}{\epsilon} - \frac{\Delta}{2}, \quad \Delta \equiv \gamma_E + \ln \pi, \quad (2.161)$$

that works unchanged for UV and CL divergences. Soft divergences, and in particular the squared log's coming from overlapping soft and CL divergences, cancel out in fully inclusive observables.

A significant difference between FDR and DR arise from the contraction of two metric tensors coming from the Feynman rules: indeed, $g_{\alpha\beta}g^{\alpha\beta}$ respectively gives 4 and n in FDR and DR. For this reason, FDR one-loop results explicitly correspond to expressions calculated in $\overline{\text{DRed}}$ [76], rather than standard DR with $\overline{\text{MS}}$; the transition rules from $\overline{\text{DRed}}$ to DR are known [68, 77], and they can be directly applied to FDR. Recall that DRed was introduced in order to extend the use of DR to supersymmetric theories, which require that observed external states are treated in four dimensions. For the same reason, FDR was naturally born as a suitable scheme to be used with SUSY models.

At two loops, a correspondence between FDR and DR expressions is less transparent, essentially because FDR drops all subdivergences at the very beginning, while in DR one has to undertake a careful order-by-order renormalization to obtain the correct answer. However, as shown in [59] for various theories – QCD included –, the vacuum content extracted from an amplitude via FDR defining expansion corresponds to the contribution that the addition of standard counter terms to the Lagrangian would add to the amplitude itself. This establishes a relationship between the two frameworks that makes it possible to transfer the results from one into the other.

2.3 Calculating IR-Safe Observables in FDR

In this section, we explain how FDR deals with real radiation in the final state, i.e. with the phase space integration of the matrix elements of a process with massless external particles. Indeed, when a massless particle is soft or collinear to another one, and it cannot be observed, its contribution cannot be considered without that of the same particle if it was emitted virtually. In particular, the spurious IR infinities that open up as one calculates the virtual or real radiation alone cancel exactly in the combination of the two contributions, as guaranteed by the BN and KLN theorems [44, 45]. In the virtual radiation, the infinities arise as we perform the loop integral, which we have learnt abundantly how to treat in DR. In the real case, the infinities come up at the level of the phase space integration: in this section we give an FDR interpretation to the phase space integral, so that the matching between virtual and real can be realized. Moreover, because the real radiation quickly reach a complexity that makes it futile to try and cope with it analytically, we have designed a numerical strategy, in which the real part is integrated with the Monte Carlo method and then combined with the analytical expression of the virtual. This is possible in FDR thanks to the fact that all singularities are at most logarithmic, making the problems due to numerical instability much less severe than in a DR-based Monte Carlo. We then develop the idea of constructing a novel local subtraction method at NLO, in which the cancellation of the IR divergences happen at the integrand level; in particular, we want to extract a counterterm for the real directly from the virtual, on which we usually have an analytic handle. Finally, in the last section we discuss the generalization of the FDR approach to IR radiation beyond NLO. The last two topics presented in this section concern some very preliminary work, and are meant more as an invitation than as a complete account. Studies on initial state radiation are currently being performed too, but they go beyond the scope of this thesis.

2.3.1 Real radiation

In Section 2.1.9, we discussed IR divergences in loop integrals, explaining how the deformation of loop momentum prescribed by FDR automatically cures also the IR singularities. We now show how the virtual radiation is matched by a particular treatment of the real radiation, allowing a neat realization of the KLN theorem.



Figure 2.4: Splitting regulated by massive (thick) unobserved particles. The one-particle cut in (a) contributes to the virtual part, the two-particle cut of (b) to the real radiation.

As a starting point, consider how the divergent $1 \rightarrow 2$ splitting is regulated in the loop integrals. The situation is depicted in figure 2.4(a), where thick lines represent unobserved loop particles – whose propagator is made massive by the addition of μ^2 – and the cut line is an external observed massless particle. The real counterpart of this splitting is provided by the pattern of fig. 2.4(b), where thick lines are unobserved external particles merging into an internal observed massless one. In both situations unobserved particles get a mass μ and unitarity relates the two cases as follows

$$\frac{1}{q^2 - \mu^2} \rightarrow \delta(q^2 - \mu^2) \theta(q^{(0)}) . \quad (2.162)$$

Indeed, with this relation, it is possible to interpret a phase-space integral as a loop one, which provides a guideline to give an FDR meaning to phase-space integration.

Just like the loop momenta are regulated by the replacement $q^2 \rightarrow \bar{q}^2$, would-be-massless external particles with momenta p_i are given a mass μ , that is $p_i^2 \rightarrow p_i^2 = \mu^2$. This is achieved

- by trading the original massless m -body phase space $d\Phi_m$ for a massive one, denoted by $d\bar{\Phi}_m$;
- by replacing

$$\frac{1}{2(p_i \cdot p_j)} \rightarrow \frac{1}{(p_i + p_j)^2} \equiv \frac{1}{s_{ij}} \quad (2.163)$$

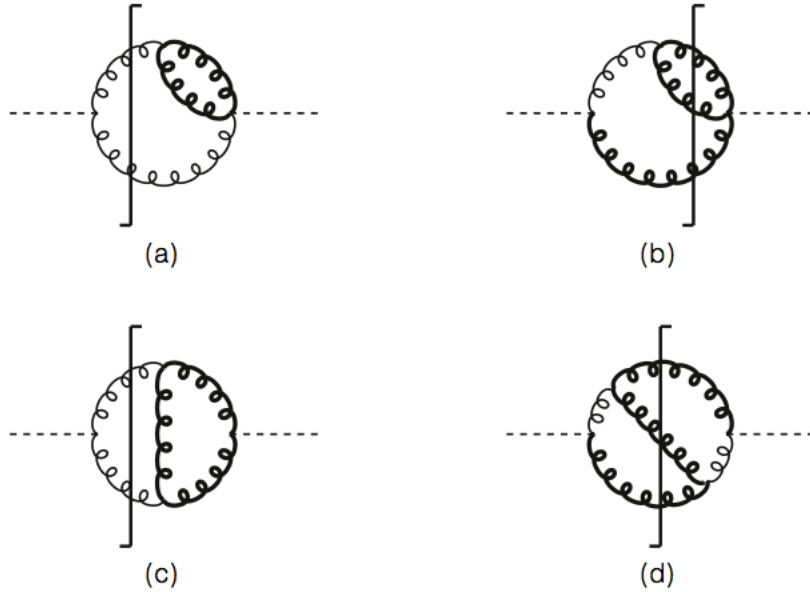


Figure 2.5: Typical cut-diagrams contributing to $H \rightarrow gg(g)$ in HEFT. In the first column, (a) and (c) are virtual cuts, i.e. they contribute to the product of the tree-level and the one-loop amplitude for $H \rightarrow gg$. These are matched by the real cuts in the second column, respectively (b) and (d), which contribute to the squared amplitude at the tree-level of the process $H \rightarrow ggg$.

in any possible singular denominator of the real matrix element.

In this way, singular configurations produce logarithms which cancel the IR dependence on μ^2 of the virtual contribution, for example that of eq. (2.147) in Section 2.1.9. Once the matching is done, all $\ln \mu$ cancel, as prescribed by the KLN theorem, and one can safely take the limit $\mu \rightarrow 0$.

This strategy has been successfully adopted in [78] to derive the inclusive decay rate for $H \rightarrow gg(g)$ at NLO, in Higgs effective field theory (HEFT), as explained in Section 3.4. In fig. 2.5, we show some typical cut-diagrams for this one-loop process, to give an example of the correspondence between virtual and real contributions that was sketched in fig. 2.4.

2.3.2 Naive numerical matching

In the calculation of the NLO decay rate of $H \rightarrow gg(g)$ [78], both the virtual and the real contribution were computed analytically,

$$\begin{aligned}\sigma_V(H \rightarrow gg) &= v_0 + v_1 \log \mu_0 + v_2 \log^2 \mu_0, \\ \sigma_R(H \rightarrow ggg) &= r_0 + r_1 \log \mu_0 + r_2 \log^2 \mu_0,\end{aligned}\tag{2.164}$$

where $\mu_0 = \mu^2/s^2$ and $s = M_H^2$; when summing up the two quantities, the cancellation of $\ln \mu_0$ is neat, because it turns out that $v_1 = -r_1$, and $v_2 = -r_2$; therefore, the limit

$$\sigma(H \rightarrow gg(g)) = \lim_{\mu \rightarrow 0} \left(\sigma_V(H \rightarrow gg + X) + \sigma_R(H \rightarrow gg + X) \right) = v_0 + r_0\tag{2.165}$$

is well-defined. Unfortunately, as the complexity of the process of interest increases, it is not always possible to have the analytic expressions of both contributions. Often it is the real part that poses the biggest issue when computing full inclusive observables. Indeed, there is no general method to analytically perform the phase space integral for arbitrarily involved final states; on the other hand, loop integrals are generally more manageable, and analytical results can be usually achieved. In this section we discuss the possibility of numerically integrating the real part, in an FDR calculation at NLO.

Consider the inclusive cross section of a process with n observed particles in the final state; the contributions can be schematically expressed as follows:

$$\begin{aligned}\sigma_V(\ln \mu) &= \int d\Phi_n \int [d^4q] V(\bar{q}, \Phi_n), \\ \sigma_R(\ln \mu) &= \int d\bar{\Phi}_{n+1} R(\bar{\Phi}_{n+1}).\end{aligned}\tag{2.166}$$

where Φ_m as the argument of V and R is a synthetic notation referring to the kinematical information about the final state, i.e. all scalar products of external particle momenta ($p_i \cdot p_j$). As far as the virtual part is concerned, the dependence on $\ln \mu$ comes from the loop integral, while the phase space integration is trivial. In the real case, we have used the notation of the previous section, denoting by $\bar{\Phi}_{n+1}$ the massive phase space modified à la FDR. Here, divergences are generated at the level of the phase space integration. Suppose we know the analytic expression of $R(\bar{\Phi}_{n+1})$, but we are not able

to perform the integral analytically. By choosing a small but finite value of μ , we can integrate $R(\overline{\Phi})$ numerically with a Monte Carlo method; then, we would like the combination

$$\sigma_V(\ln \mu) + \sigma_R(\ln \mu) = \sigma_\mu \quad (2.167)$$

to converge to a single value

$$\sigma = \lim_{\mu \rightarrow 0} \sigma_\mu$$

as we take smaller and smaller values of μ . Here is where FDR comes into play: this limit is numerically stable thanks to the fact that we are combining infinities that –in FDR– are at most logarithmic. In DR, such an approach would not work as well, because it would require the numerical cancellation of poles $1/\epsilon$, which is highly unstable.

It is worthwhile to comment on the fact that in eq. (2.166) we have assumed that the full analytic knowledge on $R(\Phi_{n+1})$ is available. Indeed, by writing $R(\overline{\Phi}_{n+1})$, i.e. having substituted $\Phi_{n+1} \rightarrow \overline{\Phi}_{n+1}$, we are actually implying that the replacement

$$\frac{1}{2(p_i \cdot p_j)} \rightarrow \frac{1}{s_{ij}}, \quad (2.168)$$

with s_{ij} as in eq. (2.163), has taken place in all divergent terms of R , and this is only feasible if the analytic expression of $R(\Phi_{n+1})$ is known.

We now want to generalize the procedure deligned above to those cases in which $R(\Phi_{n+1})$ is obtained via some numerical algorithm. Indeed, the replacement of eq. (2.168), instead of being enforced by hand, can be implemented by multiplying the massless $R(\Phi_{n+1})$ by all possible \hat{s}_{ij}/s_{ij} , where

$$\hat{s}_{ij} = 2(p_i \cdot p_j) = s - 2\mu^2$$

is the massless version of s_{ij} . What we are saying is that

$$\sigma_R(\ln \mu) \approx \int d\overline{\Phi}_{n+1} R(\Phi_{n+1}) \prod_{i,j=1}^n \frac{\hat{s}_{ij}}{s_{ij}}. \quad (2.169)$$

The rational behind this equation is the fact that at NLO the divergent pieces of $R(\Phi_{n+1})$ are all proportional to either

$$\frac{1}{\hat{s}_{ij}} \quad \text{or} \quad \frac{1}{\hat{s}_{ij}\hat{s}_{jk}}, \quad (2.170)$$

and that adding μ^2 to convergent terms has no significant effect when μ is small. Therefore $\prod(\hat{s}_{ij}/s_{ij})$ is effectively an operator that automatically produces the replacement of eq. (2.168) and that can be incorporated in a fully numerical strategy to obtain σ_R .

This approach, both that of eq. (2.166) and the purely numerical one of eq. (2.169), has been successfully tested for the simple process $H \rightarrow gg$, as we explain in Section 3.4 where we also add some technical details to the present discussion; its application to $H \rightarrow ggg(g)$ is under construction.

As a final point, let us remark that this numerical approach in FDR is somehow similar to the phase space slicing method [79]. The latter however has a few drawbacks that in FDR are avoided. Indeed, being based on DR, it still requires the analytic calculation of the poles in ϵ ; moreover, an extra IR cut-off δ is introduced, on which the cross sections depend logarithmically analogously to the FDR μ . Instead in FDR no new unphysical scale needs to be added in the calculation, and the cancellation can be completely brought about numerically.

For these reasons, we envisage that such a method can be also extended at NNLO. It may not return the most accurate result, but it is solid enough to be used in preliminary studies.

2.3.3 FDR local subtraction

Since the real radiation is generally more difficult to calculate analytically, when designing a scheme for the matching of virtual and real radiation, we want to aim at a method that exploits to the maximum the analytical knowledge on the virtual, and that treats numerically the real. In the last section, we proposed a naive numerical method, in which the real was integrated by Monte Carlo and then combined with the analytic expression of the virtual: in FDR the cancellation of the logarithmic IR infinities is stable, and such simple procedure is feasible and effective. However, it would be much more convenient to cancel the IR divergences at the integrand level: the subsequent numerical integration would be extremely fast and safe.

This is the idea of subtraction methods such as the dipole method [9] and FKS [8]: by partially integrating the real part, i.e. integrating over the momentum of the unobserved particle, they obtain an object that can be put together with the virtual at the integrand level. The problem of such an approach is that it is not always possible to partially integrate the real, even more so when the real integrand $R(\Phi_{n+1})$ is not known analytically. A

way to proceed then is that of cleverly guessing the divergent structure of $R(\Phi_{n+1})$, subtracting this counterterm from the real and adding it back to the virtual. Schematically, the two “cured” contributions read

$$\int d\Phi_{n+1} \left(R(\Phi_{n+1}) + R_{ct}(\Phi_{n+1}) \right), \quad \int d\Phi_n \left(V(\Phi_n) - V_{ct}(\Phi_n) \right), \quad (2.171)$$

where the integrals can be performed numerically, and

$$\int d\Phi_{n+1} R_{ct}(\Phi_{n+1}) = \int d\Phi_n V_{ct}(\Phi_n). \quad (2.172)$$

The main drawback of this type of approach is that, since R_{ct} and V_{ct} are unphysical, the cancellations expected in eq. (2.171) sometimes can be plagued by numerical instability, especially for high multiplicities.

To avoid this problem, a different strategy can be designed that exploits the analytical knowledge of the virtual, rather than trying to integrate the poorly known real part. The idea is that of *disintegrating* the virtual, i.e. rewriting the $\ln \mu^2$ arising from the virtual as local counterterm of the real part.

Let us play around this idea, limiting the discussion to the NLO level. We want to separate the IR-safe and the IR-divergent part in the integrand of the virtual, schematically

$$\int d\Phi_n \int [d^4q] V(q, \Phi_n) = \int d\Phi_n \int [d^4q] \left(V_F(q, \Phi_n) + V_{div}(q, \Phi_n) \right). \quad (2.173)$$

By trading the loop momentum for an extra external one, we can translate V_{div} into a counterterm for the real part, i.e.

$$\int d\Phi_n \int [d^4q] V_{div}(q, \Phi_n) = \int_{\mu} d\Phi_{n+1} R_{ct}(\Phi_{n+1}), \quad (2.174)$$

in practice doing the opposite of eq. (2.172). We can then cancel the IR singularities of the real at the integrand level, by taking

$$\int_{\mu} d\Phi_{n+1} \lim_{\mu \rightarrow 0} \left(R(\Phi_{n+1}) + R_{ct}(\Phi_{n+1}) \right), \quad (2.175)$$

where the integral at this point can be safely performed numerically, over the massive phase-space prescribed by FDR.

The question now is whether the *disintegration* of the virtual, i.e. eq. (2.174), can be realized. Unitarity may help to this goal, if we make use of the relation sketched in eq. (2.162). More precisely [80],

$$\frac{1}{\bar{q}^2 + i0 - \mu^2} \leftrightarrow -2\pi i \delta(\bar{q}^2 - \mu^2) \theta(q^{(0)}) + \frac{1}{\bar{q}^2 - i0 q^{(0)}}, \quad (2.176)$$

where the second term is regular, and can thus be neglected when inserted in a realistic Feynman integrand.

At NLO, the only type of divergent integrands in the real part are those of eq. (2.170); these are the shapes of the counterterms to the real that we must be able to read from the virtual. As far as

$$\frac{1}{s_{ij}s_{jk}}$$

is concerned, the one-loop three point function of eq. (2.147) is enough to reconstruct all local counterterms. Indeed,

$$\int d\Phi_2 \Re \left(\int [d^4q] \frac{1}{\bar{q}^2 \bar{D}_1 \bar{D}_2} \right) = \int d\bar{\Phi}_3 \frac{1}{s_{13}s_{32}}, \quad (2.177)$$

which means that each $\ln^2 \mu^2$ of the virtual must be replaced according to the following equation

$$\ln^2 \frac{\mu^2}{s} - \pi^2 = \frac{8s}{\pi^2} \int d\bar{\Phi}_3 \frac{1}{s_{ij}s_{jk}}, \quad (2.178)$$

or alternatively, one can put to zero the integrands of the type $1/\bar{q}^2 \bar{D}_1 \bar{D}_2$ in the virtual, and then correct the real with the addition of $1/(s_{ij}s_{ik})$.

Regarding the terms of the type

$$\frac{s_{ij}^a}{s_{ik}},$$

they can also be read from the virtual, from terms like $2(q \cdot p_j)^a / \bar{q}^2 \bar{D}_k$ or from the collinear behaviour of the Altarelli-Parisi splitting functions.

The method has been applied to $H \rightarrow gg(g)$ and work is ongoing towards its application to $H \rightarrow ggg(g)$.

2.3.4 A possible scheme beyond NLO

When going to NNLO, a few comments are required in order to generalize the FDR approach to IR infinities in a consistent way. Let's review the strategy deligned in Section 2.3.1 as applied to a NNLO calculation: our guideline will be gauge invariance, i.e. we must make sure that the procedures that we set up respect the symmetries of the Lagrangian.

To illustrate the way to proceed we consider m -jet production at NNLO in e^+e^- annihilation, as a formal example. The building blocks of the calculation depend on the set of invariants

$$\{s_{i_1 \div i_m}\} \equiv \{s_{i_1 i_2}, s_{i_1 i_2 i_3}, \dots, s_{i_1 \dots i_m}\}, \quad s_{i \dots j} = (p_i + \dots + p_j)^2, \quad (2.179)$$

where $p_i^2 = 0$. They are:

- the Born contribution $d\sigma_{\text{LO}}^B\{s_{i_1 \div i_{m-1}}\}$,
- the virtual and real NLO corrections, $d\sigma_{\text{NLO}}^V\{s_{i_1 \div i_{m-1}}\}$ and $d\sigma_{\text{NLO}}^R\{s_{i_1 \div i_m}\}$,
- the NNLO two-loop part $d\sigma_{\text{NLO}}^{V,2}\{s_{i_1 \div i_{m-1}}\}$,
- the one-loop corrections to the NLO real radiation, $d\sigma_{\text{NNLO}}^{V,1}\{s_{i_1 \div i_m}\}$,
- the double radiation $d\sigma_{\text{NNLO}}^R\{s_{i_1 \div i_{m+1}}\}$.

After α_S renormalization, they give a m -jet cross section accurate up to NNLO

$$d\sigma = d\sigma_{\text{LO}} + d\sigma_{\text{NLO}} + d\sigma_{\text{NNLO}}, \quad (2.180)$$

where

$$\begin{aligned} d\sigma_{\text{LO}} &= \int_{d\Phi_m} d\sigma_{\text{LO}}^B\{s_{i_1 \div i_{m-1}}\}, \\ d\sigma_{\text{NLO}} &= \int_{d\Phi_m} d\sigma_{\text{NLO}}^V\{s_{i_1 \div i_{m-1}}\} + \int_{d\Phi_{m+1}} d\sigma_{\text{NLO}}^R\{s_{i_1 \div i_m}\}, \\ d\sigma_{\text{NNLO}} &= \int_{d\Phi_m} d\sigma_{\text{NNLO}}^{V,2}\{s_{i_1 \div i_{m-1}}\} + \int_{d\Phi_{m+1}} d\sigma_{\text{NNLO}}^{V,1}\{s_{i_1 \div i_m}\} \\ &\quad + \int_{d\Phi_{m+2}} d\sigma_{\text{NNLO}}^R\{s_{i_1 \div i_{m+1}}\}. \end{aligned} \quad (2.181)$$

The integrands behave as

$$d\sigma\{\dots\} \sim \frac{1}{s_{ij}}, \quad \text{if } s_{ij} \rightarrow 0 \quad \text{and} \quad d\sigma\{\dots\} \sim \frac{1}{s_{ijk}^2}, \quad \text{if } s_{ijk} \rightarrow 0 \quad (2.182)$$

therefore the integrations over single- and double-unresolved massless phase-spaces (Φ_{m+1} and Φ_{m+2} , respectively) generate logarithmic IR divergences which have to be regulated.

In DR, the last two lines of eq. (2.181) are interpreted as a limit to $\epsilon \rightarrow 0$ of integrals computed in $n = 4 + \epsilon$ dimensions. We instead define a mapping from massless to massive invariants as follows

$$\begin{aligned} s_{i_1 \dots i_m} &\rightarrow \hat{s}_{i_1 \dots i_m} \equiv \sum_{k < l}^m \hat{s}_{i_k i_l}, \\ \hat{s}_{ij} &= \bar{s}_{ij} = (\bar{p}_i + \bar{p}_j)^2, \\ \bar{p}_i^2 &= \mu^2, \end{aligned} \quad (2.183)$$

and rewrite

$$\begin{aligned} d\sigma_{\text{NLO}} &= \int_{d\Phi_m} d\sigma_{\text{NLO}}^V \{s_{i_1 \div i_{m-1}}\} + \lim_{\mu \rightarrow 0} \int_{d\bar{\Phi}_{m+1}} d\sigma_{\text{NLO}}^R \{\hat{s}_{i_1 \div i_m}\}, \\ d\sigma_{\text{NNLO}} &= \int_{d\Phi_m} d\sigma_{\text{NNLO}}^{V,2} \{s_{i_1 \div i_{m-1}}\} + \lim_{\mu \rightarrow 0} \int_{d\bar{\Phi}_{m+1}} d\sigma_{\text{NNLO}}^{V,1} \{\hat{s}_{i_1 \div i_m}\} \\ &\quad + \lim_{\mu \rightarrow 0} \int_{d\bar{\Phi}_{m+2}} d\sigma_{\text{NNLO}}^R \{\hat{s}_{i_1 \div i_{m+1}}\} W_{\text{NNLO}} \{\hat{s}_{i_1 i_2 i_3}\}_{m+2}, \end{aligned} \quad (2.184)$$

where μ is the same regulator used in the IR divergent loop integrals, and

$$W_{\text{NNLO}} \{\hat{s}_{i_1 i_2 i_3}\}_{m+2} = \prod_{i < j < k}^{m+2} \left(\frac{\hat{s}_{ijk}}{\bar{s}_{ijk}} \right)^2, \quad \bar{s}_{ijk} = (\bar{p}_i + \bar{p}_j + \bar{p}_k)^2. \quad (2.185)$$

The proof that eq. (2.184) converges to the right results is simple. First note that the mapping in eq. (2.183) preserves all formal properties of massless kinematics. For instance

$$\hat{s}_{123} = \hat{s}_{12} + \hat{s}_{13} + \hat{s}_{23}. \quad (2.186)$$

Thus, $d\sigma_{\text{NLO}}^R$, $d\sigma_{\text{NNLO}}^{V,1}$ and $d\sigma_{\text{NNLO}}^R$ are gauge invariant by construction. As for the NLO real emission, $\frac{1}{s_{ijk}^2}$ poles are always screened by the requirement

of observing m particles. Therefore, the only possible singular behavior is

$$d\sigma_{\text{NLO}}^R\{\hat{s}_{i_1\div i_m}\} \sim \frac{1}{\hat{s}_{ij}} = \frac{1}{\bar{s}_{ij}} = \frac{1}{(\bar{p}_i + \bar{p}_j)^2}, \quad (2.187)$$

which, being the internal propagator massless, matches the virtual IR poles, as in figure 2.4(b). In the NNLO case, $d\sigma_{\text{NNLO}}^R\{\hat{s}_{i_1\div i_{m+1}}\}$ contains additional $\frac{1}{\hat{s}_{ijk}^2}$ poles, which no longer have the form of massless propagators. In fact, a spurious mass is generated by the gauge invariant mapping of eq. (2.183):

$$\hat{s}_{ijk} = \bar{s}_{ijk} + 3\mu^2 = (\bar{p}_i + \bar{p}_j + \bar{p}_k)^2 + 3\mu^2. \quad (2.188)$$

To cure this, $d\sigma_{\text{NNLO}}^R$ is multiplied by the weight factor in eq. (2.185), which changes – in a gauge invariant way – any pole $\frac{1}{\hat{s}_{ijk}^2}$ to the correct value $\frac{1}{\bar{s}_{ijk}^2}$. The additional integrals, generated when each term in W_{NNLO} does not meet its corresponding pole, vanish in the limit $\mu \rightarrow 0$. This last property follows from the fact that the integral is at most logarithmically divergent.

The reason why a pole cannot be changed *by hand* only in the terms where it appears, is that the logarithmic behavior is reached only *after* gauge cancellations, which should not be altered. This can be easily understood with a toy model:

$$d\sigma_{\text{NNLO}}^R|_{\text{toy}} = \frac{1}{\hat{s}_{12}^2} - \frac{(\hat{s}_{12} + \hat{s}_{13} + \hat{s}_{23})^2}{\hat{s}_{12}^2 \hat{s}_{123}^2}. \quad (2.189)$$

The correct procedure gives

$$\lim_{\mu \rightarrow 0} \int_{d\bar{\Phi}_{m+2}} d\sigma_{\text{NNLO}}^R|_{\text{toy}} W_{\text{NNLO}}\{\hat{s}_{i_1 i_2 i_3}\}_{m+2} = 0, \quad (2.190)$$

while

$$\lim_{\mu \rightarrow 0} \int_{d\bar{\Phi}_{m+2}} \left[\frac{1}{\hat{s}_{12}^2} - \frac{(\hat{s}_{12} + \hat{s}_{13} + \hat{s}_{23})^2}{\hat{s}_{12}^2 \bar{s}_{123}^2} \right] \neq 0. \quad (2.191)$$

We have extended the FDR treatment of the real radiation to NNLO. The outlined strategy opens the possibility of a numerical treatment of NNLO calculations like the one described in Section 2.3.2, similar to the phase-space slicing method at NLO [79]: $\ln \mu^2$ are extracted analytically from the virtual contribution and are then matched with the logs obtained numerically

from the real part. The procedure presented in this section clearly works only when all the integrands of eq. (2.184) are known analytically; nonetheless it can be generalized to allow for a purely numerical treatment of the real in the same way as eq. (2.169) does at NLO. Work to test this NNLO scheme has been planned, but remains out the scope of this thesis.

Chapter 3

FDR at work

After describing all the features of FDR, in this chapter we show them at work on some simple case studies. The calculations presented here are the first ever performed in FDR [74,81], and they stood as a test of the method and as an opportunity of development.

In Section 3.1, the calculation of the amplitude for $H \rightarrow \gamma\gamma$ at one-loop in arbitrary R_ξ -gauge is reported; this calculation provided a powerful test of gauge invariance in FDR, and the first opportunity to work with strings of internal fermions at one loop

In Section 3.2, we treat the gluonic corrections to the same process, $H \rightarrow \gamma\gamma$, in the approximation of large top mass, which required the use of the technology for the computation of two-loop vacuum integrals. The advantages of performing this calculation in FDR, with respect to other more traditional methods, are here summarized:

- order by order renormalization is avoided;
- because the parameter, m_t , does not appear in the final result, its renormalization, compulsory in DR, is avoided altogether in FDR;
- factorizable two-loop integrals are calculated as the product of two one-loop integrals, without any further operation (e.g. the Taylor expansion in ϵ demanded by DR);

Moreover, the properties of the vacuum content subtracted from the definition of the FDR integral were used to design a test for the calculation.

In Section 3.3, the QED Ward identity for $H \rightarrow \gamma\gamma$ is verified at one and two loops, at the integrand level. This illustrates the mechanism that allows FDR to respect gauge invariance.

Finally, in Section 3.4, we consider $H \rightarrow gg$ in HEFT at NLO, as an example of calculation with massless final state, to study the interplay of virtual and real radiation, within FDR-based methods. The analytic computation performed in [78] is reported for completeness, together with various tests for the viability of the numerical approaches.

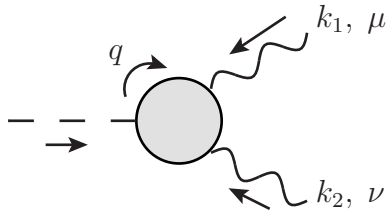


Figure 3.1: Sketch of the Feynman diagrams contributing to the process; the loop can be either fermionic or bosonic (see figures 3.3 and 3.2). The momenta are considered to be all incoming, and the virtual loop momentum q is outgoing from the Higgs vertex.

3.1 $H \rightarrow \gamma\gamma$ at one loop in R_ξ -gauge

We present the first application of FDR [74] to a complete calculation in the EW theory. In order to keep the most general approach, we have decided to work in an arbitrary R_ξ -gauge, thereby explicitly verifying that the method respects gauge invariance. We have chosen to compute the 1-loop on-shell amplitude for the Higgs boson decay into two photons, which has been known since a long time [83–86] and, given its relevance and simplicity, it has been reconsidered a few years ago by several authors [87–97].

Because there is no $H\gamma\gamma$ interaction at tree level in the SM, the process is finite and indirect: it is mediated by either bosonic or fermionic loops. No renormalization is needed, nevertheless infinities arise at intermediate steps of the calculation, which demands to work within a divergence-safe framework, such as FDR. Calculating the bosonic contribution stands as a strong test of the gauge invariance property of FDR. On the other hand, the fermionic contribution gives us the opportunity of illustrating FDR in the presence of fermionic loops.

The two contributions are independent of each other and separately gauge-invariant, so that the generic amplitude can be written as

$$\mathcal{M}(\beta, \eta) = \left(\mathcal{M}_W(\beta) + \sum_f N_c Q_f^2 \mathcal{M}_f(\eta) \right), \quad (3.1)$$

where β and η are dimensionless kinematic parameters defined as

$$\beta = \frac{4 M_W^2}{M_H^2}, \quad \eta = \frac{4 m_f^2}{M_H^2}. \quad (3.2)$$

By denoting with k_1 and k_2 the momenta of the photons, as in figure 3.1, the amplitude reads

$$\mathcal{M} = \mathcal{M}^{\mu\nu} \varepsilon_\mu^*(k_1) \varepsilon_\nu^*(k_2). \quad (3.3)$$

The tensorial structure of $\mathcal{M}^{\mu\nu}$ is dictated by on-shellness and gauge invariance, i.e. $k_i \cdot \varepsilon(k_i) = 0$ and $k_1^\mu \mathcal{M}_{\mu\nu} = k_2^\nu \mathcal{M}_{\mu\nu} = 0$, so that

$$\mathcal{M}^{\mu\nu}(\beta, \eta) = \left(\widetilde{\mathcal{M}}_W(\beta) + \sum_f N_c Q_f^2 \widetilde{\mathcal{M}}_f(\eta) \right) T^{\mu\nu}, \quad (3.4)$$

where $\widetilde{\mathcal{M}}_W$ and $\widetilde{\mathcal{M}}_f$ are scalar form factors of mass dimension -1, and

$$T^{\mu\nu} = k_1^\nu k_2^\mu - (k_1 \cdot k_2) g^{\mu\nu}. \quad (3.5)$$

$\widetilde{\mathcal{M}}_W$ and $\widetilde{\mathcal{M}}_f$ are obtained from the diagrams depicted in figure 3.2 and 3.3 respectively, with the Feynman rules of Appendix C.1. Because we work in an arbitrary R_ξ gauge, also ghost, scalar and mixed vectorial-scalar loops contribute to the bosonic part. Notice that diagrams can be distinguished according to the charge flow in the loop; however, because loops only couple to photons, graphs with the same topology but oppositely charged loops equally contribute to the amplitude. Schematically, naming the contribution of each diagram after the type of particles running in the loop,

$$\mathcal{M}_f = 2 \mathcal{M}_{FFF}, \quad (3.6)$$

as far as the fermionic contribution is concerned, and

$$\begin{aligned} \mathcal{M}_W = & +2 \mathcal{M}_{SSS} + 2 \mathcal{M}_{VVV} + 2 \mathcal{M}_{SVS} + 2 \mathcal{M}_{SSV} + 2 \mathcal{M}_{VSS} \\ & +2 \mathcal{M}_{SVV} + 2 \mathcal{M}_{VVS} + 2 \mathcal{M}_{VSV} + 2 \mathcal{M}_{GGG_+} + 2 \mathcal{M}_{GGG_-} \\ & +2 \mathcal{M}_{SV} + 2 \mathcal{M}_{VS} + \mathcal{M}_{SS} + \mathcal{M}_{VV}, \end{aligned} \quad (3.7)$$

for the bosonic part. Because we work in the R_ξ -gauge, each bosonic diagram depends on the gauge parameter, e.g. $\mathcal{M}_{SV} = \mathcal{M}_{SV}(\beta, \xi)$, but their sum is gauge-invariant, i.e. $\mathcal{M}_W = \mathcal{M}_W(\beta)$.

Even though the final result is finite, UV divergent loop integrals are encountered at intermediate steps. In particular, after simplifying reducible numerators, we deal with integrals with 2 or 3 internal legs and up to tensorial rank 2. Furthermore, the analytic structure of each diagram is characterized

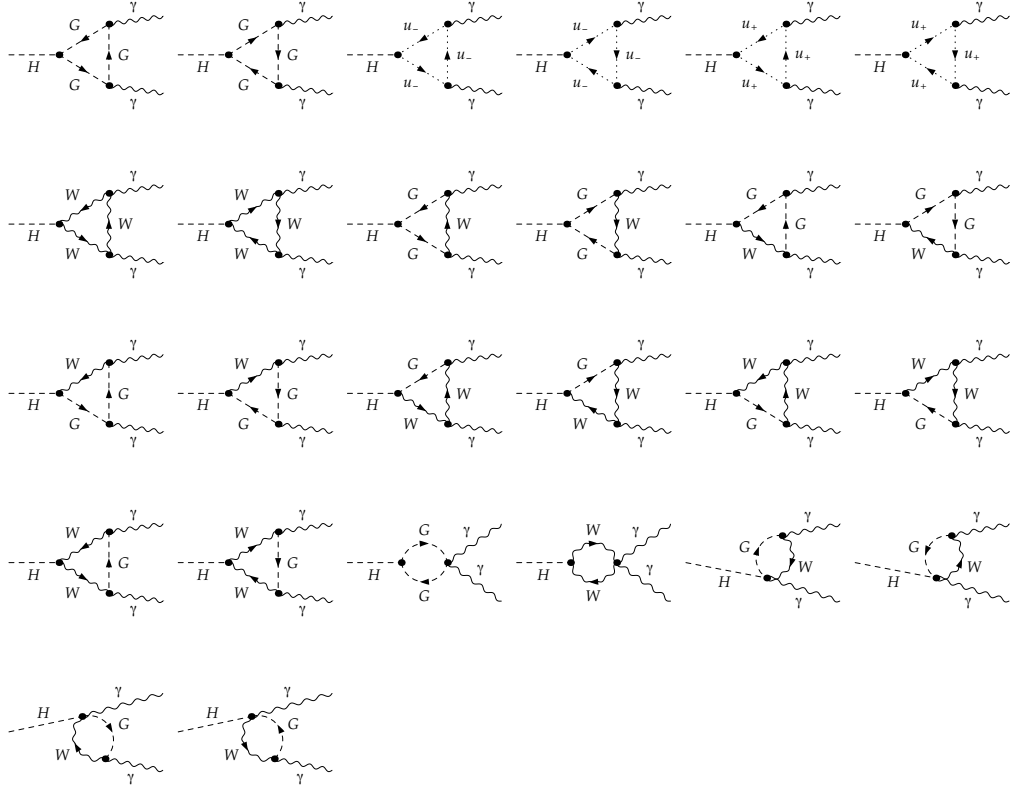


Figure 3.2: Diagrams contributing to the bosonic part of the amplitude (obtained with *FeynArts* [98]). G denotes Goldstone bosons, while u^\pm and \bar{u}^\pm are the charged ghost and anti-ghost fields, respectively.

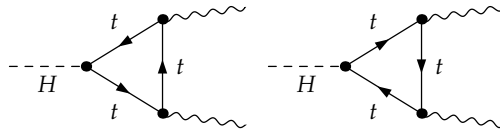


Figure 3.3: Diagrams contributing to the fermionic part of the amplitude (obtained with *FeynArts* [98]).

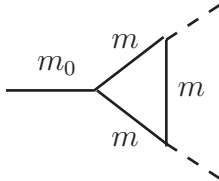


Figure 3.4: Scalar triangle $C_0(0, 0, m_0; m, m, m)$; dashed lines refer to massless particles, solid lines to massive ones.

by either a single threshold, M_W^2 or m_f^2 , or two thresholds M_W^2 and ξM_W^2 . To regularize the infinities, we have used the FDR method described in chapter 2. Instead of calculating the integrals directly, we reduced the amplitude to scalar integrals by using the FDR version of PV reduction explained in Section 2.1.8.2. The amplitude, expressed in terms of tadpoles, self-energies and triangles (A_0 , B_0 and C_0 , respectively), is manifestly gauge-invariant, so that there remain only scalar integrals with a single physical threshold to be evaluated. In particular, all divergent integrals cancel out, and only scalar triangles must be computed, of the type given in figure 3.4. Indeed, by combining the diagrams, performing the PV reduction, and evaluating the scalar integrals, we come by a result consistent with that in [97], which was obtained in DR, i.e.

$$\widetilde{\mathcal{M}}_W(\beta) = \frac{i e^3}{(4\pi)^2 s_W M_W} \left[2 + 3\beta + 3\beta(2 - \beta)f(\beta) \right], \quad (3.8)$$

$$\widetilde{\mathcal{M}}_f(\eta) = \frac{-i e^3}{(4\pi)^2 s_W M_W} 2\eta \left[1 + (1 - \eta)f(\eta) \right], \quad (3.9)$$

where $s_W = \sin \theta_W$ is the sine of the Weinberg mixing angle, and

$$f(x) = -\frac{1}{4} \ln^2 \left(\frac{1 + \sqrt{1-x+i\varepsilon}}{-1 + \sqrt{1-x+i\varepsilon}} \right) = \begin{cases} \arctan^2 \left(\frac{1}{\sqrt{x-1}} \right) & \text{if } x \geq 1 \\ -\frac{1}{4} \left[\ln \left(\frac{1 + \sqrt{1-x}}{1 - \sqrt{1-x}} \right) - i\pi \right]^2 & \text{if } x < 1, \end{cases}$$

where $\varepsilon > 0$ is a small imaginary part allowing for the analytic continuation of the result to any value of x . Indeed, $f(x)$ is a parametrization of the scalar triangle

$$C_0(0, 0, s; M, M, M) = -\frac{2i\pi^2}{s} f(x), \quad x \equiv \frac{4M^2}{s}. \quad (3.10)$$

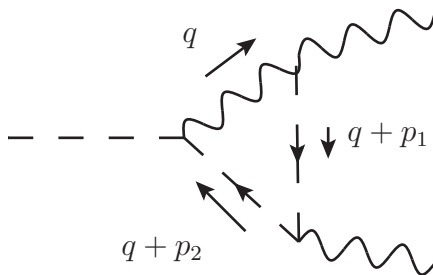


Figure 3.5: Vector-scalar-scalar loop diagram contributing to the bosonic part of the amplitude.

Note that the bosonic form factor in eq. (3.8) contains a constant term, independent of the kinematics. FDR automatically leads to its correct value, while in non-gauge-invariant frameworks it is necessary to enforce gauge-invariance [90,99] or momentum routing invariance [87] as an extra constraint to recover it.

3.1.1 The W loop contribution

In this section, we work out in some detail the contribution to the amplitude coming from the diagram in figure 3.5. This stands as an example to illustrate how to use the FDR method in practice. In particular, we are interested in showing that, thanks to the global treatment of the μ parameter, the integrand within an FDR integral can be algebraically manipulated just in the same way as any integrand of a standard 4- or n -dimensional loop integral. This fact, together with the FDR shift invariance property (see Section 2.1.3), preserves all cancellations required by gauge invariance.

The analytic contribution of the diagram in figure 3.5 to the amplitude \mathcal{M}_W is given by

$$\mathcal{M}_{VSS}^{\mu\nu} = \int [d^4q] J_{VSS}^{\mu\nu}(\bar{q}^2), \quad (3.11)$$

where, according to the Feynman rules in Appendix C.1,

$$J_{VSS}^{\mu\nu}(\bar{q}^2) = \frac{e^3 M_W}{2 s_W} \frac{(2q + p_1 + p_2)^\nu (q + 2p_2)_\rho}{\bar{D}_0 \bar{D}_1 \bar{D}_2} \left[g^{\mu\rho} - \frac{(1 - \xi) q^\mu q^\rho}{(\bar{q}^2 - \xi M_w^2)} \right], \quad (3.12)$$

with $M_0^2 \equiv d_0 = M_w^2$, $M_1^2 = M_2^2 = \xi M_w^2$ and $p_n = \sum_{i=1}^n k_i$. After contracting Lorentz indices, q^2 should be promoted to \bar{q}^2 , as implied by the definition of the FDR integral. The usual algebraic manipulations can then be performed on $J_{VSS}(\bar{q}^2)$.

After simplifying all tensorial integrands appearing in J_{VSS} to irreducible ones, we obtain

$$\begin{aligned} \mathcal{M}_{VSS}^{\mu\nu} = & \frac{e^3 M_W}{2 s_W} \left\{ \frac{-1}{M_W^2} \left[2 \left(B_{2\text{thr}}^{\mu\nu} - B_{1\text{thr}}^{\mu\nu} \right) + (p_1 + p_2)^\nu \left(B_{2\text{thr}}^\mu - B_{1\text{thr}}^\mu \right) \right] \right. \\ & - \left(\xi - \frac{p_2^2}{M_W^2} \right) \left[2 \left(C_{2\text{thr}}^{\mu\nu} - C_{1\text{thr}}^{\mu\nu} \right) + (p_1 + p_2)^\nu \left(C_{2\text{thr}}^\mu - C_{1\text{thr}}^\mu \right) \right] \\ & \left. + \left(2 C_{2\text{thr}}^{\mu\nu} + (p_1 + p_2)^\nu C_{2\text{thr}}^\mu \right) + 2 p_2^\mu \left(2 C_{2\text{thr}}^\nu + (p_1 + p_2)^\nu C_{2\text{thr}} \right) \right\}, \end{aligned} \quad (3.13)$$

where the remaining integrals are scalar and tensorial bubbles and triangles in FDR, to be further reduced via PV reduction. In eq. (3.13) the subscript ‘ n thr’ indicates the number of different thresholds; explicitly

$$\begin{aligned} C_{2\text{thr}}^{\mu_1 \dots \mu_r} &= \int [d^4 q] \frac{q^{\mu_1} \dots q^{\mu_r}}{\overline{D}_0(M_W^2) \overline{D}_1(\xi M_W^2) \overline{D}_2(\xi M_W^2)}, \\ C_{1\text{thr}}^{\mu_1 \dots \mu_r} &= \int [d^4 q] \frac{q^{\mu_1} \dots q^{\mu_r}}{\overline{D}_0(\xi M_W^2) \overline{D}_1(\xi M_W^2) \overline{D}_2(\xi M_W^2)}, \\ B_{2\text{thr}}^{\mu_1 \dots \mu_r} &= \int [d^4 q] \frac{q^{\mu_1} \dots q^{\mu_r}}{\overline{D}_0(M_W^2) \overline{D}_1(\xi M_W^2)}, \\ B_{1\text{thr}}^{\mu_1 \dots \mu_r} &= \int [d^4 q] \frac{q^{\mu_1} \dots q^{\mu_r}}{\overline{D}_0(\xi M_W^2) \overline{D}_1(\xi M_W^2)}, \end{aligned} \quad (3.14)$$

where we have put between parentheses the mass appearing in each propagator.

By similarly treating the other diagrams and putting the contributions together, one obtains the bosonic form factor of eq. (3.8).

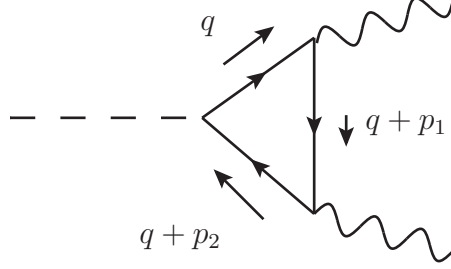


Figure 3.6: Fermionic loop diagram contributing to the amplitude.

3.1.2 The fermionic loop contribution

The contribution to the decay amplitude mediated by a loop of a charged fermion with mass m_f is given by

$$\mathcal{M}_{FFF}^{\mu\nu} = \frac{-e^3 m_f}{2 s_W M_W} \int [d^4 q] \frac{\text{Tr}[(\bar{q} + \not{p}_2 + m_f)\gamma^\nu(\bar{q} + \not{p}_1 + m_f)\gamma^\mu(\bar{q} + m_f)]}{\bar{D}_0 \bar{D}_1 \bar{D}_2}, \quad (3.15)$$

with $M_0 = M_1 = M_2 = m_f$, and where two types of traces containing twice the integration momentum appear, namely

$$\begin{aligned} \text{Tr}[\bar{q} \gamma^\mu \bar{q} \gamma^\nu] &= \text{Tr}[(\not{q} \pm \mu) \gamma^\mu (\not{q} \pm \mu) \gamma^\nu], \\ \text{Tr}[\bar{q} \gamma^\mu \gamma^\nu \bar{q}] &= \text{Tr}[(\not{q} \pm \mu) \gamma^\mu \gamma^\nu (\not{q} \mp \mu)], \end{aligned} \quad (3.16)$$

with \bar{q} defined in accordance with eq. (2.84). This again allows all the usual algebraic manipulations at the level of the FDR integrand; for example

$$\begin{aligned} \int [d^4 q] \frac{\text{Tr}[\bar{q} \gamma^\mu \gamma^\nu \bar{q}]}{\bar{D}_0 \bar{D}_1 \bar{D}_2} &= \int [d^4 q] \frac{4 \bar{q}^2 g^{\mu\nu}}{\bar{D}_0 \bar{D}_1 \bar{D}_2} \\ &= 4 g^{\mu\nu} \left(\int [d^4 q] \frac{1}{\bar{D}_1 \bar{D}_2} + \int [d^4 q] \frac{m_f^2}{\bar{D}_0 \bar{D}_1 \bar{D}_2} \right). \end{aligned} \quad (3.17)$$

After simplifying all reducible numerators we obtain

$$\mathcal{M}_{FFF}^{\mu\nu} = -\frac{e^3 m_f^2}{s_W M_W} \left\{ \begin{aligned} &- 2g^{\mu\nu} B + \left[2(p_1^\mu p_2^\nu + p_2^\mu p_1^\nu) - M_H^2 g^{\mu\nu} \right] C \\ &+ 4(p_1 + p_2)^\nu C^\mu + 4p_1^\mu C^\nu + 8C^{\mu\nu} \end{aligned} \right\}, \quad (3.18)$$

where

$$C^{\mu_1 \dots \mu_r} = \int [d^4 q] \frac{q^{\mu_1} \dots q^{\mu_r}}{\overline{D}_0 \overline{D}_1 \overline{D}_2} \quad \text{and} \quad B = \int [d^4 q] \frac{1}{\overline{D}_0 \overline{D}_2}. \quad (3.19)$$

After a PV reduction of C^μ and $C^{\mu\nu}$ the result of eq. (3.9) easily follows.

3.1.3 Conclusions

We made use of the loop-mediated decay $H \rightarrow \gamma\gamma$ to illustrate some key features of FDR. In particular, we pointed out the mechanisms which lead to an automatic preservation of gauge invariance. To this aim, we performed the calculation in a generic R_ξ gauge, showing that, unlike other four-dimensional methods, FDR naturally produces the correct rational part of the amplitude, with no need to impose extra constraints.

3.2 $H \rightarrow \gamma\gamma$ at two loops

The point of this section is to investigate the behaviour of the FDR method at two loops. We have taken the process $H \rightarrow \gamma\gamma$ as a case study, calculating the $\mathcal{O}(\alpha_S)$ QCD corrections to the on-shell amplitude. The result has been known for a long time [100,101]. For simplicity, we have decided to work in the large top mass limit: the photon production is mediated solely by the top quark, and all scales other than the top mass are neglected. In practice this means that we only deal with vacuum integrals.

In the exact calculation, the top mass renormalization should be performed. In the large top mass limit, because the mass dependence is dropped, UV infinities cancel independently in the diagrams and counter-term diagrams, making the renormalization unnecessary. This is true in FDR as a consequence of the full subtraction of local vacua. In other frameworks, in DR for example, counter-terms do contribute to the finite part of the amplitude, and are therefore required, even though the mass parameter does not appear in the final result.

3.2.1 The calculation

The diagrams contributing to the QCD corrections of the top-loop-mediated Higgs decay into two photons are depicted in figure 3.7. The amplitude reads

$$\mathcal{M} = \mathcal{M}^{\mu\nu} \varepsilon_\mu(p_1) \varepsilon_\nu^*(p_2), \quad (3.20)$$

where p_1 and $-p_2$ are the momenta of the outgoing photons. One has

$$\mathcal{M}^{\mu\nu} = \frac{1}{(2\pi)^2} \frac{\alpha}{\pi} \frac{T^{\mu\nu}}{v} \frac{4}{3} \eta \mathcal{F}(\eta), \quad (3.21)$$

with v being the vacuum expectation value (vev) of the Higgs boson and

$$\eta = \frac{4m^2}{s}, \quad m = m_{\text{top}}, \quad s = (p_1 - p_2)^2 = M_H^2, \quad T^{\mu\nu} = p_2^\mu p_1^\nu + \frac{s}{2} g^{\mu\nu}. \quad (3.22)$$

\mathcal{M} is well defined in the limit $m \rightarrow \infty$ we are interested in. This means that, order by order, the form factor $\mathcal{F}(\eta)$ can be written as

$$\mathcal{F}(\eta) = \mathcal{F}_0 + \frac{\mathcal{F}_1}{\eta} + \frac{\mathcal{F}_2}{\eta^2} + \dots \quad (3.23)$$

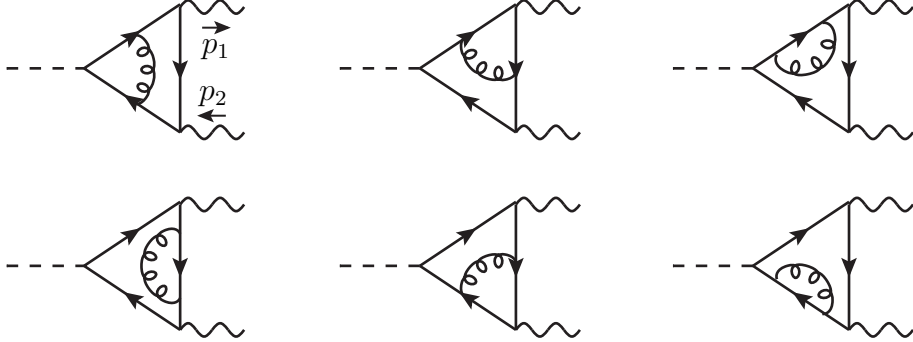


Figure 3.7: Feynman diagrams contributing to the QCD corrections of the top-loop-mediated Higgs decay into two photons. The same diagrams with the electric charge flowing counterclockwise also contribute.

with

$$\mathcal{F}_0 = 0. \quad (3.24)$$

By inserting eq. (3.23) into the expansion in α_S of $\mathcal{F}(\eta)$, one obtains, up to two loops and neglecting $\mathcal{O}(\frac{1}{\eta^2})$ terms,

$$\begin{aligned} \mathcal{F}(\eta) &= \mathcal{F}^{(1)}(\eta) - i \frac{\alpha_S}{3\pi^3} \mathcal{F}^{(2)}(\eta) \\ &\equiv \left(\mathcal{F}_0^{(1)} + \frac{\mathcal{F}_1^{(1)}}{\eta} \right) - i \frac{\alpha_S}{3\pi^3} \left(\mathcal{F}_0^{(2)} + \frac{\mathcal{F}_1^{(2)}}{\eta} \right). \end{aligned} \quad (3.25)$$

At one loop $\mathcal{F}_0^{(1)} = 0$ and (see, for example, [74])

$$\mathcal{F}_1^{(1)} = \frac{4i\pi^2}{3}. \quad (3.26)$$

We re-derive – within the FDR framework – the known result at two loops [102]

$$\begin{aligned} \mathcal{F}_0^{(2)} &= 0, \\ \mathcal{F}_1^{(2)} &= 4\pi^4, \end{aligned} \quad (3.27)$$

which implies that the QCD corrections factorize the one-loop amplitude

$$\mathcal{M} = \mathcal{M}^{(1)} \left(1 - \frac{\alpha_S}{\pi} \right) + \mathcal{O}(\alpha_S^2) + \mathcal{O}\left(\frac{1}{\eta}\right). \quad (3.28)$$

We have used the Feynman rules reported in Appendix C.2.

3.2.2 The building blocks

Since we are working in the large top mass limit, denominators can be expanded as follows

$$\begin{aligned} \frac{1}{(q_i + p_j)^2 - m^2} &= \frac{1}{q_i^2 - m^2} \left(1 - \frac{2(q_i \cdot p_j) + p_j^2}{(q_i + p_j)^2 - m^2} \right) \\ &= \frac{1}{q_i^2 - m^2} \left(1 - \frac{2(q_i \cdot p_j)}{q_i^2 - m^2} + \dots \right), \end{aligned} \quad (3.29)$$

where the on-shell condition $p_j^2 = 0$ for the photons has been used. An expansion to the second order, as the one above, is sufficient to the level of accuracy we are interested in, i.e. $\mathcal{O}(1/\eta)$. All external momenta can then be neglected and the top mass is the only relevant scale. As a consequence, we only have to deal with vacuum integrals.

After cancelling between numerator and denominator the \bar{q}_1^2 , \bar{q}_2^2 , \bar{q}_{12}^2 terms generated by the Feynman rules, tensor integrals up to rank 4 contribute to the amplitude. Because there is no dependence on external momenta, odd rank integrals vanish and we use the formulas collected in Section 2.1.8.1 to perform the tensorial reduction.

Recall that denominators can then be reconstructed by rewriting

$$\begin{aligned} q_1^2 &= \bar{q}_1^2 + \mu^2|_1, & q_2^2 &= \bar{q}_2^2 + \mu^2|_2, \\ 2(q_1 \cdot q_2) &= \bar{q}_{12}^2 - \bar{q}_1^2 - \bar{q}_2^2 + \mu^2|_{12} - \mu^2|_1 - \mu^2|_2. \end{aligned} \quad (3.30)$$

During this tensor decomposition, the $\mu^2|_1$, $\mu^2|_2$, $\mu^2|_{12}$ terms are kept only when they generate a non zero contribution. This means that they should be power-counted as the corresponding squared loop momenta, and contribute only if the integral is divergent (see Section 2.1.5.1). The final result can then be completely expressed in terms of scalar two-loop integrals, products of two one-loop integrals and extra integrals containing $\mu^2|_j$ ($j = 1, 2, 12$).

For convenience, we use the notation

$$[\alpha m] = \int \frac{[d^4 q]}{(\bar{q}^2 - m^2)^\alpha}, \quad (3.31)$$

$$[\alpha m_1 | \beta m_2] = \int \frac{[d^4 q_1]}{(\bar{q}_1^2 - m_1^2)^\alpha} \times \int \frac{[d^4 q_2]}{(\bar{q}_2^2 - m_2^2)^\beta}, \quad (3.32)$$

$$[\alpha m_1 | \beta m_2 | 0] = \int \frac{[d^4 q_1][d^4 q_2]}{(\bar{q}_1^2 - m_1^2)^\alpha (\bar{q}_2^2 - m_2^2)^\beta \bar{q}_{12}^2}, \quad (3.33)$$

and

$$[\alpha m](\mu^2) = \int \frac{[d^4 q] \mu^2}{(\bar{q}^2 - m^2)^\alpha}, \quad (3.34)$$

$$[\alpha m_1 | \beta m_2](\mu^2|_1) = \int \frac{[d^4 q_1] \mu^2|_1}{(\bar{q}_1^2 - m_1^2)^\alpha} \times \int \frac{[d^4 q_2]}{(\bar{q}_2^2 - m_2^2)^\beta},$$

$$[\alpha m_1 | \beta m_2 | 0](\mu^2|_j) = \int \frac{[d^4 q_1][d^4 q_2] \mu^2|_j}{(\bar{q}_1^2 - m_1^2)^\alpha (\bar{q}_2^2 - m_2^2)^\beta \bar{q}_{12}^2}. \quad (3.35)$$

As explained in Section 2.1.7, recall that eq. (3.32) is simply the product of two integrals of the kind given in eq. (3.31); this does not happen in DR, where terms of $\mathcal{O}(\epsilon)$ must be added to the one-loop functions appearing in a two-loop calculation. Moreover, the one-loop and factorizable integrals of eqs. (3.31) and (3.32) can be computed as derivatives of the quadratically divergent one-loop tadpole

$$[\alpha m] = \frac{1}{\Gamma(\alpha)} \frac{d^{\alpha-1}[m]}{d(m^2)^{\alpha-1}}, \quad [m] = -i\pi^2 m^2 \left(\log \frac{m^2}{\mu^2} - 1 \right), \quad (3.36)$$

while those in eq. (3.33) are obtained by deriving with respect to the mass parameters the basic integral $[2m_1 | m_2 | 0]$ of eq. (2.114), that is

$$[\alpha m_1 | \beta m_2 | 0] = \frac{1}{\Gamma(\alpha)\Gamma(\beta)} \frac{d^{\alpha-2}}{d(m_1^2)^{\alpha-2}} \frac{d^{\beta-1}}{d(m_2^2)^{\beta-1}} [2m_1 | m_2 | 0]. \quad (3.37)$$

This implies that for each of the diagrams in figure 3.7 the routing of the momenta is chosen in such a way that as the gluon line gets the momentum q_{12} . This is allowed due to the shift invariance properties of the FDR integration (see Section 2.1.3).

All extra integrals relevant for our calculation can be determined from eqs. (2.77 to 2.79) and eq. (2.62), by using

$$\begin{aligned}
[\alpha m_1 | \beta m_2 | 0](\mu^2|_j) &= \frac{1}{\Gamma(\alpha)\Gamma(\beta)} \frac{d^{\alpha-2}}{d(m_1^2)^{\alpha-2}} \frac{d^{\beta-2}}{d(m_2^2)^{\beta-2}} [2m_1 | 2m_2 | 0](\mu^2|_j), \\
\int [d^4q] \frac{\mu^2}{(\bar{q}^2 - m^2)^\alpha} &= \frac{1}{\Gamma(\alpha)} \frac{d^{\alpha-1}}{d(m^2)^{\alpha-1}} \int [d^4q] \frac{\mu^2}{(\bar{q}^2 - m^2)}. \tag{3.38}
\end{aligned}$$

All two loop integrals necessary for this calculation are reported in Appendix 3.8.

3.2.3 The result

By summing all Feynman diagrams and performing the tensor reduction we end up with

$$\begin{aligned}
\mathcal{F}_0^{(2)} &= -2 [2m | 2m] + 4 [3m | m] - 4m^2 [3m | 2m] + 12m^2 [4m | m] \\
&+ 4 [2m | m | 0] + 12m^2 (2 [3m | m | 0] + [2m | 2m | 0]) \\
&+ 24m^4 ([4m | m | 0] + [3m | 2m | 0]) + 4 [3m | 2m](\mu^2|_1) \\
&+ 8 [3m | m | 0](\mu^2|_1) + 4 [2m | 2m | 0](\mu^2|_1) - 2 [2m | 2m | 0](\mu^2|_{12}) \\
&+ 8m^2 ([3m | 2m | 0](\mu^2|_2) - [3m | 2m | 0](\mu^2|_{12})), \tag{3.39}
\end{aligned}$$

and

$$\begin{aligned}
\mathcal{F}_1^{(2)} = & +\frac{176}{9}m^2 [3m | 2m] - \frac{56}{3}m^2 [4m | m] \\
& - 4m^4 \left(\frac{10}{9} [3m | 3m] - \frac{10}{3} [4m | 2m] + \frac{16}{3} [5m | m] \right) \\
& + 4m^6 \left(\frac{10}{3} [4m | 3m] + 4 [5m | 2m] - \frac{20}{3} [6m | m] \right) \\
& - \frac{320}{9}m^2 [3m | m | 0] - \frac{136}{9}m^2 [2m | 2m | 0] \\
& - \frac{176}{3}m^4 \left([4m | m | 0] + [3m | 2m | 0] \right) \\
& - \frac{224}{3}m^6 \left([5m | m | 0] + [4m | 2m | 0] + \frac{1}{2} [3m | 3m | 0] \right) \\
& - \frac{160}{3}m^8 \left([6m | m | 0] + [5m | 2m | 0] + [4m | 3m | 0] \right) \\
& - 8m^2 [3m | 3m](\mu^2|_1) - 8m^4 [3m | 4m](\mu^2|_1) \\
& + \frac{64}{9}m^2 [3m | 2m | 0](\mu^2|_2) + \frac{80}{9}m^2 [3m | 2m | 0](\mu^2|_{12}) \\
& - 16m^4 \left([4m | 2m | 0](\mu^2|_2) - [4m | 2m | 0](\mu^2|_{12}) \right) \\
& - \frac{64}{3}m^6 \left([5m | 2m | 0](\mu^2|_2) - [5m | 2m | 0](\mu^2|_{12}) \right). \tag{3.40}
\end{aligned}$$

The final result in eq. (3.27) follows by inserting the expressions of the scalar and extra integrals computed as explained in Section 2.1.7.2.

It is important to stress once more that at two loops the one-to-one correspondence between DR and FDR is lost and it is no longer true that FDR integrals are obtained from DR ones after subtracting poles (and universal constants). For example, if we were to interpret the integrals appearing in eq. (3.39) as dimensionally regulated ones, we would not get zero and a $1/\epsilon$ pole would even remain. This can be understood because two different mechanisms to preserve gauge invariance are used by DR and FDR, the latter avoiding an order-by-order renormalization, as we see in the next section.

3.2.4 Renormalization

The results reported in the last section do not require renormalization. This directly follows from the discussion in section 2.2.2.1. FDR renormalization amounts to the mere operation of fixing results in terms of physical quantities, and since the top mass disappears due to the limit $m_{\text{top}} \rightarrow \infty$, no fixing is needed. This *is not* the case when using DR, where renormalization

$$\begin{array}{c} p \\ \curvearrowright \\ \xrightarrow{k} \quad \xrightarrow{j} \\ \text{---} \end{array} = i \delta_{jk} \Sigma(p)$$

Figure 3.8: Top self-energy at $\mathcal{O}(\alpha_S)$.

is necessary in order to compensate spurious ϵ/ϵ constants generated in the limit $n \rightarrow 4$.

Here we demonstrate that if we insist with an order-by-order renormalization we obtain a vanishing contribution to $\mathcal{F}_0^{(2)}$ and $\mathcal{F}_1^{(2)}$. At $\mathcal{O}(\alpha_S)$ the bare (m_0) and physical on-shell (m) top masses satisfy the relation

$$m_0 = m + \delta m, \delta m = \Sigma(m), \quad (3.41)$$

where $\Sigma(p)$ is the top self-energy depicted in figure 3.8 and

$$\Sigma(m) = m \frac{\alpha_S}{3\pi} \left(3 \ln \frac{m^2}{\mu^2} - 5 \right). \quad (3.42)$$

This gives the one-loop counterterms and diagrams of figure 3.9, which generate a contribution to $\mathcal{F}_0^{(2)}$ and $\mathcal{F}_1^{(2)}$ proportional to

$$\mathcal{F}_{0,ct}^{(2)} = i \delta m C_{0,ct} \quad \text{and} \quad \mathcal{F}_{1,ct}^{(2)} = i \delta m C_{1,ct}. \quad (3.43)$$

One computes

$$\begin{aligned} C_{0,ct} &= 8m^2 [3m] + 12m^4 [4m] + 4 [3m] (\mu^2) = 0, \\ C_{1,ct} &= -\frac{16m^2}{3} \left([3m] + 4m^2 [4m] + 5m^4 [5m] + 5m^6 [6m] \right) = 0. \end{aligned} \quad (3.44)$$

Therefore renormalization does not have any effect.

In DR renormalization is necessary. Indeed,

$$C_{0,ct}|_{\text{DR}} = 0 \quad \text{and} \quad C_{1,ct}|_{\text{DR}} = \mathcal{O}(\epsilon), \quad (3.45)$$

so that $C_{1,ct}|_{\text{DR}}$ contributes to the amplitude when multiplied against the $1/\epsilon$ pole contained in $\delta m|_{\text{DR}}$, i.e. the DR counterpart of δm , which is obtained from eq. (3.42) through the replacement of eq. (2.106).

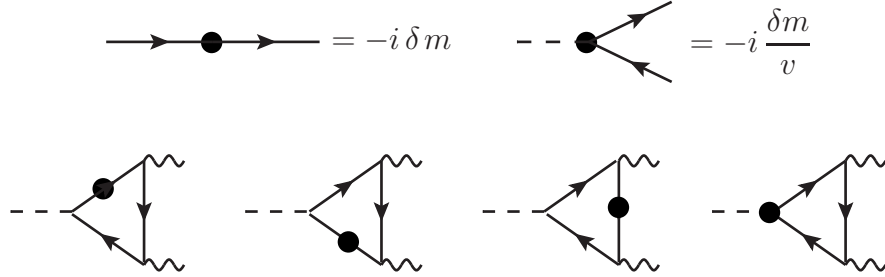


Figure 3.9: One-loop counterterms and diagrams generated by eq. (3.41).

Finally notice that

$$C_{2,\text{ct}} \neq 0, \quad (3.46)$$

and it renormalizes the $\mathcal{O}(\frac{1}{\eta^2})$ of the amplitude, which does depend on the top mass.

3.2.5 The Vacuum Content

In Section 2.1.4, we explained that order by order the vacuum content of an integral has the same dependence on the regulator μ as that of the FDR integral. As a consequence one can consistently trade the UV regulator μ with the renormalization scale μ_R . For brevity, we have so far equated $\mu = \mu_R$, however in the context of this section it is useful to distinguish them.

This property can be exploited to design a test for calculations in the FDR framework: the vacuum content of an amplitude, calculated in any regularization scheme, must have exactly the same dependence on $\log \mu$ as the amplitude itself. In particular, a physical amplitude, being *finite*, is completely independent of μ , and so must be its vacuum content.

The vacuum content of a two-loop integral can be expressed in terms of

three scalar vacua:

$$\begin{aligned} V_1(\mu) &\equiv \int_R d^4q \left[\frac{1}{\bar{q}^4} \right], & V_2(\mu) &\equiv \int_R d^4q_1 d^4q_2 \left[\frac{1}{\bar{q}_1^4} \right] \left[\frac{1}{\bar{q}_2^4} \right], \\ V_3(\mu) &\equiv \int_R d^4q_1 d^4q_2 \left[\frac{1}{\bar{q}_1^4 \bar{q}_2^2 \bar{q}_{12}^2} \right], \end{aligned} \quad (3.47)$$

which are easily calculated by using eq. (2.108) for the first two, and eq. (2.114) for the latter, with μ playing the role of the mass. For example, depending on the scheme used,

$$\begin{aligned} V_3 \Big|_{DR} &= \pi^4 \left\{ \frac{-1}{\epsilon^2} - \left(\frac{1}{\epsilon} + \log \frac{\mu^2}{\mu_R^2} + \Delta \right)^2 + \frac{1}{\epsilon} + \log \frac{\mu^2}{\mu_R^2} + \Delta - \frac{1}{2} - \frac{\pi^2}{12} - f \right\}, \\ V_3 \Big|_{FDR} &= \pi^4 \left(\log \frac{\mu^2}{\mu_R^2} - \frac{1}{2} \log^2 \frac{\mu^2}{\mu_R^2} + f \right), \end{aligned} \quad (3.48)$$

where, in the second equation, we have used FDR as a regularization scheme, upon the introduction of new arbitrary scale which we have called μ_R .

In general,

$$V_i(\mu) = \sum_{j=1,2} \alpha_{ij}^R \log^j \frac{\mu^2}{\mu_R^2} + c_i. \quad (3.49)$$

where μ is the FDR “mass” parameter, whilst μ_R is the arbitrary scale of the regularization scheme elected on which also the constants α_{ij}^R may depend. Recalling eq. (??) from Section 2.2.2.1, we can write a generic two-loop integrand as

$$J(q_1, q_2) = a_0(q_1, q_2) + a_1(q) V_1(\mu) + a_2 V_2(\mu) + a_3 V_3(\mu). \quad (3.50)$$

If J corresponds to a physical (finite) quantity, all $\log(\mu)$ must cancel, which gives a parametric condition on the coefficients a_i 's:

$$\begin{aligned} a_1 &= - \left(\frac{\alpha_{21}}{\alpha_{11}} - \frac{\alpha_{31} \alpha_{22}}{\alpha_{11} \alpha_{32}} \right) t \\ a_2 &= t \\ a_3 &= - \frac{\alpha_{22}}{\alpha_{32}} t. \end{aligned} \quad (3.51)$$

From this, it follows that the vacuum content of a two-loop quantity is in the form

$$\int_R d^4q_1 d^4q_2 J_{INF}(q_1, q_2) = A \left(2i\pi^2 V_1(\mu) + V_2(\mu) - 2V_3(\mu) \right) + B_R, \quad (3.52)$$

where A and B_R do not depend on μ .

In the case of our calculation of interest, we have explicitly verified that the vacuum content of F_0 and F_1 is independent of μ . We introduce the following notation:

$$[I]_R(\mu) = \int_R d^4q_1 d^4q_2 J_{INF}(q_1, q_2) \quad (3.53)$$

if I is the integral of the integrand J whose vacuum configurations are J_{INF} .

By taking the divergent part of eq. (3.39) and (3.40) and replacing each integral with its vacuum configurations, we have obtained

$$[F_0]_{DR} = -8\pi^4 \left(\frac{1}{\epsilon} + \ln \frac{m^2}{\mu_R^2} + \Delta + 1 + \frac{f_{11}}{2} \right), \quad [F_1]_{DR} = 0, \quad (3.54)$$

by working with DR-regulated integrals, and

$$[F_0]_{FDR} = 4\pi^4 f_{11}, \quad [F_1]_{FDR} = 0. \quad (3.55)$$

by using FDR.

Moreover, $[F_0]$ respects eq. (3.52):

$$[F_0] = -2 \left(2i\pi^2 V_1(\mu) + V_2(\mu) - 2V_3(\mu) \right) + B_R \quad (3.56)$$

with

$$B_{FDR} = 0, \quad \text{and} \quad B_{DR} = -2\pi^4 \left(\frac{2}{\epsilon} + 4 \ln \frac{m^2}{\mu_R^2} + 3 \right). \quad (3.57)$$

The constants do not cancel out because the FDR definition implies a subtraction of something more than just the poles.

3.2.5.1 Calculating the vacuum content of an integral

Here we collect some technical remarks regarding the calculation of the vacuum content of an integral.

- The vacuum of the product of integrals is not the product of the vacuum contents of the factors. If $I_i = F_i + [I_i]$,

$$[I_1 I_2] = [I_1]F_2 + [I_2]F_1 - [I_1][I_2] \quad (3.58)$$

The generalization of this formula is trivial.

- The vacuum content of an extra integral is null in FDR, however it is finite and non-null in all other regularization methods. In particular, if $I(\mu^2)$ is a generic extra-integral, from eq. (2.10), we have that

$$[I(\mu^2)]_{FDR} = 0, \quad [I(\mu^2)]_R = -I(\mu^2)|_{FDR}. \quad (3.59)$$

The constants generated in this way play a role in the determination of the vacuum content, for example if one of I_1, I_2 in eq. (3.58) is an extra-integral.

3.2.5.2 Tensorial reduction of the vacuum content

In FDR, also the tensorial vacuum configurations are subtracted. Since tensors, beyond one loop, are not defined in the same way in DR and FDR, it is not obvious that one could perform a tensorial reduction over the vacuum configurations.

Consider an example:

$$\int [d^4 q_1][d^4 q_2] \frac{q_1^\mu q_1^\nu}{\overline{D}_1^3 \overline{D}_2 \overline{D}_{12}} = g^{\mu\nu} \sum_i c_i \int d^4 q_1 d^4 q_2 S_i(q_1, q_2) \quad (3.60)$$

where

$$\frac{q_1^\mu q_1^\nu}{\overline{D}_1^3 \overline{D}_2 \overline{D}_{12}} = J_V^{\mu\nu}(q_1, q_2) + J_F^{\mu\nu}(q_1, q_2) \quad (3.61)$$

and

$$J_F^{\mu\nu}(q_1, q_2) = g^{\mu\nu} \sum_i c_i S_i(q_1, q_2) \quad (3.62)$$

Alternatively:

$$\int [d^4 q_1][d^4 q_2] \frac{q_1^\mu q_1^\nu}{\overline{D}_1^3 \overline{D}_2 \overline{D}_{12}} = g^{\mu\nu} \sum_i c_i \int d^4 q_1 d^4 q_2 \tilde{S}_i(q_1, q_2) \quad (3.63)$$

and

$$\tilde{S}_i(q_1, q_2) = V_i(q_1, q_2) + S_i(q_1, q_2). \quad (3.64)$$

However, the vacuum by construction is

$$J_V^{\mu\nu}(q_1, q_2). \quad (3.65)$$

In the present case, also

$$J_V^{\mu\nu}(q_1, q_2) = g^{\mu\nu} \sum_i c_i V_i(q_1, q_2). \quad (3.66)$$

Moreover, we have verified that the tensorial vacuum is equal to the vacuum of the tensorially reduced amplitude in the case of $H \rightarrow \gamma\gamma$. We may conjecture that this is always the case as long as physical quantities are concerned; further investigation is needed in this respect.

3.2.6 Conclusions

The calculation presented in this section was the first ever performed in FDR at two loops. The $\mathcal{O}(\alpha_S)$ corrections to the $H \rightarrow \gamma\gamma$ amplitude –mediated by an infinitely heavy top loop– have been computed in a fully four-dimensional fashion. This example has allowed us to demonstrate that FDR is an approach to loop calculations in which

- order-by-order renormalization is avoided;
- a finite renormalization is only needed to fix the parameters of the theory in terms of experimental observables;
- ℓ -loop integrals are directly re-usable in $(\ell+1)$ -loop calculations, with no need of further expanding in ϵ .

Due to its four-dimensionality we envisage a great potential of FDR in further simplifying NNLO computations. More investigation is needed in this direction, that we plan to undertake in the near future.

3.3 Ward identities for $H \rightarrow \gamma\gamma$ at one and two loops

In the two previous sections the one- and two-loop amplitude for the process $H \rightarrow \gamma\gamma$ have been derived by entirely working in the FDR framework. The gauge-invariant results that were obtained stand as a strong test that the method respects gauge invariance. In this section we explicitly verify the Ward identities at the integrand level for the one- and two-loop amplitudes, to make more transparent the diagrammatic argument that proves gauge invariance in FDR.

3.3.1 The QED Ward identity

The Ward identity is a direct consequence of gauge invariance. Classically, gauge fields couple to conserved currents, i.e. the Lagrangian exhibits a term

$$A^\mu j_\mu \quad \text{with} \quad \partial^\mu j_\mu = 0 . \quad (3.67)$$

In quantum mechanics, this is rephrased as the current being transverse with respect to the direction of the photon momentum p , i.e.

$$p^\mu j_\mu = 0 . \quad (3.68)$$

If $\varepsilon^\mu(p)$ is the polarization vector of the photon, the amplitude

$$\mathcal{M}(p) = \varepsilon^\mu(p) \mathcal{M}_\mu(p) \quad (3.69)$$

vanishes if we replace the polarization vector with the momentum, of the photon i.e.

$$p^\mu \mathcal{M}_\mu(p) = 0 . \quad (3.70)$$

In other words, the amplitude itself must be transverse to the photon momentum. Eq. (3.70) is the QED Ward identity; it can be shown that it is valid to all orders in perturbation theory [103].

Gauge invariance is a property of the amplitude. As such, it must be satisfied at the integrand level, i.e. the diagram level, before traces over fermionic lines are calculated, or the tensorial reduction is performed. The subsequent manipulations that one does may break gauge invariance, depending on the

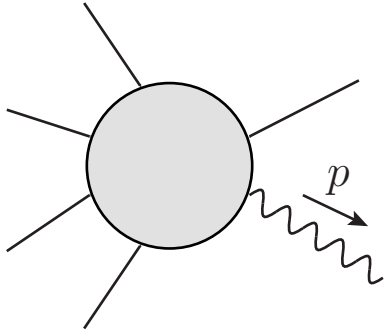


Figure 3.10: amplitude for a generic process with an external photon of momentum p : $\mathcal{M}(p) = \varepsilon^\mu \mathcal{M}_\mu(p)$. The Ward identity states that the amplitude vanishes if we replace the photon polarization vector with its momentum, i.e. $p^\mu \mathcal{M}_\mu(p) = 0$.

method used. For example, concerning tensorial reduction, we have seen PV reduction as a technique that preserves gauge invariance. In the same way, at the level of the calculation of the integrals, where a regularization scheme must be introduced, DR does respect gauge invariance, while other techniques, such as a trivial cut-off method, Pauli-Villars or BPHZ, break this property of the amplitude, and can be used only upon restauration of gauge invariance by hand.

This is why in sec. 2.2.1 was suggested that gauge invariance implies a tight interplay between numerator and denominator: being a property of the integrand, the regularization scheme, in order for it to preserve gauge invariance, must be as respectful as possible of the structure of the integrand. With this perspective it is easily understood why DR preserves gauge invariance: changing the dimension of the integral measure, although not physically transparent, leaves the integrand untouched.

Within the FDR framework, while the actual integral one performs is a four-dimensional standard one (linear, shift-invariant, ...), the integrand is altogether changed. Its mechanism for preserving gauge invariance is a bit more sophisticated with respect to DR, and it involves the global prescription and the definition of extra-integrals. It is therefore interesting to verify gauge invariance at the integrand level in FDR, to convince ourselves that the manipulations that we make are indeed safe.

3.3.2 The Feynman identity

We will take $H \rightarrow \gamma\gamma$, mediated by a fermion with mass m , as a case study. In this case The proof of gauge invariance relies on the graphical equivalence depicted in figure 3.11, which, in turn, is realized by the Feynman

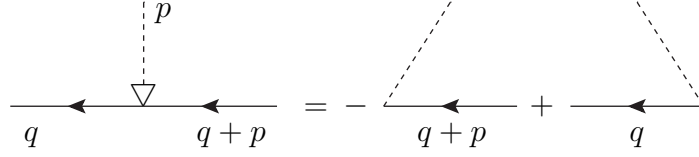


Figure 3.11: Graphical representation of the Feynman identity in eq. (3.71). The dashed line represents a scalar photon.

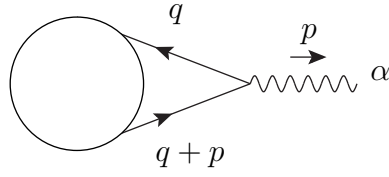


Figure 3.12: Generic ℓ -loop amplitude with an external photon with momentum p . The blob stands for the rest of the amplitude and q is an integration momentum.

identity [71]

$$\frac{\not{q} + m}{D} \not{p} \frac{\not{q} + \not{p} + m}{D_p} = \frac{\not{q} + m}{D} - \frac{\not{q} + \not{p} + m}{D_p}, \quad (3.71)$$

where

$$D = q^2 - m^2 \quad \text{and} \quad D_p = (q + p)^2 - m^2. \quad (3.72)$$

Consider now the generic ℓ -loop amplitude in figure 3.12. Its integrand reads

$$\varepsilon_\alpha(p) J^\alpha = \varepsilon_\alpha(p) \sum_i \frac{1}{DD_p} \text{Tr} [(\not{q} + m) \gamma^\alpha (\not{q} + \not{p} + m) (\Gamma_o^i + \Gamma_e^i)], \quad (3.73)$$

where the sum is over all contributing Feynman diagrams, while Γ_o^i and Γ_e^i are proportional to a product of respectively an odd or an even number of gamma matrices. In general, $J^\alpha = J^\alpha(q, \dots, q_\ell)$, and also $\Gamma_{o,e}^i = \Gamma_{o,e}^i(q, \dots, q_\ell)$. Gauge invariance requires that

$$p_\alpha \int [d^4 q] \cdots [d^4 q_\ell] \bar{J}^\alpha(q, \dots, q_\ell) = 0, \quad (3.74)$$

where \bar{J}^α is the integrand in eq. (3.73) regulated *à la* FDR by replacing $q_i^2 \rightarrow q_i^2 - \mu^2$ in both numerators and denominators according to the global prescription. Eq. (3.74) can be directly proven at the integrand level. With this aim, we first concentrate on the replacements responsible for the conservation of the specific current in figure 3.12:

$$J^\alpha \rightarrow J'^\alpha = \sum_i \frac{1}{\overline{D}\overline{D}_p} \left(Tr [\not{q}\gamma^\alpha \not{q}\Gamma_o^i] + Tr [\not{q}\gamma^\alpha \not{p}\Gamma_o^i] + m^2 Tr [\gamma^\alpha \Gamma_o^i] \right. \\ \left. + m Tr [\gamma^\alpha (\not{q} + \not{p})\Gamma_e^i] + m Tr [\not{q}\gamma^\alpha \Gamma_e^i] \right), \quad (3.75)$$

where the loop denominators in $\Gamma_{o,e}^i$ are also barred. In the previous equation

$$\not{q} = \not{q} \pm \mu, \quad (3.76)$$

with the sign chosen as in eq. (2.84), has the effect of changing q^2 to \bar{q}^2 in the first trace; in the remaining traces, the same replacement has no effect, because it generates a term proportional to a vanishing trace of an odd number of Dirac matrices. With more photons, replacements as in eq. (3.76) have to be performed for all integration momenta appearing in the trace, after summing over all internal indices.

Back to eq. (3.75), when contracting with p , it is possible to reconstruct the denominators \overline{D} and \overline{D}_p in the numerator, and subsequently simplify with the denominator

$$p_\alpha J'^\alpha = \sum_i \frac{1}{\overline{D}} \left(Tr [\not{q}\Gamma_o^i] + m Tr [\Gamma_e^i] \right) \\ - \frac{1}{\overline{D}_p} \left(Tr [(\not{q} + \not{p})\Gamma_o^i] + m Tr [\Gamma_e^i] \right), \quad (3.77)$$

in agreement with the Feynman identity in eq. (3.71). This clearly shows that the Feynman identity, within a realistic amplitude, is satisfied thanks to the possibility of reconstructing the denominators; this is why it is crucial to correctly put into practice the global prescription. After that, the Ward identity

$$p_\alpha \int [d^4q] \cdots [d^4q_\ell] J'^\alpha(q, \cdots, q_\ell) = 0 \quad (3.78)$$

directly follows from the shift invariance properties of the loop integrals, as in DR. In the following two sections we explicitly test eq. (3.78) at one and two loops for $H \rightarrow \gamma\gamma$ in FDR.

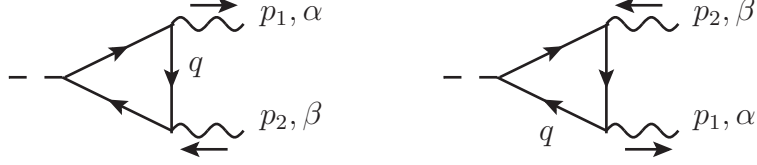


Figure 3.13: Feynman diagrams contributing to the amplitude for $H \rightarrow \gamma\gamma$ mediated by fermions at one loop. The loop momentum q has been assigned to the internal line that follows the vertex with the photon p_1 , so that in both diagrams the momentum routing of fig. 3.12 is respected.

3.3.3 The Ward Identity at one loop

We now apply the general treatment of the last section to our case study, i.e. $H \rightarrow \gamma\gamma$ at one loop, as in fig. 3.13. We use the notation:

$$\overline{D}_i = (q + p_i)^2 - m^2 - \mu^2, \quad p_0 = 0, \quad (3.79)$$

$$p_{12} = p_1 - p_2. \quad (3.80)$$

At one loop,

$$\mathcal{M}_1(H \rightarrow \gamma\gamma) \propto \varepsilon_\alpha^*(p_1) \varepsilon_\beta^*(p_2) \int [d^4q] J_1^{\alpha\beta}(q), \quad (3.81)$$

where

$$J_1^{\alpha\beta} = \frac{\text{Tr}[\gamma^\alpha (\not{q} + \not{p}_1 + m) (\not{q} + \not{p}_2 + m) \gamma^\beta (\not{q} + m)]}{\overline{D}_0 \overline{D}_1 \overline{D}_2} + (p_1, \alpha \leftrightarrow -p_2, \beta). \quad (3.82)$$

By shifting the loop momentum of the second diagram so that it reflects the routing of fig. 3.13, $J_1^{\alpha\beta}$ can be rewritten in the form of eq. (3.73), that is

$$J_1^{\alpha\beta} = \frac{1}{\overline{D}_0 \overline{D}_1} \text{Tr} [(\not{q} + m) \gamma^\alpha (\not{q} + \not{p}_1 + m) (\Gamma_o^\beta + \Gamma_e^\beta)], \quad (3.83)$$

with

$$\Gamma_o^\beta = m \gamma^\beta \left(\frac{1}{\overline{D}_2} + \frac{1}{\overline{D}_{12}} \right) \equiv \Gamma_o^{\beta,(1)}(q) + \Gamma_o^{\beta,(2)}(q), \quad (3.84)$$

$$\Gamma_e^\beta = \frac{\not{q} + \not{p}_2}{\overline{D}_2} \gamma^\beta + \gamma^\beta \frac{\not{q} + \not{p}_{12}}{\overline{D}_{12}} \equiv \Gamma_e^{\beta,(1)}(q) + \Gamma_e^{\beta,(2)}(q). \quad (3.85)$$

The indices (1) and (2) in the above expressions refer to the first and second diagram of fig. 3.13. By applying the Feynman identity on the product $J_1^{\alpha\beta} p_{1\alpha}$ one obtains

$$\frac{\text{Tr}[\not{q} \Gamma_o^\beta] + m \text{Tr}[\Gamma_e^\beta]}{\overline{D}_0} = \frac{\text{Tr}[(\not{q} + \not{p}_1) \Gamma_o^\beta] + m \text{Tr}[\Gamma_e^\beta]}{\overline{D}_1}, \quad (3.86)$$

like in eq. (3.77). The Ward identity of eq. (3.78) is realized if the loop momentum is conveniently shifted in the terms of the last equation. Namely, by noticing that

$$\frac{\not{q} \Gamma_o^{\beta,(1)}(q)}{\overline{D}_0} = \frac{-m \Gamma_e^{\beta,(1)}(-q - p_2)}{\overline{D}_0} \quad (3.87)$$

$$\frac{\not{q} \Gamma_o^{\beta,(2)}(q)}{\overline{D}_0} = \frac{-m \Gamma_e^{\beta,(2)}(-q - p_{12})}{\overline{D}_0} \quad (3.88)$$

and

$$\frac{(\not{q} + \not{p}_1) \Gamma_o^{\beta,(1)}(q)}{\overline{D}_1} = \frac{-m \Gamma_e^{\beta,(1)}(-q - p_{12})}{\overline{D}_1} \quad (3.89)$$

$$\frac{(\not{q} + \not{p}_1) \Gamma_o^{\beta,(2)}(q)}{\overline{D}_1} = \frac{-m \Gamma_e^{\beta,(2)}(-q - p_2)}{\overline{D}_1} \quad (3.90)$$

one can verify that

$$p_{1\alpha} \int [d^4 q] J_1^{\alpha\beta} = 0. \quad (3.91)$$

To prove eq. (3.91) we made explicit use of the Feynman identity. In the following we show that the same result can be obtained by reconstructing the denominators in eq. (3.82) directly. Indeed, by performing some algebra in the trace, $J_1^{\alpha\beta}$ of eq. (3.82) can be rearranged as

$$\begin{aligned} J_1^{\alpha\beta} = \frac{m}{\overline{D}_0 \overline{D}_1 \overline{D}_2} & \left(2m^2 \text{Tr}[\gamma^\alpha \gamma^\beta] - 2\overline{q}^2 \text{Tr}[\gamma^\alpha \gamma^\beta] + 8 \{ \gamma^\alpha, \not{q} \} \{ \gamma^\beta, \not{q} \} \right. \\ & + 4 \{ \gamma^\alpha, \not{q} \} \{ \gamma^\beta, \not{p}_2 \} + 4 \{ \gamma^\beta, \not{q} \} \{ \gamma^\alpha, \not{p}_1 \} \\ & \left. + \text{Tr}[\gamma^\alpha \not{p}_1 \not{p}_2 \gamma^\beta] + \text{Tr}[\gamma^\beta \not{p}_2 \not{p}_1 \gamma^\alpha] \right). \quad (3.92) \end{aligned}$$

where the curly brackets represent an anticommuting operator, i.e. $\{ \gamma^\alpha, \gamma^\beta \} = \gamma^\alpha \gamma^\beta + \gamma^\beta \gamma^\alpha$. By contracting with $p_{1\alpha}$, we reconstruct the denominator \overline{D}_1

so that

$$\begin{aligned}
J_1^{\alpha\beta} p_{1\mu} &= \frac{m}{\overline{D}_0 \overline{D}_1 \overline{D}_2} \left(-4 \overline{D}_0 \{ \gamma^\beta, \not{p}_1 \} + 8 (\overline{D}_1 - \overline{D}_0) \{ \gamma^\beta, \not{q} \} \right. \\
&\quad \left. + 4 (\overline{D}_1 - \overline{D}_0) \{ \gamma^\beta, \not{p}_2 \} \right) \\
&= 4m \frac{\{ \gamma^\beta, \not{q} + \not{p}_2 \}}{\overline{D}_0 \overline{D}_2} - 4m \frac{\{ \gamma^\nu, \not{q} + \not{p}_2 \}}{\overline{D}_0 \overline{D}_1} \\
&\quad + 4m \frac{\{ \gamma^\nu, \not{q} \}}{\overline{D}_0 \overline{D}_2} - 4m \frac{\{ \gamma^\nu, \not{q} + \not{p}_1 \}}{\overline{D}_1 \overline{D}_2}. \tag{3.93}
\end{aligned}$$

With the shift $q \rightarrow -q - p_2$ the first term cancels the third one; similarly the second term cancels the fourth by shifting $q \rightarrow -q - p_1 - p_2$. This proves again eq. (3.91).

3.3.4 The Ward Identity at two loops

We now verify eq. (3.78) for $H \rightarrow \gamma\gamma$ at two loops. We refer to fig. (3.7) and we use the following notation:

$$\overline{D}_{i,j} = (q_i + p_j)^2 - m^2 - \mu_i^2 \tag{3.94}$$

$$q_{12} = q_1 - q_2 \tag{3.95}$$

$$p_{12} = p_1 - p_2, \quad p_0 = 0. \tag{3.96}$$

For the purpose of this section, there is no need to take the limit of large top mass as in Section 3.2, so that the denominators do contain external momenta. The two-loop correction to the amplitude can be expressed in terms of the integrand $J_2^{\alpha\beta}$, that is

$$\mathcal{M}_2 \propto \varepsilon_\alpha^*(p_1) \varepsilon_\beta^*(p_2) \int [d^4 q_1] [d^4 q_2] J_2^{\alpha\beta}(q_1, q_2), \tag{3.97}$$

and the Ward identities we are interested in verifying reads

$$p_{1\alpha} \int [d^4 q_1] [d^4 q_2] J_2^{\alpha\beta}(q_1, q_2) = 0. \tag{3.98}$$

Let us indicate with I_i , where $i = 1, \dots, 12$, each Feynman diagram contracted with the photon momentum p_1^α . In fig. 3.7, diagrams are labelled from 1 to 6 starting from the top left one; the same diagrams, with photons

exchanged, are labelled with the indices 7 to 12. The Ward identity is then rephrased: since

$$p_{1\alpha} J_2^{\alpha\beta} \equiv \sum_{i=1}^{12} I_i, \quad \text{then} \quad \sum_{i=1}^{12} \int [d^4 q_1][d^4 q_2] I_i(q_1, q_2) = 0. \quad (3.99)$$

At two loops, each I_i is a made of large expression. For shortness we introduce some extra notation. The fermionic lines are indicated by

$$f(q_i, p_j) \equiv \frac{\not{q}_i + \not{p}_j + m}{D_{i,j}} \equiv \not{f}(i, j) + m d(i, j), \quad (3.100)$$

where

$$\not{f}(i, j) \equiv \frac{\not{q}_i + \not{p}_j}{D_{i,j}}, \quad d(i, j) \equiv \frac{1}{D_{i,j}}. \quad (3.101)$$

In terms of this functions, the Feynman identity for the photon with momentum p_1 is rewritten as

$$f(q_1, 0) \not{p}_1 f(q_1, p_1) = f(q_1, 0) - f(q_1, p_1) \equiv \overline{f(q_1, 0)}. \quad (3.102)$$

The contributions of the diagrams can be organized in three patterns:

$$\begin{aligned}
& \text{Tr}[\gamma^\rho f(q_{i_1}, p_{j_1}) \gamma^\nu f(q_{i_2}, p_{j_2}) \gamma_\rho f(q_{k_1}, p_{h_1}) f(q_{k_2}, p_{h_2})] \\
&= \left\{ -2m \text{Tr}[\gamma^\nu \mathfrak{f}(i_1, j_1) \mathfrak{f}(k_1, h_1) \mathfrak{f}(i_2, j_2)] d(k_2, h_2) \right. \\
&\quad - 2m^3 \text{Tr}[\gamma^\nu \mathfrak{f}(k_1, h_1)] d(i_1, j_1) d(i_2, j_2) d(k_1, h_1) \\
&\quad \left. ((k_1, h_1) \leftrightarrow (k_2, h_2)) \right\} + \\
&+ \left\{ 2m \text{Tr}[\gamma^\nu \mathfrak{f}(i_1, j_1)] d(i_2, j_2) \{ \mathfrak{f}(k_1, h_1), \mathfrak{f}(k_2, h_2) \} \right. \\
&\quad + 4m^3 \text{Tr}[\gamma^\nu \mathfrak{f}(i_1, j_1)] d(i_2, j_2) d(k_1, h_1) d(k_2, h_2) \\
&\quad \left. ((i_1, j_1) \leftrightarrow (i_2, j_2)) \right\} \\
&\equiv \text{Tr}_1(\nu, (i_1, j_1), (k_1, h_1), (k_2, h_2), (i_2, j_2)), \tag{3.103}
\end{aligned}$$

$$\begin{aligned}
& \text{Tr}[\gamma^\rho f(q_i, p_j) \gamma_\rho f(q_{k_1}, p_{h_1}) f(q_{k_2}, p_{h_2}) \gamma^\nu f(q_{k_3}, p_{h_3})] \\
&= \left\{ -2m \text{Tr}[\mathfrak{f}(i, j) \mathfrak{f}(k_1, h_1) \mathfrak{f}(k_2, h_2) \gamma^\nu] d(k_3, h_3) \right. \\
&\quad - 2m \text{Tr}[\mathfrak{f}(i, j) \mathfrak{f}(k_1, h_1) \gamma^\nu \mathfrak{f}(k_3, h_3)] d(k_2, h_2) \\
&\quad - 2m \text{Tr}[\mathfrak{f}(i, j) \mathfrak{f}(k_2, h_2) \gamma^\nu \mathfrak{f}(k_3, h_3)] d(k_1, h_1) \\
&\quad - m \text{Tr}[\mathfrak{f}(k_1, h_1) \mathfrak{f}(k_2, h_2) \gamma^\nu \mathfrak{f}(k_3, h_3)] d(i, j) \\
&\quad + \left(m^3 \text{Tr}[\gamma^\nu \mathfrak{f}(k_1, h_1)] d(i, j) d(k_2, h_2) d(k_3, h_3) \right. \\
&\quad \quad \left. + (1 \leftrightarrow 2) + (1 \leftrightarrow 3) \right) \\
&\quad \left. - 2m^3 \text{Tr}[\gamma^\nu \mathfrak{f}(i, j)] d(k_1, h_1) d(k_2, h_2) d(k_3, h_3) \right\} \\
&\equiv \text{Tr}_2(\nu, (k_3, h_3), (i, j), (k_1, h_1), (k_2, h_2)), \tag{3.104}
\end{aligned}$$

$$\begin{aligned}
& \text{Tr}[\gamma^\rho f(q_i, p_j) \gamma_\rho f(q_{k_1}, p_{h_1}) \gamma^\nu f(q_{k_2}, p_{h_2}) f(q_{k_3}, p_{h_3})] \\
&= \left\{ -2m \text{Tr}[\mathfrak{f}(i, j) \mathfrak{f}(k_1, h_1) \gamma^\nu \mathfrak{f}(k_2, h_2)] d(k_3, h_3) \right. \\
&\quad - 2m \text{Tr}[\mathfrak{f}(i, j) \mathfrak{f}(k_1, h_1) \gamma^\nu \mathfrak{f}(k_3, h_3)] d(k_2, h_2) \\
&\quad - 2m \text{Tr}[\mathfrak{f}(i, j) \gamma^\nu \mathfrak{f}(k_2, h_2) \mathfrak{f}(k_3, h_3)] d(k_1, h_1) \\
&\quad - m \text{Tr}[\mathfrak{f}(k_1, h_1) \gamma^\nu \mathfrak{f}(k_2, h_2) \mathfrak{f}(k_3, h_3)] d(i, j) \\
&\quad + \left(m^3 \text{Tr}[\gamma^\nu \mathfrak{f}(k_1, h_1)] d(i, j) d(k_2, h_2) d(k_3, h_3) \right. \\
&\quad \quad \left. + (1 \leftrightarrow 2) + (1 \leftrightarrow 3) \right) \\
&\quad \left. - 2m^3 \text{Tr}[\gamma^\nu \mathfrak{f}(i, j)] d(k_1, h_1) d(k_2, h_2) d(k_3, h_3) \right\} \\
&\equiv \text{Tr}_3(\nu, (k_2, h_2), (k_3, h_3), (i, j), (k_1, h_1)). \tag{3.105}
\end{aligned}$$

Tr_1 , Tr_2 and Tr_3 keep their form under shift of integration momenta. For example,

$$\text{Tr}_i(\nu, (1, 0), (2, 12), (2, 0), (1, 12)) \xrightarrow{q_i \rightarrow q_i + p_2} \text{Tr}_i(\nu, (1, 2), (2, 1), (2, 2), (1, 1)).$$

By routing the internal momenta in such a way that the vertex of fig. 3.12 is recreated in each diagram, all I_i are proportional to the factor $\overline{f(q_1, 0)}$ as defined in eq. (3.102). This means that we can use the Feynman identity, so that

$$I_i = \text{Tr}[\overline{f(q_1, 0)} \dots] = I_i^{(0)} - I_i^{(1)} \quad (3.106)$$

$$\text{with } I_i^{(0)} = \text{Tr}[f(q_1, 0) \dots], \quad \text{and } I_i^{(1)} = \text{Tr}[f(q_1, p_1) \dots] \quad (3.107)$$

In table 3.1 we report the contribution of each I_i in terms of the functions Tr_j . Looking at the shape of these contributions – i.e. whether they can be expressed as Tr_1 , Tr_2 or Tr_3 functions) – one can argue that, in order to satisfy the Ward identity of eq. (3.99), cancellations must take place within the following subgroups:

$$\begin{aligned} I_1 + I_5 + I_7 + I_8 &\rightarrow 0 \\ I_2 + I_4 + I_6 + I_{12} &\rightarrow 0 \\ I_3 + I_9 + I_{10} + I_{11} &\rightarrow 0. \end{aligned} \quad (3.108)$$

The convenient shifts in loop momenta must be designed, by looking for particular symmetries relating the diagrams of each subgroup.

Taking $I_i^{(n)} = I_i^{(n)}(q_1, q_2)$ as a function of the internal momenta, the following equations hold:

$$\begin{aligned} I_1^{(1)}(q_1, q_2) &= -I_5^{(2)}(q_2, q_1), \\ I_7^{(2)}(q_1, q_2) &= -I_8^{(1)}(q_2, q_1), \\ I_5^{(1)}(q_2, q_1) &= -I_8^{(2)}(q_2 - p_{12}, q_1 - p_{12}), \\ I_7^{(1)}(q_1, q_2) &= -I_1^{(2)}(q_1 - p_2, q_2 - p_2). \end{aligned} \quad (3.109)$$

These imply that the first of (3.108) is true, i.e.

$$\int [d^4 q_1][d^4 q_2] \left(I_1 + I_5 + I_7 + I_8 \right) = 0. \quad (3.110)$$

$$\begin{aligned}
I_1 &= \text{Tr} \left[\overline{f(q_1, 0)} \gamma^\rho f(q_2, p_1) f(q_2, p_2) \gamma^\rho f(q_1, p_2) \gamma^\nu \right] \\
&= \text{Tr}_1(\nu, (1, 2), (2, 1), (2, 2), (1, 0)) - \text{Tr}_1(\nu, (1, 2), (2, 1), (2, 2), (1, 1)) \\
I_7 &= \text{Tr} \left[\overline{f(q_1, 0)} \gamma^\nu f(q_1, p_{12}) \gamma^\rho f(q_2, p_{12}) f(q_2, p_0) \gamma^\rho \right] \\
&= \text{Tr}_1(\nu, (1, 0), (2, 12), (2, 0), (1, 12)) - \text{Tr}_1(\nu, (1, 1), (2, 12), (2, 0), (1, 12)) \\
I_2 &= \text{Tr} \left[\overline{f(q_1, 0)} \gamma^\rho f(q_2, p_1) f(q_2, p_2) \gamma^\nu f(q_2, p_0) \gamma^\rho \right] \\
&= \text{Tr}_2(\nu, (2, 0), (1, 0), (2, 1), (2, 2)) - \text{Tr}_2(\nu, (2, 0), (1, 1), (2, 1), (2, 2)) \\
I_8 &= \text{Tr} \left[\overline{f(q_1, 0)} \gamma^\rho f(q_2, p_1) \gamma^\nu f(q_2, p_{12}) \gamma^\rho f(q_1, p_{12}) \right] \\
&= \text{Tr}_1(\nu, (2, 1), (1, 12), (1, 0), (2, 12)) - \text{Tr}_1(\nu, (2, 1), (1, 12), (1, 0), (2, 12)) \\
I_3 &= \text{Tr} \left[\overline{f(q_1, 0)} f(q_1, p_2) \gamma^\rho f(q_2, p_2) \gamma^\rho f(q_1, p_2) \gamma^\nu \right] \\
&= \text{Tr}_3(\nu, (1, 0), (1, 2), (2, 2), (1, 2)) - \text{Tr}_3(\nu, (1, 1), (1, 2), (2, 2), (1, 2)) \\
I_9 &= \text{Tr} \left[\overline{f(q_1, 0)} \gamma^\nu f(q_1, p_{12}) f(q_1, p_0) \gamma^\rho f(q_2, p_0) \gamma^\rho \right] \\
&= \text{Tr}_3(\nu, (1, 12), (1, 0), (2, 0), (1, 0)) - \text{Tr}_3(\nu, (1, 12), (1, 0), (2, 0), (1, 1)) \\
I_4 &= \text{Tr} \left[\overline{f(q_1, 0)} f(q_1, p_2) \gamma^\nu f(q_1, p_0) \gamma^\rho f(q_2, p_0) \gamma^\rho \right] \\
&= \text{Tr}_2(\nu, (1, 0), (2, 0), (1, 0), (1, 2)) - \text{Tr}_2(\nu, (1, 0), (2, 0), (1, 1), (1, 2)) \\
I_{10} &= \text{Tr} \left[\overline{f(q_1, 0)} \gamma^\rho f(q_2, p_1) \gamma^\rho f(q_1, p_1) \gamma^\nu f(q_1, p_{12}) \right] \\
&= \text{Tr}_3(\nu, (1, 12), (1, 0), (2, 1), (1, 1)) - \text{Tr}_3(\nu, (1, 12), (1, 1), (2, 1), (1, 1)) \\
I_5 &= \text{Tr} \left[\overline{f(q_1, 0)} f(q_1, p_2) \gamma^\rho f(q_2, p_2) \gamma^\nu f(q_2, p_0) \gamma^\rho \right] \\
&= \text{Tr}_1(\nu, (2, 2), (1, 0), (1, 2), (2, 0)) - \text{Tr}_1(\nu, (2, 2), (1, 1), (1, 2), (2, 0)) \\
I_{11} &= \text{Tr} \left[\overline{f(q_1, 0)} \gamma^\rho f(q_2, p_1) \gamma^\nu f(q_2, p_{12}) f(q_2, p_0) \gamma^\rho \right] \\
&= \text{Tr}_3(\nu, (2, 12), (2, 0), (1, 0), (2, 1)) - \text{Tr}_3(\nu, (2, 12), (2, 0), (1, 1), (2, 1)) \\
I_6 &= \text{Tr} \left[\overline{f(q_1, 0)} \gamma^\rho f(q_2, p_1) \gamma^\rho f(q_1, p_1) f(q_1, p_2) \gamma^\nu \right] \\
&= \text{Tr}_2(\nu, (1, 0), (2, 1), (1, 1), (1, 2)) - \text{Tr}_2(\nu, (1, 1), (2, 1), (1, 1), (1, 2)) \\
I_{12} &= \text{Tr} \left[\overline{f(q_1, 0)} \gamma^\nu f(q_1, p_{12}) \gamma^\rho f(q_2, p_{12}) \gamma^\rho f(q_1, p_{12}) \right] \\
&= \text{Tr}_2(\nu, (1, 12), (2, 12), (1, 12), (1, 0)) - \text{Tr}_2(\nu, (1, 12), (2, 12), (1, 12), (1, 1))
\end{aligned}$$

Table 3.1: Contribution to $p_{1\alpha} J_2^{\alpha\beta}$ of each Feynman diagram appearing in fig. 3.7.

Analogously

$$\begin{aligned}
I_4^{(2)}(q_1, q_2) &= -I_2^{(1)}(q_2, q_1), \\
I_6^{(1)}(q_1, q_2) &= -I_2^{(2)}(q_2, q_1), \\
I_4^{(1)}(q_1, q_2) &= -I_{12}^{(2)}(q_1 - p_{12}, q_2 - p_{12}), \\
I_6^{(2)}(q_1, q_2) &= -I_{12}^{(1)}(q_1 + p_2, q_2 + p_2),
\end{aligned} \tag{3.111}$$

and

$$I_9^{(2)}(q_1, q_2) = -I_{11}^{(2)}(q_2, q_1) \tag{3.112}$$

$$I_{10}^{(1)}(q_1, q_2) = -I_{11}^{(2)}(q_2, q_1) \tag{3.113}$$

$$I_{10}^{(2)}(q_1, q_2) = -I_5^{(1)}(q_1 + p_{12}, q_2 + p_{12}) \tag{3.114}$$

$$I_9^{(1)}(q_1, q_2) = -I_5^{(2)}(q_1 - p_2, q_2 - p_2) \tag{3.115}$$

respectively imply the second and last of eq. (3.108). Altogether this proves eq. (3.99), i.e the Ward identity at two loops for $H \rightarrow \gamma\gamma$.

3.4 $H \rightarrow gg$ at NLO

We consider the NLO gluonic correction to $H \rightarrow gg(g)$ mediated by an infinitely massive top loop as a case study for putting into practice the FDR treatment of IR divergences, as outlined in Section 2.3. First we review the analytic result [78]. Despite its simplicity this process provides a rich example as it involves the renormalization of α_S and the combination of real and virtual radiation in order to cancel the IR $\ln \mu$.

We then move on to computing the inclusive and differential decay rate numerically with a MC. We explore the three approaches described in Section 2.3.2 and Section 2.3.3: naive numerical combination with and without analytic knowledge on the integrand, and numerical integration after local subtraction.

3.4.1 Preliminaries

For this calculation we use purely gluonic QCD and the HEFT model, as described in Appendix C.3, where the Feynman rules used in this section can also be found. The diagrams contributing to the decay rate at NLO are depicted in fig. 3.14. The inclusive decay rate reads [78]

$$\Gamma_{NLO}(H \rightarrow gg(g)) = \Gamma_0 + \Gamma_1 = \Gamma^{(0)}(\alpha_S(M_H^2)) \left(1 + \frac{95}{4} \frac{\alpha_S}{\pi} \right), \quad (3.116)$$

where the Born decay rate is given by

$$\Gamma_0 = \Gamma^{(0)}(H \rightarrow gg) = A^2 \frac{M_H^3}{8\pi} = \frac{\alpha_S^2 M_H^3}{72 \pi^3 v^2}, \quad (3.117)$$

while the NLO radiative correction is the result of the combination of the virtual and real radiation, i.e.

$$\Gamma_1 = \Gamma_V^{(1)}(H \rightarrow gg) + \Gamma_R^{(0)}(H \rightarrow ggg) = \frac{95}{4} \frac{\alpha_S}{\pi}. \quad (3.118)$$

$\Gamma_V^{(1)}(H \rightarrow gg)$ is the renormalized decay rate at one-loop, and $\Gamma_R^{(0)}(H \rightarrow ggg)$ is at tree-level. The analytic expressions for $\Gamma_V^{(1)}$ and $\Gamma_R^{(0)}$ calculated in [78] are reported in eq. (3.125) and eq. (3.135).

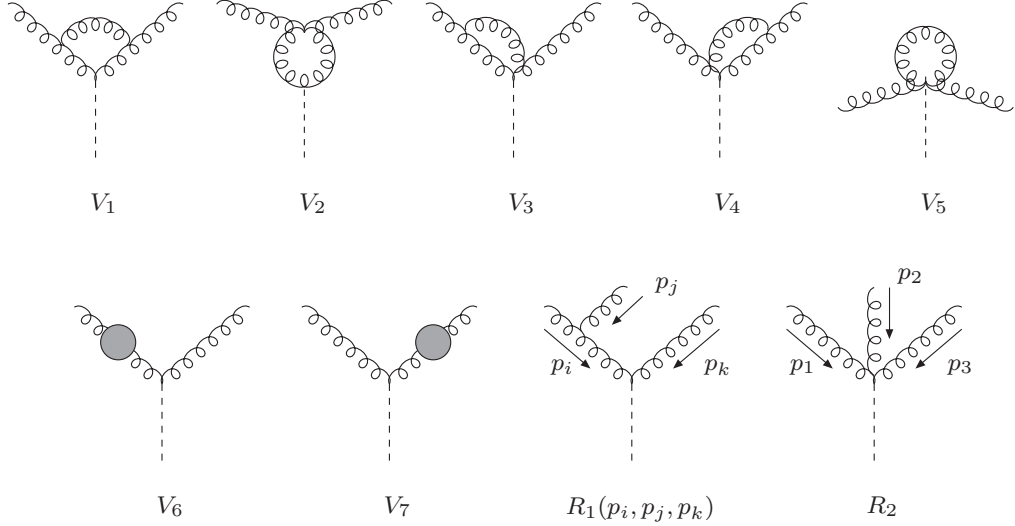


Figure 3.14: Feynman diagrams contributing to the NLO decay rate of $H \rightarrow gg$. V_1 to V_7 represent the virtual corrections at one loop; the gray blobs stand for gluon wave function correction. $R_1(p_i, p_j, p_k)$, corresponding to three diagrams with permuted gluons, and R_2 contribute to the real correction.

3.4.1.1 Renormalization

At NLO, the process is affected by the renormalization of α_S , which must be taken into account in order to cancel the $\ln \mu = \ln \mu_R$ of UV origin arising in the one-loop amplitude of $H \rightarrow gg$. Because FDR integrals are already finite, the procedure to undertake is a finite renormalization (see Section 2.2.2), with the aim of relating the bare coupling constant to a physical observable. In practice, for α_S , this means replacing it with the running coupling constant, thereby trading the renormalization scale μ_R for a physical one relevant for the process, in this case $s = M_H^2$. At one loop, the QCD running coupling constant reads

$$\alpha_S(M_H^2) = \frac{\alpha_S(\mu^2)}{1 + \frac{\alpha_S}{2\pi} \ln \frac{M_H^2}{\mu^2}}, \quad (3.119)$$

which is the usual expression calculated in $\overline{\text{MS}}$. Indeed, the expressions calculated in $\overline{\text{DRed}}$ and DR coincide, which means that eq. (3.119) can be

straightforwardly imported in FDR.

On top of the running of α_S , we must also take into account the finite renormalization of the HEFT effective coupling constant A ,

$$A = \frac{\alpha_S}{3\pi v} \left(1 + \frac{11}{4} \frac{\alpha_S}{\pi} \right). \quad (3.120)$$

By inserting these contributions into the Born decay rate of eq. (3.117), we obtain that

$$\Gamma^{(0)} + \Gamma_{ren}^{(1)} = \Gamma^{(0)}(\alpha_S(M_H^2)) \left[1 + \frac{11}{2} \frac{\alpha_S}{\pi} \left(1 + \ln \frac{M_H^2}{\mu^2} \right) \right]. \quad (3.121)$$

The $\ln(M_H^2/\mu^2)$ in the last expression will compensate the $\ln \mu$ with UV origin arising in the virtual contribution.

3.4.1.2 Analytic calculation of the virtual correction

The renormalized decay rate for $H \rightarrow gg$ at one-loop is given by the $\mathcal{O}(\alpha_S)$ contribution of the renormalization of the coupling constants -eq. (3.121)- plus the contribution of the one-loop diagrams of fig. 3.14; that is

$$\Gamma_V^{(1)}(H \rightarrow gg) = \Gamma_{ren}^{(1)} + \Gamma_{correction}^{(1)} \quad (3.122)$$

where

$$\Gamma_{correction}^{(1)} = \frac{3}{2} \frac{\alpha_S}{\pi} \Gamma^{(0)}(\alpha_S(M_H^2)) \left(\pi^2 - \ln^2 \frac{M_H^2}{\mu^2} \right). \quad (3.123)$$

To obtain the last equation, one needs to know that UV and IR divergent one-loop integrals are scaleless and vanish as explained in Section 2.1.9.1; then, with eq. (2.147), the triangle with overlapping soft and collinear divergences can be evaluated. All logs come from the loop integration, the phase space integration being trivial; indeed, since all external particles are massless,

$$\int d\Phi_2 = \frac{\pi}{2}. \quad (3.124)$$

Plugging eq. (3.123) and eq. (3.121) into $\Gamma_V^{(1)}$, we obtain that

$$\Gamma_V^{(1)}(H \rightarrow gg) = \frac{3}{2} \frac{\alpha_S}{\pi} \Gamma^{(0)}(\alpha_S(M_H^2)) \left(\pi^2 + \frac{11}{3} + \frac{11}{3} \ln \frac{M_H^2}{\mu^2} - \ln^2 \frac{M_H^2}{\mu^2} \right), \quad (3.125)$$

where all UV $\ln \mu$ cancelled with the renormalization, and the remaining $\ln \mu$ have IR origin; this means that μ is not an arbitrary scale, but an actual IR cut-off, i.e. $\mu \rightarrow 0$. The logs will cancel when eq. (3.125) is combined with the contribution coming from the real radiation.

3.4.1.3 The three-body massive phase space

Before giving the analytic result for the real contribution that was calculated in [78], it is worthwhile to spend a few words on the three-body phase space itself. In Section 2.1.9, we explained how FDR treats the real radiation in order to allow for a realization of the K.L.N. theorem: the external unobserved particles, just like virtual unobserved particles in the loop case, get a small mass μ^2 . The range over which the phase space integral is performed is then accordingly modified.

The three-body phase space differential is

$$d\Phi_3 = \prod_{i=1}^3 d^4 p_i \delta(p_i^2 - \mu^2) \theta(E_i) \delta^{(4)}(P - p_1 - p_2 - p_3), \quad (3.126)$$

with $P^2 = M_H^2 = s$. It is also useful at times to express it in other ways, e.g.

$$\begin{aligned} d\Phi_3 &= \frac{\pi^2}{4s} ds_{12} ds_{13} ds_{23} \delta(s + 3\mu^2 - s_{12} - s_{13} - s_{23}) \\ &= \frac{s \pi^2}{4} dx dy dz \delta(1 - x - y - z) \end{aligned} \quad (3.127)$$

where we have introduced the Mandelstam variables $s_{ij} = (p_i + p_j)^2$ with $i \neq j$, as well as the Dalitz variables

$$x = \frac{s_{12} - \mu^2}{s}, \quad y = \frac{s_{13} - \mu^2}{s}, \quad z = \frac{s_{23} - \mu^2}{s}, \quad (3.128)$$

obeying $x + y + z = 1$. In all equations above the external momenta p_i with $i = 1, 2, 3$ have been given a small mass μ , but notice that the momentum conservation is unchanged. The integration range is then that of three particles with identical mass, as shown in fig. ??, and it obviously depends on μ^2 :

$$\begin{aligned} s_{13} : s_{13}^{(-)} &\mapsto s_{13}^{(+)} \\ s_{12} : 4\mu^2 &\mapsto (\sqrt{s} - \mu)^2 \end{aligned} \quad (3.129)$$

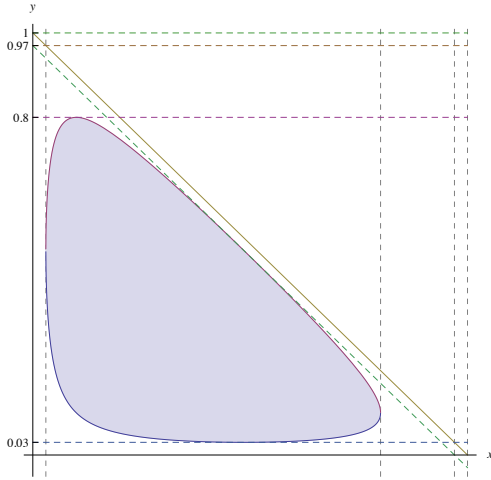


Figure 3.15: Phase space for three particles with the same mass $\mu = 0.01$, in the Dalitz plane xy . The triangle, defined by $y = 1 - x$, is the phase space for three massless particles. The borders of the triangle correspond to configurations in which at least one of the Dalitz variables is zero, thereby leading to divergences in the phase space integration. Deforming the integration region as prescribed by FDR is a way of avoiding these problematic regions.

where

$$s_{13}^{(\pm)} = \frac{(s - \mu^2)^2 - (sR_0 \mp sR_1)^2}{4s_{12}}$$

$$sR_0 = \sqrt{s_{12}(s_{12} - 4\mu^2)}, \quad sR_1 = \sqrt{(s - s_{12} + \mu^2)^2 - 4\mu^4}. \quad (3.130)$$

3.4.2 Analytic calculation of the real correction

The computation of the decay rate of $H \rightarrow ggg$ is easy at the level of matrix elements, because the Born amplitude is all we need; the phase space integration, on the other hand, is more complicated than the two-body case, because more legs are involved, and because divergences arise when integrating over external momenta that get small or collinear to each other.

The tree-level matrix elements for $H \rightarrow ggg$, read from the real emission diagrams of fig. 3.14, are given by

$$|\mathcal{M}|^2 = 192 \pi \alpha_S A^2 R(s_{12}, s_{13}, s_{23}) \quad (3.131)$$

with $R(s_{12}, s_{13}, s_{23}) = f(s_{12}, s_{13}, s_{23}) + f(s_{12}, s_{23}, s_{13}) + f(s_{23}, s_{13}, s_{12})$, and

$$f(s_{12}, s_{13}, s_{23}) = \frac{s_{23}^3}{s_{12}s_{13}} + \frac{2(s_{12}^2 + s_{13}^2) + 3s_{12}s_{13}}{s_{23}} + 6s_{23} \quad (3.132)$$

where the FDR replacement of eq. (2.163), $2(p_i \cdot p_j) \rightarrow s_{ij}$, has been brought about, with the logic explained in Section 2.3.1 and depicted in fig. 2.5. In

order to evaluate the decay rate for $H \rightarrow ggg$, given by

$$\Gamma_R^{(1)}(H \rightarrow ggg) = \frac{1}{12 (2\pi)^5 M_H} \int_{\mu} d\Phi_3 |\mathcal{M}(H \rightarrow ggg)|^2, \quad (3.133)$$

we need the following phase space integrals:

$$\begin{aligned} \Phi_3(s) &\equiv \int d\Phi_3 = \frac{\pi^2 s}{8}, \\ F(s) &\equiv \int d\Phi_3 s_{ij} = \frac{\pi^2 s^2}{24}, \\ J_p(s, \mu^2) &\equiv \int_{\mu} d\Phi_3 \frac{(s_{ij})^p}{s_{kl}} = -\frac{\pi^2 s^p}{4(p+1)} \left(\log \frac{\mu^2}{s} + \frac{1}{1+p} + 2 \sum_{n=1}^{p+1} \frac{1}{n} \right), \\ I(s, \mu^2) &\equiv \int_{\mu} d\Phi_3 \frac{1}{s_{kl} s_{ij}} = \frac{\pi^2}{8s} \left(\log^2 \frac{\mu^2}{s} - \pi^2 \right). \end{aligned} \quad (3.134)$$

Notice that the last two equations are valid only for small values of μ (i.e. any polynomial dependence of μ has been dropped). With these results at hand, and taking $s = M_H^2$, it is easily shown that

$$\Gamma_R^{(0)}(H \rightarrow ggg) = \frac{3}{2} \frac{\alpha_S}{\pi} \Gamma^{(0)}(\alpha_S(M_H^2)) \left(-\pi^2 + \frac{73}{6} - \frac{11}{3} \ln \frac{M_H^2}{\mu^2} + \ln^2 \frac{M_H^2}{\mu^2} \right). \quad (3.135)$$

The combination of this equation and of eq. (3.125) returns the NLO correction to the decay rate of eq. (3.118). All logs have cancelled exactly; in particular, the cancellation of the double log, originated by overlapping soft and collinear singularities, is due to the following relation:

$$\text{Re} \left[\frac{C(s, \mu^2)}{i\pi^2} \right] = \frac{4}{\pi^2} I(s, \mu^2) \quad (3.136)$$

where $C(s, \mu^2)$ is the loop triangle of eq. (2.147) and $I(s, \mu^2)$ is the last integral of eq. (3.134).

3.4.2.1 Comparing with DR

As explained in Section 2.1.7.1, at one loop, there is a one-to-one relationship between integrals calculated in DRed and FDR,

$$\ln \mu \rightarrow \ln \mu - \frac{1}{\epsilon} - \frac{\Delta}{2}, \quad \Delta \equiv \gamma_E + \ln \pi. \quad (3.137)$$

This correspondence goes beyond the loop integrals, in that also the IR logs obtained from phase space integration in FDR can be mapped into single or double poles in DRed.

As a consistency check, let's test this statement on the divergent integrals of eq. (3.134). As far as purely collinear singularities are concerned, the DR version of J_p reads

$$\begin{aligned} J_p^{\text{DR}}(s) &= \frac{\pi^{2+\frac{\epsilon}{2}} s^{p+\frac{\epsilon}{2}}}{2\Gamma(1+\frac{\epsilon}{2})} \int dx dy dz \frac{x^p}{y} \delta(1-x-y-z) (xyz)^{\frac{\epsilon}{2}} \\ &= -\frac{\pi^2 s^p}{4(p+1)} \left(\ln \frac{\mu^2}{s} - \frac{2}{\epsilon} - \Delta \right) + \frac{1}{p+1} + 2 \sum_{n=1}^{p+1} \frac{1}{n} \end{aligned} \quad (3.138)$$

which indeed coincides with J_p in eq. (3.134), if we remove the pole and the universal constants.

Regarding the overlapping IR/CL singularities that generate the $\ln^2(\mu^2)$ term in $I(s, \mu^2)$, they drop when adding virtual and fully inclusive real contributions, as a consequence of eq. (3.136). Exactly the same happens also in DR. Indeed,

$$\mathcal{R}e \left[\frac{1}{i\pi^2} \int d^n q \frac{1}{q^2(q+p_1)^2(q+p_2)^2} \right] = \frac{1}{s} (\pi s)^{\frac{\epsilon}{2}} \Gamma\left(1 - \frac{\epsilon}{2}\right) \left[\frac{4}{\epsilon^2} - \frac{2}{3} \pi^2 \right], \quad (3.139)$$

where $p_1^2 = p_2^2 = 0$ and $s = -2(p_1 \cdot p_2)$, and

$$\begin{aligned} I^{\text{DR}}(s) &= \frac{\pi^{2+\frac{\epsilon}{2}} s^{\frac{\epsilon}{2}-1}}{4\Gamma(1+\frac{\epsilon}{2})} \int dx dy dz \frac{1}{xy} \delta(1-x-y-z) (xyz)^{\frac{\epsilon}{2}} \\ &= \frac{\pi^{2+\frac{\epsilon}{2}} s^{\frac{\epsilon}{2}-1}}{4} \Gamma\left(1 - \frac{\epsilon}{2}\right) \left[\frac{4}{\epsilon^2} - \frac{2}{3} \pi^2 \right]. \end{aligned} \quad (3.140)$$

In summary, eq. (3.137) is the only needed relation to relate FDR and DRed expressions at one loop.

3.4.3 Naive numerical combination

In general, the dependence on $\ln \mu$ of the virtual part comes from the loops, which makes it straightforward to perform the phase space integral analytically. As for the real part, the phase-space integration depends logarithmically on μ . In the simple case we are considering, an analytic result

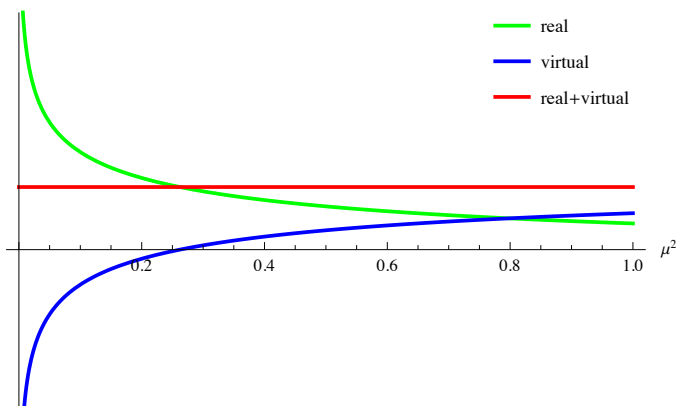


Figure 3.16: We have plotted the analytic expression of $\Gamma_{\mathcal{V}}^{(1)}$ and $\Gamma_{\mathcal{R}}^{(0)}$, together with their combination, against μ^2 , with $s = 100$. The sum of the two contributions is a constant, obtained, when $\mu^2 \ll 1$, as the cancellation of big numbers; for this reason, a numerical approach is potentially unstable in this region.

can be achieved, but as the process becomes more involved the phase space integration quickly reaches a complexity that makes it futile to tackle the problem analytically. In general, it is more convenient to set up a MC integration, as described in Section 2.3.2 and Section 2.3.3 in Chapter 2.

A first rough numerical approach to the problem consist in verifying the convergence of the limit

$$\lim_{\mu \rightarrow 0} \left(\Gamma_{\mathcal{V}}^{(1)}(\ln \mu_0, \ln^2 \mu_0) + \Gamma_{\mathcal{R}}^{(0)}(\ln \mu_0, \ln^2 \mu_0) \right) = \Gamma_1, \quad (3.141)$$

with $\mu_0 = \mu^2/s$; in fig. 3.16 the analytic realization of such limit is represented. In the following, we take the analytic expression of eq. (3.125) for the virtual contribution, and the numeric integral for the real radiation, that is

$$\Gamma_{\mathcal{R}}^{(0)}|_{MC} = \frac{4\alpha_S \Gamma^{(0)}(\alpha_S(s))}{\pi^3 s^2} \int_{MC} d\Phi_3 R(s_{12}, s_{13}, s_{23}) \quad (3.142)$$

where $R(s_{12}, s_{13}, s_{23})$ is defined in eq. (3.132), and the MC employed is a multi-channel approach optimized on this process (see Appendix D). In fig. 3.17, we have plotted the combination of these two contributions, normalized to one, against small values of μ^2 . Notice that as μ^2 becomes larger, the error decreases because the integrand is less peaked, but the central value gets less and less compatible with the normalization, which was obtained in

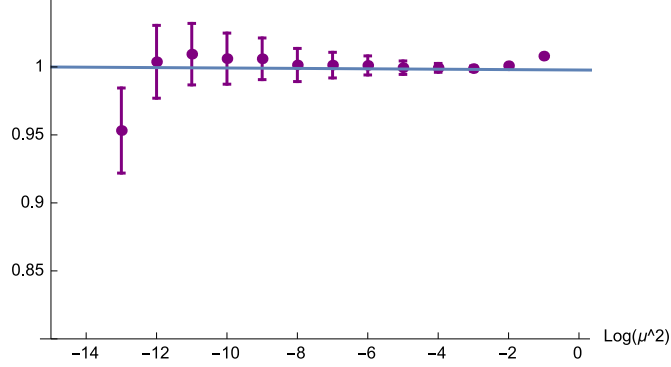


Figure 3.17: The combination of $\Gamma_{\mathcal{R}}^{(0)}|_{MC}$ and $\Gamma_{\mathcal{V}}^{(1)}$ - normalized to one - is plotted against μ^2 in logarithmic scale. For this result we have employed $s = 100$, and $N_{MC} = 10^7$ random points to generate the phase space.

the limit $\mu \rightarrow 0$. On the other side of the plot, for very small values of μ , deviations from one are due to numerical fluctuations, up to a level in which they become fatal to the MC. Despite this, we can conclude that for

$$\mu^2 \geq 10^{-12},$$

the naive numerical combination described in Section 2.3.2 produces a consistent result.

On the technical side, we have used the massive kinematics prescribed by FDR, i.e

$$p_i^2 = \mu^2, \quad p_{ij}^2 = (p_i + p_j)^2 = s_{ij}, \quad (p_1 + p_2 + p_3)^2 = s. \quad (3.143)$$

We chose a multi-channel MC approach, in order to accomodate the different shapes of the terms in the integrand of eq. (3.132). In particular, three types of channel appear:

- the single-pole channel $\frac{1}{s_{ij}}$, for which

$$\int d\Phi_3(p_1, p_2, p_3) \frac{1}{s_{ij}} = \int \frac{ds_{ij}}{s_{ij}} d\Phi_2(p_i, p_j) d\Phi_2(p_k, p_{ij}). \quad (3.144)$$

In a MC generator, first one needs to produce the distribution of s_{ij} in the range

$$2\mu \leq \sqrt{s_{ij}} \leq \sqrt{s} - \mu, \quad (3.145)$$

then one can generate the subsequent two-body decays, respecting the conditions of on-shellness and momentum conservation.

- the double pole $\frac{1}{s_{ij}s_{kl}}$, for which

$$\int d\Phi_3 \frac{1}{s_{i_1 i_2} s_{i_3 i_4}} = \int_R \frac{ds_{i_1 i_2}}{s_{i_1 i_2}} \frac{ds_{i_3 i_4}}{s_{i_3 i_4}}. \quad (3.146)$$

Both distributions are produced as independent singly-peaked functions within the range of (3.145); then a veto is put on the points that do not respect

$$y_-(x) < y < y_+(x) \quad (3.147)$$

where x , y and y_{\pm} are defined respectively in (3.128) and (3.129) after a change of variable.

- finally the convergent part, which is integrated using a flat channel, namely *RAMBO* [104].

More details on the MC technique employed are discussed in Appendix D.

3.4.3.1 Naive purely numerical combination

Here we put into practice the approach described in the second part of Section 2.3.2, where we don't need to have analytic hold over the integrand of the real. The replacement $2(p_i \cdot p_j) \rightarrow s_{ij}$ is not possible for a numerically generated integrand, which we can then dub as

$$f_{num} = f_{num}(\hat{s}_{12}, \hat{s}_{13}, \hat{s}_{23}) \quad \text{with} \quad \hat{s}_{ij} = 2(p_i \cdot p_j) = s_{ij} - 2\mu^2. \quad (3.148)$$

The function to be integrated with the MC is then

$$f_{num}(\hat{s}_{12}, \hat{s}_{13}, \hat{s}_{23}) \times \frac{\hat{s}_{12}}{s_{12}} \frac{\hat{s}_{13}}{s_{13}} \frac{\hat{s}_{23}}{s_{23}} \quad (3.149)$$

so that the FDR prescription $2(p_i \cdot p_j) \rightarrow s_{ij}$ is automatically achieved.

At the technical level, we have generated the usual massive momenta with our MC, so that the integration range is still the massive one demanded by the FDR treatment. Then we have forced the momenta to be massless, i.e.

$$p_i \rightarrow \hat{p}_i = (|\mathbf{p}_i|, \mathbf{p}_i), \quad (3.150)$$

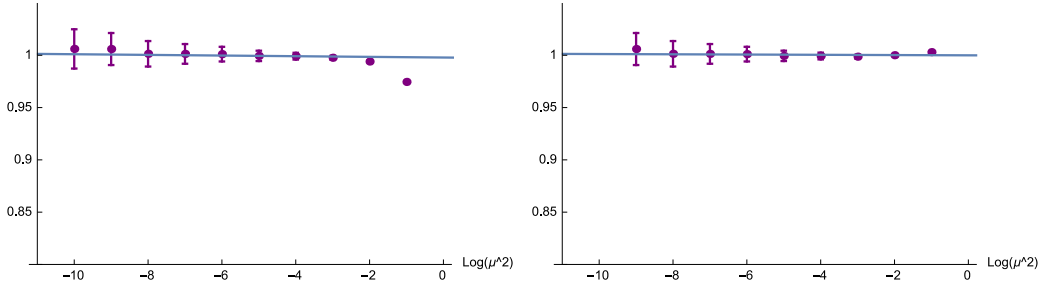


Figure 3.18: The combination of $\Gamma_{\mathcal{R}}^{(0)}|_{MC}$ and $\Gamma_{\mathcal{V}}^{(1)}$ - normalized to one - is plotted against μ^2 in logarithmic scale. $\Gamma_{\mathcal{R}}^{(0)}|_{MC}$ was obtained with a purely numerical method, where we have forced the momenta generated by the MC to be massless; we have used the definition of eq. (3.150) and of eq. (3.152) respectively for the figure on the left and on the right. For this result we have employed $s = 100$, and $N_{MC} = 10^7$ random points to generate the phase space.

and we have built the new massless Mandelstam variables with them, $\hat{s}_{ij} = 2(\hat{p}_i \cdot \hat{p}_j)$. Alternatively, in order to maintain the original energy conservation law, we have generated massless momenta scaled so that

$$\hat{p}'_1 + \hat{p}'_2 + \hat{p}'_3 = \sqrt{s}, \quad (3.151)$$

that is

$$p_i \rightarrow \hat{p}'_i = \frac{E_i}{|\mathbf{p}_i|} (|\mathbf{p}_i|, \mathbf{p}_i), \quad \text{where } E_i^2 - |\mathbf{p}_i|^2 = \mu^2. \quad (3.152)$$

The combination of the real obtained in these two ways and the analytic expression of the virtual is shown in fig. 3.18, as it varies along with μ^2 .

We find that these approximations work well for $10^{-10} < \mu^2 < 10^{-4}$.

3.4.4 FDR local subtraction

Finally, we have tried at work the approach proposed in Section 2.3.3, in which the real contribution is made convergent -at the integrand level- by adding a local counterterm, read from the analytic expression of the virtual.

In practice, given $\Gamma_{\mathcal{V}}^{(1)}(\ln \mu_0, \ln^2 \mu_0)$ of eq. (3.125), we have replaced the

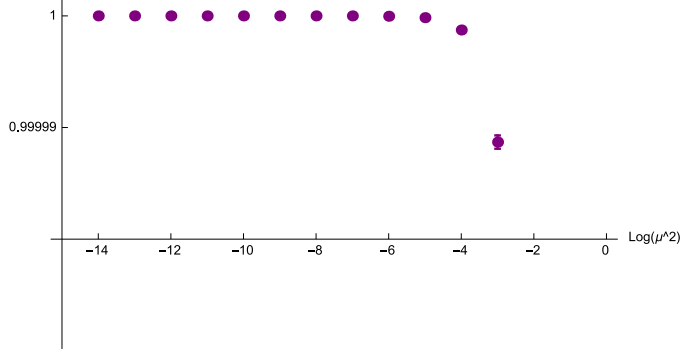


Figure 3.19: The combination of $\Gamma_{\mathcal{R}}^{(0)}|_{subtr.}$ and $\Gamma_{\mathcal{V}}^{(0)}|_{fin}$ -normalized to one- is plotted against μ^2 in logarithmic scale. Both contributions were obtained numerically, with a flat MC (*RAMBO*). For this result we have employed $s = 100$, and $N_{MC} = 10^6$ random points to generate the phase space.

single and double logs with the appropriate *3-body* phase-space integrals:

$$\begin{aligned} \ln^2 \frac{\mu^2}{s} &= \pi^2 + C_3 \\ \ln \frac{\mu^2}{s} &= -\frac{1}{11} \left(18 C_0 - 27 C_1 + 3 C_2 + \frac{43}{2} \right), \end{aligned} \quad (3.153)$$

where the counterterm functions are

$$\begin{aligned} C_0 &= \frac{8}{3 \pi^2} \int d\Phi_3 \left(\frac{1}{s_{12}} + \frac{1}{s_{13}} + \frac{1}{s_{23}} \right), \\ C_1 &= \frac{4}{3 \pi^2 s} \int d\Phi_3 \left(\frac{s_{12} + s_{13}}{s_{23}} + \frac{s_{12} + s_{23}}{s_{13}} + \frac{s_{13} + s_{23}}{s_{12}} \right), \\ C_2 &= \frac{4}{3 \pi^2 s} \int d\Phi_3 \left(\frac{s_{12}^2 + s_{13}^2}{s_{23}} + \frac{s_{12}^2 + s_{23}^2}{s_{13}} + \frac{s_{13}^2 + s_{23}^2}{s_{12}} \right), \\ C_3 &= \frac{8 s}{3 \pi^2} \int d\Phi_3 \left(\frac{1}{s_{12} s_{13}} + \frac{1}{s_{13} s_{23}} + \frac{1}{s_{12} s_{23}} \right). \end{aligned} \quad (3.154)$$

The first one of eqs. (3.153) is simply a version of eq. (3.136), i.e. it comes from the one-to-one correspondence between the triangle loop and the double-pole phase space integral. The second equation can be obtained from the universal behavior of the gluon splitting functions at one loop. In this particular case, because the analytic expression of the real is known, C_0 , C_1 and

C_2 can be extracted from eq. (3.135). Clearly, this would not be useful in a realistic calculation, but it served in the present study, interested in the numerical performance, rather than the way of extracting the counterterms.

The virtual contribution can be rewritten as

$$\Gamma_V^{(1)} = \frac{3}{2} \frac{\alpha_S}{\pi} \Gamma^{(0)}(\alpha_S(M_H^2)) \left(\frac{46}{3} + \int d\Phi_3 R_{ct}(s_{12}, s_{13}, s_{23}) \right), \quad (3.155)$$

where R_{ct} is the integrand counterterm to the real contribution, and it reads

$$\begin{aligned} R_{ct}(s_{12}, s_{13}, s_{23}) = \frac{4}{\pi^2} & \left[\left(\frac{1}{s_{12}} + \frac{1}{s_{13}} + \frac{1}{s_{23}} \right) \right. \\ & + \frac{1}{3s^2} \left(\frac{s_{12}^2 + s_{13}^2}{s_{23}} + \frac{s_{12}^2 + s_{23}^2}{s_{13}} + \frac{s_{13}^2 + s_{23}^2}{s_{12}} \right) \\ & \left. - \frac{2s}{3} \left(\frac{1}{s_{12}s_{13}} + \frac{1}{s_{13}s_{23}} + \frac{1}{s_{12}s_{23}} \right) \right]. \quad (3.156) \end{aligned}$$

After defining the subtracted real contribution,

$$\Gamma_{\mathcal{R}}^{(0)}|_{subtr.} = \frac{3}{2} \frac{\alpha_S}{\pi} \Gamma^{(0)}(\alpha_S(M_H^2)) \int_{MC} d\Phi_3 \left(R(s_{12}, s_{13}, s_{23}) + R_{ct}(s_{12}, s_{13}, s_{23}) \right), \quad (3.157)$$

and the finite virtual contribution,

$$\Gamma_V^{(0)}|_{fin} = \Gamma_V^{(1)} = 23 \frac{\alpha_S}{\pi} \Gamma^{(0)}(\alpha_S(M_H^2)), \quad (3.158)$$

we have set up a flat MC (*RAMBO*) in order to perform the integral in eq. (3.157). The combination of the two contributions thus defined is shown in fig. 3.19, as it varies along with different values of μ^2 . We see that the distribution of the central values is extremely stable, and that errors are tiny. For bigger values of μ^2 the deviation is due to the poor accordance with the limit $\mu \rightarrow 0$ with which the analytic result was obtained, just like in fig. 3.17.

3.4.5 Conclusions and outlooks

By considering gluon production via Higgs decay in the infinitely heavy top effective theory, we have shown that it is possible to implement an FDR-based MC that combines the real and virtual radiation in order to obtain a finite result. This is achieved thanks to the fact that in FDR IR infinities

are expressed in terms of logarithms of a vanishing scale, and not in terms of poles; this feature guarantees a good numerical stability up to very small values of μ . To improve the efficiency of the MC, the FDR local subtraction method proposes to regularize the real contribution at the integrand level, by reading a counterterm from the virtual contribution. This we have done and implemented in a MC: because all integrals are now finite, the MC performance is stable and extremely efficient. It was out of the scope of this thesis to study a technique to systematically extract the counterterms from the virtual, but studies are ongoing in this direction.

These techniques are ready to be applied to the differential decay rate of $H \rightarrow ggg$ at one-loop, in order to study their performance with a higher number of legs.

The next steps involve extending the methods to higher loop levels, and designing an FDR-compatible treatment for initial state radiation. As far as the first issue is concerned, we highlight once more that the naive numerical combination, especially in its purely numerical version, can be straightforwardly generalized to NNLO and beyond, with the extra cost of potentially losing some stability. In any case we envisage in this simple method, unapplicable in a DR-based calculation, a powerful tool for preliminary studies.

Chapter 4

Conclusions

After motivating the study of new calculation techniques for radiative corrections in the introduction, in Chapter 2 we have given an exhaustive description of FDR, pointing out the mechanisms that allow its correct functioning, and in Chapter 3 we have moved onto applying the method on some realistic calculations. This discussion hopefully is able to yield enough confidence on the method, particularly on the fact that it is on the way of accomplishing its original purpose, that of providing a viable alternative to DR in the calculation of radiative corrections in pQFT.

Let's summarize the properties of FDR. At the level of loop calculus,

- the FDR integral is finite in the UV region and it depends solely on an arbitrary scale μ_R , no UV cut-off is needed; infinities, both global and local ones, are fully subtracted at the integrand level;
- multi-loop Feynman diagrams are treated in a way that respects sub-integration consistency;
- amplitudes are automatically gauge-invariant and respectful of the symmetries of the theory, thanks to the fact that the FDR integral is shift-invariant and that simplifications between the numerator and denominator are respected;
- renormalization is built in the integral, no counterterms must be added to the Lagrangian, only a finite renormalization must be performed in order to relate the predictions with physical observables; with this procedure the dependence on μ_R can be traded for that on a physical

scale. This means, among the other things, that parameters that do not appear in the final result never need to be renormalized in FDR.

This is all achieved in a fully four-dimensional framework. Together with the fact that UV infinities are not parametrized but dropped altogether, four-dimensionality means that

- with respect to DR, there appear no term of the type ϵ/ϵ , which is notably a source of difficulties especially in higher order calculations; for example, this is why order by order renormalization is avoided, and why factorizable two-loop integrals are just the product of one-loop integrals;
- FDR is directly applicable to SUSY theories, like the DR variants of DRed and FDH;
- the space time dimension is not an obstacle to a numeric approach to the integration.

Also IR divergences can be treated in FDR. Indeed, thanks to unitarity, it is possible to give an FDR meaning to the phase space integral, by putting slightly off-shell the external momenta. This implies the introduction of an IR regulator $\mu \rightarrow 0$, on which non-inclusive quantities depend at most logarithmically. The same KLN matching that allows for the cancellation of poles $1/\epsilon$ in DR takes place in FDR, where the dependence on $\ln \mu$ drops away in inclusive observables. Thanks to four-dimensionality and to the fact that infinities are at most logarithmic, the combination of virtual and real radiation can be brought about numerically, with the integration over the phase space being performed with a MC.

At the practical level, if one were to decide to adopt the FDR method, it is worth recalling that

- all usual algebraic manipulations can be done at the integrand level; the FDR definition, extraction of vacua and so forth, only needs to be applied on the master integrals;
- PV reduction and IBP identities can be used to simplify FDR expressions;
- FDR is a scheme of renormalization, which can be connected, via a finite renormalization, to any other scheme (in particular, at one-loop it

is equivalent to $\overline{\text{DRed}}$); this means that pdfs, α_S , master integrals, and all pieces of a calculation that are already known in another framework can be translated to FDR;

- regarding new unknown pieces of calculation, it is conceivable that these can be maybe attacked numerically in the framework of FDR.

Using the work reported in this thesis as a stepping stone, some natural possible directions of further studies are here proposed:

- testing the naive numerical matching method on processes with higher multiplicity, for example the differential decay rate of $H \rightarrow ggg(g)$;
- developing the FDR local subtraction method, studying a way of consistently reading from the virtual integral a counterterm for the integrand of the real.

The next step would be to prepare the pathway towards a purely numerical NNLO computation, for which -we trust- FDR will provide a significant progress opportunity.

Appendix A

The basic two-loop vacuum integral

In sec. 2.1.7 we have reported that

$$[2 m_1 | m_2 | m_{12}] = \pi^4 \left\{ \ln \frac{m^2}{\mu^2} - \frac{1}{2} \ln^2 \frac{m^2}{\mu^2} - f(a, b) + f \right\}, \quad (\text{A.1})$$

where

$$a = \frac{m_2^2}{m_1^2}, \quad b = \frac{m_{12}^2}{m_1^2}, \quad (\text{A.2})$$

as the basic two-loop integral from which all other two-loop vacuum integrals can be deduced.

We now explain how eq. (2.114) has been obtained. Two different approaches are feasible:

- an indirect approach, by taking the difference of the integral in DR minus the vacuum configurations, also calculated in DR;
- a direct approach, by evaluating in 4 dimensions the finite terms of eq. (A.12).

We have pursued both strategies, thereby verifying at 2-loop that the two definitions of FDR integral are equivalent.

Preliminary 1: The function $f(a, b)$

The function $f(a, b)$ is symmetric under the exchange of a and b ; in integral form,

$$f(a, b) = \int_0^1 dx \left[\text{Li}_2(1 - \mathcal{M}_{a,b}^2(x)) - \frac{\mathcal{M}_{a,b}^2(x) \log \mathcal{M}_{a,b}^2(x)}{1 - \mathcal{M}_{a,b}^2(x)} \right], \quad (\text{A.3})$$

with

$$\mathcal{M}_{a,b}^2(x) = \frac{ax + b(1-x)}{x(1-x)}. \quad (\text{A.4})$$

The constant $f = f(1, 1)$ can be calculated numerically, using

$$\begin{aligned} f &= -\sqrt{\frac{2}{3}} \text{Cl}\left(\frac{\pi}{3}\right) = \frac{i}{\sqrt{3}} (\text{Li}_2(e^{i\frac{\pi}{3}}) - \text{Li}_2(e^{-i\frac{\pi}{3}})) \\ &= \frac{1}{36} \left[-\psi_1\left(\frac{1}{6}\right) - \psi_1\left(\frac{1}{3}\right) + \psi_1\left(\frac{2}{3}\right) + \psi_1\left(\frac{5}{6}\right) \right] \\ &= -1.17195361\dots \end{aligned} \quad (\text{A.5})$$

where $\text{Cl}(x)$ is the Clausius function as defined in [65], and $\psi_n(x)$ is the polygamma function.

If $a \neq b$, $f(a, b)$ can be evaluated analytically, so that

$$\begin{aligned} f(a, b) &= -\frac{1}{2} \log a \log b + \frac{1-a-b}{S} \left[\zeta_2 + \text{Li}_2\left(\frac{-x_2}{y_1}\right) + \text{Li}_2\left(\frac{-y_2}{x_1}\right) \right] \\ &\quad + \frac{1}{4} \log^2\left(\frac{x_2}{y_1}\right) + \frac{1}{4} \log^2\left(\frac{y_2}{x_1}\right) + \frac{1}{4} \log^2\left(\frac{x_1}{y_1}\right) - \frac{1}{4} \log^2\left(\frac{x_2}{y_2}\right) \Big], \end{aligned} \quad (\text{A.6})$$

where

$$x_{1,2} = \frac{1}{2} (1 - a + b \pm S), \quad (\text{A.7})$$

$$y_{1,2} = \frac{1}{2} (1 + a - b \pm S), \quad (\text{A.8})$$

$$S = \sqrt{1 - 2(a+b) + (a-b)^2}. \quad (\text{A.9})$$

For $b = 0$,

$$f(a, 0) = \text{Li}_2(1-a), \quad \text{and} \quad f(1, 0) = 0. \quad (\text{A.10})$$

For completeness, we also collect here the derivatives of $f(a, b)$ in the limits $m_2 \rightarrow m_1$ and $m_{12} \rightarrow 0$, which are needed when applying the formula of eq. (2.113):

$$\begin{aligned}
\lim_{a \rightarrow 1, b \rightarrow 0} \frac{df}{da} &= -1, & \lim_{a \rightarrow 1, b \rightarrow 0} \frac{d^2 f}{da^2} &= \frac{1}{2}, \\
\lim_{a \rightarrow 1, b \rightarrow 0} \frac{d^3 f}{da^3} &= -\frac{2}{3}, & \lim_{a \rightarrow 1, b \rightarrow 0} \frac{d^4 f}{da^4} &= \frac{3}{2}, \\
\lim_{a \rightarrow 1, b \rightarrow 0} b^q \frac{d^{p+q}}{da^p db^q} f &= 0 & \text{for } p \geq 0, q > 0. & \quad (\text{A.11})
\end{aligned}$$

Preliminary 2: The FDR defining expansion

$$\begin{aligned}
\frac{1}{\overline{D}_1^2 \overline{D}_2 \overline{D}_{12}} &= \left[\frac{1}{\overline{q}_1^4 \overline{q}_2^2 \overline{q}_{12}^2} \right] + \left(\frac{2m_1^2}{\overline{q}_1^4 \overline{D}_1} + \frac{m_1^4}{\overline{q}_1^4 \overline{D}_1^2} \right) \left[\frac{1}{\overline{q}_2^4} \right] + \\
&- 2m_1^2 \frac{q_1^2 + 2(q_1 \cdot q_2)}{(\overline{q}_1^4 \overline{D}_1) \overline{q}_2^4 \overline{q}_{12}^2} - m_1^4 \frac{q_1^2 + 2(q_1 \cdot q_2)}{(\overline{q}_1^4 \overline{D}_1^2) \overline{q}_2^4 \overline{q}_{12}^2} + \\
&+ \frac{m_2^2}{(\overline{q}_1^2 \overline{D}_1)(\overline{q}_2^2 \overline{D}_2) \overline{q}_{12}^2} + \frac{m_1^2 m_2^2}{(\overline{q}_1^2 \overline{D}_1^2)(\overline{q}_2^2 \overline{D}_2) \overline{q}_{12}^2} + \\
&+ \frac{m_{12}^2}{(\overline{q}_1^2 \overline{D}_1) \overline{q}_2^2 (\overline{q}_{12}^2 \overline{D}_{12})} + \frac{m_1^2 m_{12}^2}{(\overline{q}_1^2 \overline{D}_1^2) \overline{q}_2^2 (\overline{q}_{12}^2 \overline{D}_{12})} + \\
&+ \frac{m_2^2 m_{12}^2}{(\overline{q}_1^2 \overline{D}_1)(\overline{q}_2^2 \overline{D}_2)(\overline{q}_{12}^2 \overline{D}_{12})} + \frac{m_1^2 m_2^2 m_{12}^2}{(\overline{q}_1^2 \overline{D}_1^2)(\overline{q}_2^2 \overline{D}_2)(\overline{q}_{12}^2 \overline{D}_{12})}. \quad (\text{A.12})
\end{aligned}$$

A.1 The indirect approach

Following eq. (2.10), we write $[2m_1 | m_2 | m_{12}]$ as the difference of the integral calculated in DR and its vacuum configurations, that is

$$[2m_1 | m_2 | m_{12}] = [2m_1 | m_2 | m_{12}] \Big|_{\text{DR}} - \lim_{\mu_i \rightarrow 0} \int d^n q_1 d^n q_2 J_V(q_1, q_2, m_1), \quad (\text{A.13})$$

where, according to eq. (A.12),

$$J_V(q_1, q_2, m_1) = \left[\frac{1}{\overline{q}_1^4 \overline{q}_2^2 \overline{q}_{12}^2} \right] + \left(\frac{2m_1^2}{\overline{q}_1^4 \overline{D}_1} + \frac{m_1^4}{\overline{q}_1^4 \overline{D}_1^2} \right) \left[\frac{1}{\overline{q}_2^4} \right]. \quad (\text{A.14})$$

Having introduced the notation

$$\overline{\ln} \frac{M^2}{\mu_R^2} = \ln \frac{M^2}{\mu_R^2} + \Delta \quad \text{with} \quad \Delta = \gamma_E + \ln \pi. \quad (\text{A.15})$$

The DR results for the required integrals, up to $\mathcal{O}(\epsilon^0)$, are here collected:

$$\begin{aligned} \int \frac{d^n q}{\mu_R^\epsilon} \left[\frac{1}{\overline{q}^4} \right] &= -i\pi^2 \left(\frac{2}{\epsilon} + \overline{\ln} \frac{\mu^2}{\mu_R^2} \right), \\ \int \frac{d^n q_1 d^n q_2}{\mu_R^{2\epsilon}} \left[\frac{1}{\overline{q}_1^4 \overline{q}_2^2 \overline{q}_{12}^2} \right] &= \pi^4 \left\{ -\frac{2}{\epsilon^2} - \overline{\ln}^2 \frac{\mu^2}{\mu_R^2} + \frac{1}{\epsilon} + \overline{\ln} \frac{\mu^2}{\mu_R^2} + \right. \\ &\quad \left. - \frac{2}{\epsilon} \overline{\ln} \frac{\mu^2}{\mu_R^2} - \frac{1}{2} - \frac{\pi^2}{12} - f \right\}, \\ \int \frac{d^n q}{\mu_R^\epsilon} \left(\frac{2m_1^2}{\overline{q}^4 \overline{D}_1} + \frac{m_1^4}{\overline{q}^4 \overline{D}_1^2} \right) &= -i\pi^2 \left\{ \ln \frac{m_1^2}{\mu^2} \left(1 + \frac{\epsilon}{2} \Delta \right) \right. \\ &\quad \left. + \frac{\epsilon}{4} \left(\ln^2 \frac{m_1^2}{\mu_R^2} - \ln^2 \frac{\mu^2}{\mu_R^2} \right) \right\}, \end{aligned} \quad (\text{A.16})$$

plus eq. (2.116) with $m_1 = m_2 = m_{12} = \mu^2$ for the global vacuum, i.e.

$$[2\mu | \mu | \mu] \Big|_{DR} = \pi^4 \left\{ -\frac{2}{\epsilon^2} + \frac{1}{\epsilon} - \frac{2}{\epsilon} \Delta + \Delta - \Delta^2 - \frac{1}{2} - \frac{\pi^2}{12} - f \right\}. \quad (\text{A.17})$$

Combining these expressions into eq. (A.13) we obtain the analytic result of $[2m_1 | m_2 | m_{12}]$ as in eq. (A.1).

A.2 The direct approach

We perform the direct computation of the particular case $m_{12} = 0$, to obtain

$$[2m_1 | m_2 | 0] = \pi^4 \left\{ f - \text{Li}_2 \left(1 - \frac{m_2^2}{m_1^2} \right) - \frac{1}{2} \ln^2 \frac{\mu^2}{m_1^2} - \ln \frac{\mu^2}{m_1^2} \right\}, \quad (\text{A.18})$$

where we have used eq. (A.10), and f is given in eq. (A.5). It is obviously equivalent to eq. (A.1) with $b = 0$. A direct integration of the finite part of its FDR defining expansion –eq. (A.12)– gives

$$[2m_1 | m_2 | 0] = m_2^2 I_2(m_1, m_2) - m_1^2 I_1(m_1), \quad (\text{A.19})$$

where

$$\begin{aligned}
I_2(m_1, m_2) &= \lim_{\mu \rightarrow 0} \int d^4 q_1 d^4 q_2 \frac{1}{\overline{D}_1^2 (\overline{D}_2 \overline{q}_2^2) \overline{q}_{12}^2} \quad \text{and} \\
I_1(m_1) &= \lim_{\mu \rightarrow 0} \int d^4 q_1 d^4 q_2 \frac{q_1^2 + 2(q_1 \cdot q_2)}{\overline{q}_2^4 \overline{q}_{12}^2} \left(\frac{1}{\overline{D}_1 \overline{q}_1^4} + \frac{1}{\overline{D}_1^2 \overline{q}_1^2} \right) \quad (\text{A.20})
\end{aligned}$$

By power counting – due to the presence of $1/q_i^4$ terms – a logarithmic dependence on μ is expected in $I_1(m_1)$, while μ can be immediately set to zero in $I_2(m_1, m_2)$. Then $I_2(m_1, m_2)$ only depends on

$$r_{12} = \frac{m_1^2}{m_2^2}, \quad (\text{A.21})$$

and $I_1(m_1)$ on

$$\rho_1 = \frac{\mu^2}{m_1^2}, \quad (\text{A.22})$$

so no difficult integral containing both ratios needs to be computed. A simple Feynman parametrization produces

$$\begin{aligned}
I_2(m_1, m_2) &= \int_0^1 dz \int d^4 q_1 d^4 q_2 \frac{1}{\overline{D}_1^2 (q_2^2 - m_2^2 z)^2 \overline{q}_{12}^2} \\
&= \frac{\pi^4}{m_2^2} \int_0^1 dz \int_0^1 dx \int_0^1 dy \frac{y}{xyz + r_{12}(1-y)} \\
&= \frac{\pi^4}{m_2^2} \left\{ \frac{\pi^2}{6} - \text{Li}_2 \left(\frac{r_{12} - 1}{r_{12}} \right) \right\}, \quad (\text{A.23})
\end{aligned}$$

and

$$\begin{aligned}
I_1(m_1) &= 2 \lim_{\mu \rightarrow 0} \int_0^1 dz \int d^4 q_1 d^4 q_2 \frac{q_1^2 + 2(q_1 \cdot q_2)}{(\overline{q}_1^2 - m_1^2 z)^3 \overline{q}_2^4 \overline{q}_{12}^2} \\
&= \frac{2\pi^4}{m_1^2} \lim_{\mu \rightarrow 0} \int_0^1 dz \int_0^1 dx \int_0^1 dy \frac{(2x-1)y^2 x}{(z + \rho_1)x(1-x)y + \rho_1(1-y)} \\
&= \frac{\pi^4}{m_1^2} \left\{ \frac{\pi^2}{6} - f + \frac{1}{2} \ln^2 \rho_1 + \ln \rho_1 \right\}, \quad (\text{A.24})
\end{aligned}$$

from which eq. (A.18) follows.

Appendix B

Two-loop vacuum integrals

In this appendix we collect the analytic results of the two-loop vacuum integrals needed for the calculation of Section 3.2. The notation is that introduced in Chapter 2, which we report here for legibility:

$$\begin{aligned} [\alpha m_1 | \beta m_2] &= \int \frac{[d^4 q_1]}{(\bar{q}_1^2 - m_1^2)^\alpha} \times \int \frac{[d^4 q_2]}{(\bar{q}_2^2 - m_2^2)^\beta}, \\ [\alpha m_1 | \beta m_2 | \gamma m_{12}] &= \int \frac{[d^4 q_1][d^4 q_2]}{(\bar{q}_1^2 - m_1^2)^\alpha (\bar{q}_2^2 - m_2^2)^\beta (\bar{q}_{12}^2 - m_{12}^2)^\gamma}, \\ [\alpha m_1 | \beta m_2 | \gamma m_{12}] (\mu^2|_j) &= \int \frac{[d^4 q_1][d^4 q_2] \mu^2|_j}{(\bar{q}_1^2 - m_1^2)^\alpha (\bar{q}_2^2 - m_2^2)^\beta (\bar{q}^2 - m_{12}^2)^\gamma}. \end{aligned} \quad (\text{B.1})$$

The computation of all the integrals contained in this appendix can be performed according to the recipes explained in Chapter 2, Section 2.1.7.2 and Section 2.1.5.2.

Scalar two-loop vacuum integrals

$$\begin{aligned}
[2m | 2m | 0] &= +\frac{\pi^4}{m^2}, \\
[3m | m | 0] &= -\frac{\pi^4}{2m^2} \ln \frac{m^2}{\mu^2}, \\
[3m | 2m | 0] &= -\frac{\pi^4}{4m^4}, \\
[4m | m | 0] &= -\frac{\pi^4}{6m^4} \left(\frac{1}{2} - \ln \frac{m^2}{\mu^2} \right) \\
[3m | 3m | 0] &= \frac{\pi^4}{12m^6}, \\
[4m | 3m | 0] &= -\frac{\pi^4}{24m^8}, \\
[4m | 2m | 0] &= \frac{\pi^4}{9m^6}, \\
[4m | 3m | 0] &= -\frac{\pi^4}{24m^8}, \\
[5m | m | 0] &= \frac{\pi^4}{6m^6} \left(\frac{1}{3} - \frac{1}{2} \ln \frac{m^2}{\mu^2} \right), \\
[5m | 2m | 0] &= -\frac{\pi^4}{16m^8}, \\
[6m | m | 0] &= -\frac{\pi^4}{20m^8} \left(\frac{3}{4} - \ln \frac{m^2}{\mu^2} \right). \tag{B.2}
\end{aligned}$$

Two-loop extra-integrals

$$\begin{aligned}
[3m | m | 0](\mu_1^2) &= -\frac{2\pi^4}{3}f(1,1) - \frac{\pi^4}{2}, \\
[2m | 2m | 0](\mu_1^2) &= +\frac{2\pi^4}{3}f(1,1) + \frac{\pi^4}{2} \ln \frac{m^2}{\mu^2}, \\
[2m | 2m | 0](\mu_{12}^2) &= +\frac{2\pi^4}{3}f(1,1) + \pi^4 \ln \frac{m^2}{\mu^2}, \\
[3m | 2m | 0](\mu_2^2) &= [3m | 2m | 0](\mu_{12}^2) = +\frac{\pi^4}{4m^2}, \\
[4m | 2m | 0](\mu_2^2) &= [4m | 2m | 0](\mu_{12}^2) = -\frac{\pi^4}{12m^4}, \\
[5m | 2m | 0](\mu_2^2) &= [5m | 2m | 0](\mu_{12}^2) = +\frac{\pi^4}{24m^6}, \\
[\alpha m | \beta m | 0](\mu_1^2) &= 0 \quad \alpha \geq 3, \beta \geq 2, \\
[\alpha m | m | 0](\mu_1^2) &= 0 \quad \alpha \geq 4, \\
[\alpha m | \beta m | 0](\mu_2^2) &= [\alpha m | \beta m | 0](\mu_{12}^2) = 0 \quad \alpha, \beta \geq 3.
\end{aligned} \tag{B.3}$$

$$\begin{aligned}
[3m | 3m | 0](\mu_1^4) &= -\frac{\pi^4}{12m^2} \\
[3m | 3m | 0](\mu_{12}^4) &= -\frac{\pi^4}{6m^2} \\
[4m | 3m | 0](\mu_{12}^4) &= +\frac{\pi^4}{36m^4} \\
[4m | 3m | 0](\mu_2^4) &= +\frac{\pi^4}{36m^4} \\
[3m | 3m | 0](\mu_1^2 \mu_{12}^2) &= -\frac{\pi^4}{12m^2} \\
[4m | 3m | 0](\mu_2^2 \mu_{12}^2) &= +\frac{\pi^4}{36m^4}
\end{aligned} \tag{B.4}$$

Appendix C

Feynman rules

C.1 $H \rightarrow \gamma\gamma$ at one loop in R_ξ -gauge

We draw, in fig. C.1, the Feynman rules [105] used for the calculation of Section ???. The tensors $V_3^{\mu\nu\rho}$, $V_4^{\mu\nu\rho\sigma}$ and the coupling constants are given by

$$V_3^{\mu\rho\sigma} = g^{\sigma\rho}(p_+ - p_-)^\mu + g^{\rho\mu}(p_+ - q)^\sigma + g^{\mu\sigma}(q - p_-)^\rho; \quad (\text{C.1})$$

$$V_4^{\mu\nu\rho\sigma} = 2g^{\mu\nu}g^{\sigma\rho} - g^{\sigma\mu}g^{\rho\nu} - g^{\sigma\nu}g^{\mu\rho}; \quad (\text{C.2})$$

$$C_{SVV} = \begin{cases} M_W/s_W & \text{if } SVV = HW^+W^- \\ -M_W & \text{if } SVV = G^\pm W^\mp \gamma \end{cases}; \quad (\text{C.3})$$

$$C_{SSVV} = \begin{cases} 2 & \text{if } SSVV = \gamma\gamma G^+G^- \\ -1/2s_W & \text{if } SSVV = W^\pm\gamma G^\mp H \end{cases}; \quad (\text{C.4})$$

$$C_{VS_1S_2} = \begin{cases} -1 & \text{if } VS_1S_2 = \gamma G^+G^- \\ \mp \frac{1}{2s_W} & \text{if } VS_1S_2 = W^\pm G^\mp H \end{cases}. \quad (\text{C.5})$$

G denotes Goldstone bosons, while u^\pm and \bar{u}^\pm are the charged ghost and anti-ghost fields, respectively.

$$\begin{aligned}
\text{---} &= i \frac{\not{p} + m_f}{p^2 - m_f^2} & \text{---} &= -i \frac{e m_f}{2s_W M_W} & \text{---} &= -ie Q_f \gamma^\mu \\
\text{---} &= \frac{-i \left[g^{\mu\nu} - (1 - \xi) \frac{k^\mu k^\nu}{k^2 - \xi M_W^2} \right]}{k^2 - M_W^2} & \text{---} &= \frac{i}{p^2 - \xi M_W^2} \\
\text{---} &= ie V_3^{\mu\rho\sigma} & \text{---} &= -ie^2 V_4^{\mu\nu\rho\sigma} \\
\text{---} &= ieg^{\mu\nu} C_{SVV} & \text{---} &= ie^2 g^{\mu\nu} C_{SSVV} \\
\text{---} &= ie(p_1 - p_2)^\mu C_{VS_1 S_2} & \text{---} &= -i \frac{e M_H^2}{2s_W M_W} \\
\text{---} &= \frac{i}{k^2 - \xi M_W^2} & \text{---} &= -i \frac{e \xi M_W}{2s_W} & \text{---} &= \pm iep^\mu
\end{aligned}$$

Figure C.1: SM Feynman rules relevant for computing $H \rightarrow \gamma\gamma$. External momenta are considered to be incoming.

C.2 $H \rightarrow \gamma\gamma$ at two loops

We list here the Feynman rules used in the calculation of Section 3.2. Q_t , m_0 and v are the top quark charge, the top bare mass and the vacuum

expectation value of the Higgs field, respectively.

$$\begin{array}{ccc}
 \text{---} \text{---} \text{---} \begin{array}{l} \nearrow \\ \searrow \end{array} = -i \frac{m_0}{v} & \begin{array}{l} \text{---} \text{---} \text{---} \begin{array}{l} \nearrow \\ \searrow \end{array} \\ \alpha \end{array} = -ie Q_t \gamma_\alpha & \begin{array}{l} \xrightarrow{p} \\ \text{---} \end{array} = \frac{i}{\not{p} - m_0} \\
 \begin{array}{l} \begin{array}{l} \nearrow j \\ \searrow k \end{array} \\ \text{---} \text{---} \text{---} \begin{array}{l} \nearrow \\ \searrow \end{array} \\ \alpha, a \end{array} = -ig_S \gamma_\alpha T_{jk}^a & \begin{array}{l} \xrightarrow{p} \\ \text{---} \text{---} \text{---} \\ \alpha \quad \beta \end{array} = \frac{-i g_{\alpha\beta}}{p^2}
 \end{array}$$

Figure C.2: QCD Feynman rules relevant for the computation of $H \rightarrow \gamma\gamma$ at $\mathcal{O}(\alpha_S)$.

C.3 $H \rightarrow gg(g)$ and $H \rightarrow ggg(g)$ at NLO

Here we collect the Feynman rules used in the calculations of Section 3.4, Section ?? and [78]. The loop-induced interactions among Higgs boson and gluons have been described within the framework of the Higgs effective field theory (HEFT) [106]: all contributions are neglected except the top-loop, which in the limit $m_{top} \rightarrow \infty$ collapses to a vertex of a Higgs with two, three or four gluons, according to the effective Lagrangian

$$\mathcal{L}_{\text{HEFT}} = -\frac{1}{4}AHG_{\mu\nu}^a G^{a,\mu\nu}, \quad (\text{C.6})$$

where

$$A = \frac{\alpha_S}{3\pi v} \left(1 + \frac{11}{4} \frac{\alpha_S}{\pi} \right). \quad (\text{C.7})$$

At NLO, for the processes at hand only the trilinear and quadrilinear terms are relevant, as depicted in fig. C.3. The interactions among the gluons are described via the flavorless sector of the SM QCD (see fig. C.4), complemented with the ghost sector in order to restaure the transversality of the gluonic propagator (see fig. C.5).

In the following we define the tensors used in the Feynman rules:

$$\begin{aligned} H^{\alpha\beta}(p_1, p_2) &= (p_1 \cdot p_2)g^{\alpha\beta} - p_1^\beta p_2^\alpha, \\ V^{\alpha\beta\gamma}(p_1, p_2, p_3) &= (p_1 - p_2)^\gamma g^{\alpha\beta} + (p_2 - p_3)^\alpha g^{\beta\gamma} + (p_3 - p_1)^\beta g^{\alpha\gamma}, \\ G_{abcd}^{\alpha\beta\gamma\delta} &= f^{abi} f^{cdi} G^{\alpha\beta\gamma\delta} + f^{aci} f^{bdi} G^{\alpha\gamma\beta\delta} + f^{adi} f^{bci} G^{\alpha\delta\beta\gamma}, \\ G^{\alpha\beta\gamma\delta} &= g^{\alpha\gamma} g^{\beta\delta} - g^{\alpha\delta} g^{\beta\gamma}. \end{aligned} \quad (\text{C.8})$$

$$\begin{aligned}
& \text{---} \text{---} \text{---} \text{---} \begin{array}{l} \nearrow \text{wavy} \\ \searrow \text{wavy} \end{array} \begin{array}{l} p_1^{\alpha,a} \\ p_2^{\beta,b} \end{array} = iA\delta^{ab} H^{\alpha\beta}(p_1, p_2) \\
& \text{---} \text{---} \text{---} \text{---} \begin{array}{l} \nearrow \text{wavy} \\ \text{---} \text{wavy} \\ \searrow \text{wavy} \end{array} \begin{array}{l} p_3^{\gamma,cR} \\ p_2^{\beta,bR} \\ p_1^{\alpha,aR} \end{array} = -Ag f^{abc} V^{\alpha\beta\gamma}(p_1, p_2, p_3)
\end{aligned}$$

Figure C.3: Feynman rules for the HEFT Lagrangian. All momenta are considered incoming, $H^{\alpha\beta}$ and $V^{\alpha\beta\gamma}$ are defined in eq. (C.8), A is the coupling constant of HEFT as in eq. (C.7), g is the QCD coupling constant, and f^{abc} are the structure functions of the color group

$$\begin{aligned}
& \text{Diagram 1: Three-gluon vertex} & = -g f^{abc} V^{\alpha\beta\gamma}(p_1, p_2, p_3) \\
& \text{Diagram 2: Four-gluon vertex} & = -ig G_{abcd}^{\alpha\beta\gamma\delta} \\
& \text{Diagram 3: Ghost-gluon vertex} & = -i \delta^{ab} \frac{g^{\alpha\beta}}{p^2}
\end{aligned}$$

Figure C.4: Feynman rules for quarkless QCD in Feynman gauge. All momenta are incoming, g is the QCD coupling constant, f^{abc} are the structure functions of the color group, and $V^{\alpha\beta\gamma}$ and $G_{abcd}^{\alpha\beta\gamma\delta}$ are defined in eq. (C.8).

$$\begin{aligned}
& \text{Diagram 1: Ghost-gluon vertex} & = g f^{abc} p^\alpha \\
& \text{Diagram 2: Ghost-gluon vertex} & = i \frac{g^{\alpha\beta}}{p^2}
\end{aligned}$$

Figure C.5: Feynman rules for the ghost sector of quarkless QCD. All momenta are incoming, g is the QCD coupling constant $g^2 = \alpha_S$, and f^{abc} are the structure functions of the color group.

Appendix D

Monte Carlo Integration

In the MC approach, an integral is evaluated as the average of random numbers, i.e. [107]:

$$I = \int_0^1 f(x)dx = \lim_{N \rightarrow \infty} \frac{1}{N} \sum_{i=1}^N f(x_i), \quad (\text{D.1})$$

where $x_i \in [0, 1]$ is a random number, with uncertainty

$$\Delta I = \sqrt{\frac{\langle I^2 \rangle - \langle I \rangle^2}{N}} \propto \frac{1}{\sqrt{N}}. \quad (\text{D.2})$$

This can be straightforwardly extended to n variables, that is

$$\int_0^1 dx_1 \dots dx_n f(\bar{x}) = \frac{1}{N} \sum_{i=1}^N f(\bar{x}_i) \quad \bar{x} = (x_1, \dots, x_n) \quad (\text{D.3})$$

Problems arise when the function to be integrated exhibits a peak, that is an integrable singularity. For example, take

$$f(x \approx x_0) \propto g(x) \quad \text{with} \quad \int_0^1 g(x)dx = 1. \quad (\text{D.4})$$

The function $g(x)$, peaked in x_0 , is called *local density*. It is convenient to perform a change of variables such that

$$\int_0^1 g(x)dx \frac{f(x)}{g(x)} = \int_0^1 w(y)dy, \quad (\text{D.5})$$

where

$$dy = g(x)dx \quad \text{and} \quad w(y) \equiv \frac{f(x(y))}{g(x(y))}. \quad (\text{D.6})$$

The peaked behaviour is now described by the integration variable, whilst the new integrand, the *weight function* $w(y)$, is flat and it can be efficiently integrated with the MC method.

D.1 Single Peak Mapping

Consider an integrand with a pole in $x = x_0$

$$\frac{f(x)}{x - x_0}, \quad (\text{D.7})$$

where $f(x)$ is a smooth function in $[a, b]$, and for example $a = x_0 - \delta$ with $\delta \ll 1$. In order to integrate it numerically, it is best to transfer the peaked behaviour of the integrand to the random variable. We define the random variable $\rho \in [0, 1]$ such that

$$\frac{dx}{x - x_0} = H d\rho \quad (\text{D.8})$$

where H is a constant depending on the parameters x_0 , a and b . The integral is then rewritten as

$$\int_a^b dx \frac{f(x)}{x - x_0} = H \int_0^1 d\rho f(x(\rho)) \quad (\text{D.9})$$

We obtain H by integrating both sides

$$\log(x - x_0) = H\rho + c \quad (\text{D.10})$$

and applying the boundary conditions

$$\begin{aligned} \log(a - x_0) &= c, \\ \log(b - x_0) &= H + c. \end{aligned} \quad (\text{D.11})$$

We get

$$H = \log\left(\frac{b - x_0}{a - x_0}\right). \quad (\text{D.12})$$

The original variable as expressed in terms of the new random variable, $x = x(\rho)$, reads

$$x = x_0 + \frac{(b - x_0)^\rho}{(a - x_0)^{\rho-1}}. \quad (\text{D.13})$$

D.2 Multi-channel approach

If there are more than one regions in which the function peaks, a mapping is defined for each channel, such that

$$f(x \approx x_i) \propto g_i(x) \quad \text{with} \quad \int_0^1 g_i(x) dx = 1 \quad i = 1, \dots, s. \quad (\text{D.14})$$

The total probability density is defined as

$$g(x) = \sum_{i=1}^s \alpha_i g_i(x) \quad \text{with} \quad \sum_{i=1}^s \alpha_i = 1, \quad \alpha_i \geq 0, \quad (\text{D.15})$$

where the real numbers α_i are called *a-priori weights*, and are chosen accordingly to some arbitrary probabilistic function. The MC integral and its variance become

$$I = \langle w \rangle = \int dx f(x) = \int dx g(x) w(x) \quad (\text{D.16})$$

$$W_\alpha = \langle w^2 \rangle = \int dx \frac{f(x)^2}{g(x)} = \int dx g(x) w(x)^2 \quad (\text{D.17})$$

such that the error is given by

$$\Delta I_\alpha = \sqrt{\frac{W_\alpha - I^2}{N}} \quad (\text{D.18})$$

It can be shown that I is independent of $g(x)$ and of α_i ; moreover the set of a-priori weights can be changed even from one MC point to another [107]. With a suitable choice of the a-priori weights one can reduce the variance and hence the error of the MC integration.

D.2.1 Optimization of the *a-priori* weights

We have used the method described in [107]. It is an iterative procedure, starting from a uniform distribution,

$$\alpha_i^{(1)} = 1/s, \quad (\text{D.19})$$

where s is the number of channels. The new set of a-priori weights is given by

$$\alpha_i^{(n)} = \frac{\alpha_i^{(n-1)} \sigma_i}{\sum_{j=1}^s \alpha_j^{(n-1)} \sigma_j}, \quad (\text{D.20})$$

where

$$\sigma_i = \int dx g_i(x) w(x)^2, \quad w(x) = \frac{f(x)}{g(x)}. \quad (\text{D.21})$$

The number repetitions is chosen according to some convergence criterium.

In this work we have adopted this strategy with a modification: at each step we reserve a fixed percentage (namely 5%) to the flat channel. This is because it tends to count less and less, being the peaked channels dominant, even though it provides the finite (and physical) contribution to the decay amplitude, i.e. the only contribution that matters once the peaks cancel.

Bibliography

- [1] ATLAS Collaboration. Observation of a new particle in the search for the standard model higgs boson with the atlas detector at the lhc. *Physics Letters B*, B716:1–29, 2012.
- [2] CMS Collaboration. Observation of a new boson at a mass of 125 gev with the cms experiment at the lhc. *Physics Letters B*, B716:30–61, 2012.
- [3] S. Dawson and *et al.* Higgs working group report of the snowmass 2013 community planning study. 2013.
- [4] G. Peter Lepage, Paul B. Mackenzie, and Peskin Michael E. Expected precision of Higgs boson partial widths within the Standard Model. *Fermilab Publications*, 14:68, 2015.
- [5] Michal Czakon, Alexander Mitov, Michele Papucci, Joshua T. Ruderman, and Andreas Weiler. Removing gaps in the exclusion of top squark parameter space. *Phys. Rev. Lett.*, 113:201803, Nov 2014.
- [6] Michal Czakon, Paul Fiedler, and Alexander Mitov. Resolving the tevatron top quark forward-backward asymmetry puzzle. 2014.
- [7] G. Passarino and M.J.G. Veltman. One Loop Corrections for $e^+ e^-$ Annihilation Into $\mu^+ \mu^-$ in the Weinberg Model. *Nucl.Phys.*, B160:151, 1979.
- [8] S. Frixione, Z. Kunszt, and A. Signer. Three jet cross-sections to next-to-leading order. *Nucl.Phys.*, B467:399–442, 1996.
- [9] S. Catani and M.H. Seymour. A General algorithm for calculating jet cross-sections in NLO QCD. *Nucl.Phys.*, B485:291–419, 1997.

- [10] David A. Kosower. Antenna factorization of gauge theory amplitudes. *Phys.Rev.*, D57:5410–5416, 1998.
- [11] John M. Campbell, M.A. Cullen, and E.W. Nigel Glover. Four jet event shapes in electron - positron annihilation. *Eur.Phys.J.*, C9:245–265, 1999.
- [12] Stefano Catani, Stefan Dittmaier, Michael H. Seymour, and Zoltan Trocsanyi. The Dipole formalism for next-to-leading order QCD calculations with massive partons. *Nucl.Phys.*, B627:189–265, 2002.
- [13] Zoltan Nagy and Davison E. Soper. General subtraction method for numerical calculation of one loop QCD matrix elements. *JHEP*, 0309:055, 2003.
- [14] Zvi Bern, Lance J. Dixon, David C. Dunbar, and David A. Kosower. Fusing gauge theory tree amplitudes into loop amplitudes. *Nucl.Phys.*, B435:59–101, 1995.
- [15] Ruth Britto, Freddy Cachazo, and Bo Feng. Generalized unitarity and one-loop amplitudes in N=4 super-Yang-Mills. *Nucl.Phys.*, B725:275–305, 2005.
- [16] G. Ossola, C.G. Papadopoulos, and R. Pittau. Reducing full one-loop amplitudes to scalar integrals at the integrand level. *Nuclear Physics B*, B763:147–169, 2007.
- [17] Darren Forde. Direct extraction of one-loop integral coefficients. *Phys.Rev.*, D75:125019, 2007.
- [18] C. Berger, Z. Bern, L. Dixon, F. Febres Cordero, D. Forde, and et al. An automated implementation of on-shell methods for one-loop amplitudes. *Physical Review*, D78:036003, 2008.
- [19] R. Keith Ellis, Kirill Melnikov, and Giulia Zanderighi. Generalized unitarity at work: first NLO QCD results for hadronic $W + 3$ jet production. *JHEP*, 0904:077, 2009.
- [20] Stefano Catani and Massimiliano Grazzini. An NNLO subtraction formalism in hadron collisions and its application to Higgs boson production at the LHC. *Phys.Rev.Lett.*, 98:222002, 2007.

- [21] Charalampos Anastasiou, Calude Duhr, Falko Dulat, Elisabetta Furlan, Thomas Gehrmann, Herzog Franz, and Bernhard Mistlberger. Higgs boson gluon-fusion production beyond threshold in N³LO QCD. 2015.
- [22] HERAFitter developers team. Parton distribution functions at lo, nlo and nnlo with correlated uncertainties between orders. 2014.
- [23] CMS Collaboration. Measurement of the wz production cross section in the $\ell^+\ell^-\ell'\nu$ decay channel at $\sqrt{s} = 7$ and 8tev at the lhc. 2013.
- [24] T. Gehrmann, M. Grazzini, S. Kallweit, P. Maierhöfer, A. von Manteuffel, S. Pozzorini, D. Rathlev, and L. Tancredi. W^+W^- production at hadron colliders in next to next to leading order qcd. *Phys. Rev. Lett.*, 113:212001, Nov 2014.
- [25] F. Cascioli, T. Gehrmann, M. Grazzini, S.Kallweit, P. Maierhoefer, A. von Manteuffel, S. Pozzorini, D. Rathlev, L. Tancredi, and E. Weihs. $\{ZZ\}$ production at hadron colliders in $\{NNLO\}$ $\{QCD\}$. *Physics Letters B*, 735(0):311 – 313, 2014.
- [26] G. Balossini, C.M. Carloni Calame, G. Montagna, M. Moretti, O. Nicrosini, F. Piccinini, M. Treccani, and A. Vicini. Combination of electroweak and QCD corrections to single W production at the Fermilab Tevatron and the CERN LHC. *JHEP*, 13:1001, 2009.
- [27] S. Alekhin, J. Blümlein, and S. Moch. Parton distribution functions and benchmark cross sections at next-to-next-to-leading order. *Phys. Rev. D*, 86:054009, Sep 2012.
- [28] Giampiero Passarino. An Approach toward the numerical evaluation of multiloop Feynman diagrams. *Nucl.Phys.*, B619:257–312, 2001.
- [29] G. Mastrolia, P.and Ossola. On the integrand-reduction method for two-loop scattering amplitudes. *Journal of High Energy Physics*, 1111:014, 2011.
- [30] P. Mastrolia, E. Mirabella, G. Ossola, and T. Peraro. Scattering amplitudes from multivariate polynomial division. *Physics Letters B*, B718:173–177, 2012.

- [31] R. Kleiss, I. Malamos, C. G. Papadopoulos, and R. Verheyen. Counting to One: Reducibility of One- and Two-Loop Amplitudes at the Integrand Level. *Journal of High Energy Physics*, 1212:025030, 038.
- [32] Simon Badger, Hjalte Frellesvig, and Yang Zhang. Hepta-Cuts of Two-Loop Scattering Amplitudes. *JHEP*, 1204:055, 2012.
- [33] H. Johansson, D. A. Kosower, and K. J. Larsen. Two-Loop Maximal Unitarity with External Masses. *Physical Review*, D87:025030, 2013.
- [34] T. Binoth and G. Heinrich. An Automatized algorithm to compute infrared divergent multiloop integrals. *Nucl.Phys.*, B585:741–759, 2000.
- [35] Charalampos Anastasiou, Kirill Melnikov, and Frank Petriello. A New method for real radiation at NNLO. *Phys.Rev.*, D69:076010, 2004.
- [36] T. Binoth and G. Heinrich. Numerical evaluation of phase space integrals by sector decomposition. *Nucl.Phys.*, B693:134–148, 2004.
- [37] A. Gehrmann-De Ridder, T. Gehrmann, and E.W. Nigel Glover. Antenna subtraction at NNLO. *JHEP*, 0509:056, 2005.
- [38] M. Czakon. A novel subtraction scheme for double-real radiation at NNLO. *Phys.Lett.*, B693:259–268, 2010.
- [39] W. Pauli and F. Villars. On the Invariant regularization in relativistic quantum theory. *Rev.Mod.Phys.*, 21:434–444, 1949.
- [40] Gerard 't Hooft and M.J.G. Veltman. Regularization and Renormalization of Gauge Fields. *Nucl.Phys.*, B44:189–213, 1972.
- [41] N.N. Bogoliubov and O.S. and Parasiuk. On the Multiplication of the causal function in the quantum theory of fields. *Acta Math.*, 97:227–266, 1957.
- [42] Klaus Hepp. Proof of the Bogolyubov-Parasiuk theorem on renormalization. *Commun.Math.Phys.*, 2:301–326, 1966.
- [43] W. Zimmermann. Convergence of Bogolyubov's method of renormalization in momentum space. *Commun.Math.Phys.*, 15:208–234, 1969.

- [44] T. D. Lee and M. Nauenberg. Degenerate systems and mass singularities. *Physical Review*, 133:B1549–B1562, 1964.
- [45] F. Bloch and A. Nordsieck. Note on the radiation field of the electron. *Physical Review*, 52:54, 1937.
- [46] D. Z. Freedman, K. Johnson, and J. I. Latorre. Differential regularization and renormalization: A new method of calculation in quantum field theory. *Nuclear Physics B*, B371:353–414, 1992.
- [47] F. del Aguila, A. Culatti, R. Munoz-Tapia, and M. Perez-Victoria. Constraining differential renormalization in Abelian gauge theories. *Physics Letters B*, B419:263–271, 1998.
- [48] F. del Aguila, A. Culatti, R. Munoz-Tapia, and M. Perez-Victoria. Techniques for one loop calculations in constrained differential renormalization. *Nuclear Physics B*, B537:561–585, 1999.
- [49] O. Battistel, A. Mota, and M. Nemes. Consistency conditions for 4-D regularizations. *Mod.Phys.Lett.*, A13:1597–1610, 1998.
- [50] A. Cherchiglia, M. Sampaio, and M. Nemes. Systematic implementation of implicit regularization for multi-loop feynman diagrams. *Int.J.Mod.Phys.*, pages 2591–2635, 2011.
- [51] G. Cynolter and E. Lendvai. Symmetry preserving regularization with a cutoff . *Central Eur.J.Phys.*, 9:1237–1247, 2011.
- [52] Y. L. Wu. Symmetry preserving loop regularization and renormalization of qfts. *Modern Physics Letters*, A19:2191–2204, 2004.
- [53] Roberto Pittau. On the predictivity of the non-renormalizable quantum field theories. *Fortschr. Phys.* 63, 2:132–141, 2015.
- [54] Z. Bern, A. De Freitas, L. J. Dixon, and H. Wong. Supersymmetric regularization, two loop QCD amplitudes and coupling shifts. *Phys.Rev.* ., D66, 2002.
- [55] Z. Bern and A. Morgan. Massive Loop Amplitudes from Unitarity. *Nuclear Physics B*, 467:479, 1996.

- [56] G. Cullen, N. Greiner, G. Heinrich, G. Luisoni, and P. Mastrolia. Applications of NLO automation with GoSam. *European Physical Journal*, C72:1889, 2012.
- [57] F. Jegerlehner. Facts of life with gamma(5). *Eur.Phys.*, C18:673–679, 2001.
- [58] Roberto Pittau. A four-dimensional approach to quantum field theories. *JHEP*, 1211:151, 2012.
- [59] Benjamin Page and Roberto Pittau. work-in-progress. 2015.
- [60] Zvi Bern and David A. Kosower. The computation of loop amplitudes in gauge theories. *Nucl.Phys.*, B379:451–561, 1992.
- [61] Zvi Bern, A. De Freitas, L. J. Dixon, and H. L. Wong. Supersymmetric regularization, two loop QCD amplitudes and coupling shifts. *Physical Review*, D66, 2002.
- [62] William B. Kilgore. Regularization schemes and higher order corrections. *Phys.Rev.*, D83:11, 2011.
- [63] Radja Boughezal, Kirill Melnikov, and Frank Petriello. Four-dimensional helicity scheme and dimensional reconstruction. *Physical Review*, D86, 2011.
- [64] William B. Kilgore. Four dimensional helicity scheme beyond one loop. *Phys.Rev.*, D86, 2012.
- [65] J. Van Der Bij and M. Veltman. Two-loop large higgs mass correction to the ρ -parameter. *Nuclear Physics B*, 231:205–234, 1984.
- [66] P. Draggiotis, M.V. Garzelli, C.G. Papadopoulos, and R. Pittau. Feynman Rules for the Rational Part of the QCD 1-loop amplitudes. *JHEP*, 0904:072, 2009.
- [67] M.V. Garzelli, I. Malamos, and R. Pittau. Feynman rules for the rational part of the Electroweak 1-loop amplitudes. *JHEP*, 1001:040, 2010.
- [68] R. Pittau. Primary Feynman rules to calculate the epsilon-dimensional integrand of any 1-loop amplitude. *JHEP*, 1202:029, 2012.

- [69] Roberto Pittau. Integration-by-parts identities in FDR. 2014.
- [70] G.. Leibbrandt. Introduction to the technique of dimensional regularization. *Review of Modern Physics*, 47, No. 4:849–876, 1975.
- [71] George Sterman. *An Introduction to Quantum Field Theory*. Cambridge University Press, 1993.
- [72] J. Collins. Renormalization. (*Cambridge University Press, Cambridge, England*), 1984.
- [73] M. Veltman. Gauge Field Theories. *Proceedings of the VI International Symposium on Electron and Proton Interaction at High Energies*, pages 429–447, 1973.
- [74] Alice M. Donati and R. Pittau. Gauge invariance at work in fdr: $h \rightarrow \gamma\gamma$. *Journal of High Energy Physics*, 4, 2013.
- [75] Gerard 't Hooft and M.J.G. Veltman. DIAGRAMMAR. *NATO Adv.Study Inst.Ser.B Phys.*, 4:177–322, 1974.
- [76] Warren Siegel. Supersymmetric Dimensional Regularization via Dimensional Reduction. *Phys.Lett.*, B84:193, 1979.
- [77] A. Signer. Helicity method for next-to-leading order corrections in QCD. *Ph.D. Thesis*, 1995.
- [78] Roberto Pittau. QCD corrections to $H \rightarrow gg$ in FDR. *European Physics Journal C*, 74, 2014.
- [79] W.T. Giele, E.W. Nigel Glover, and David A. Kosower. Higher order corrections to jet cross-sections in hadron colliders. *Nucl.Phys.*, B403:633–670, 1993.
- [80] W. T. Giele, Z. Kunszt, and K. Melnikov. Full one-loop amplitudes from tree amplitudes. *Journal of High Energy Physics*, 2008.
- [81] Alice Maria Donati and Roberto Pittau. FDR, an easier way to NNLO calculations: a two-loop case study. *Eur.Phys.J.*, C74:2864, 2014.
- [82] Mauro Moretti, Alice Maria Donati, Fulvio Piccinini, and Roberto Pittau. work-in-progress. 2015.

- [83] J. Ellis, M. K. Gaillard, and D. V. Nanopoulos. A phenomenological profile of the higgs boson. *Nuclear Physics B*, 106:292–340, 1976.
- [84] B. Ioffe and V.A. Khoze. What can be expected from experiments on colliding $e^+ e^-$ beams with \sqrt{s} approximately equal to 100-gev? *Sov.J.Part.Nucl.*, 9:50.
- [85] M.A. Shifman, A. Vainshtein, M. Voloshin, and Zakharo V.I. Low-energy theorems for higgs boson couplings to photons. 30:711–716, 2012.
- [86] T. G. Rizzo. GLUON FINAL STATES IN HIGGS BOSON DECAY. *Physical Review*, D22:178, 1980.
- [87] A. Cherchiglia, L. Cabral, M. Sampaio, and M. Nemes. (un)determined finite regularization dependent quantum corrections: the higgs decay into two photons and the two photon scattering examples. *Physical Review*, D87:065011, 2013.
- [88] Hua-Sheng Shao, Yu-Jie Zhang, and Kuang-Ta Chao. Reduction schemes in cutoff regularization and higgs decay into two photons. *Journal of High Energy Physics*, 1, 2012.
- [89] A. Dedes and K. Suxho. Anatomy of the higgs boson decay into two photons in the unitary gauge. *arXiv:1210.0141v2*, 2012.
- [90] F. Piccinini, A. Pilloni, and A. Polosa. H to gamma gamma: A comment on the indeterminacy of non-gauge-invariant integrals. 2012.
- [91] F. Jegerlehner. Comment on H to gamma gamma and the Role of the Decoupling theorem and the Equivalence Theorem.
- [92] Y. Huang, D. Tang and Y.L. Wu. Note on higgs decay into two photons $h \rightarrow \gamma\gamma$. 57:427–434, 2012.
- [93] M. Shifman, A. Vainshtein, M. Voloshin, and V. Zakharov. Higgs decay into two photons through the w-boson loop: No decoupling in the $m_w \rightarrow 0$ limit. *Physical Review*, D85:013015, 2012.
- [94] R. Gastmans, S.L. Wu, and T.T. Wu. Higgs decay into two photons revisited. 2011.

- [95] R. Gastmans, Sau Lan Wu, and Tai Tsun Wu. Higgs Decay $H \rightarrow \gamma\gamma$ through a W Loop: Difficulty with Dimensional Regularization. 2011.
- [96] F. Bursa, A. Cherman, T. C. Hammant, R. R. Horgan, and M. Wingate. Calculation of the one w loop $h \rightarrow \gamma\gamma$ decay amplitude with a lattice regulator. *Physical Review*, D85:093009, 2012.
- [97] William J. Marciano, Cen Zhang, and Scott Willenbrock. Higgs Decay to Two Photons. *Phys.Rev.*, D85:013002, 2012.
- [98] Thomas Hahn. Generating Feynman diagrams and amplitudes with FeynArts 3. *Comput.Phys.Commun.*, 140:418–431, 2001.
- [99] A. Dedes and K. Suxho. Anatomy of the higgs boson decay into two photons in the unitary gauge. *arXiv:1210.0141v2*, 2012.
- [100] A. Djouadi, M. Spira, and P.M. Zerwas. Production of Higgs bosons in proton colliders: QCD corrections. *Phys.Lett.*, B264:440–446, 1991.
- [101] U. Aglietti, R. Bonciani, G. Degrassi, and A. Vicini. Analytic results for virtual qcd corrections to higgs production and decay. *Journal of High Energy Physics*, 01:21, 2007.
- [102] A. Djouadi, M. Spira, J. Van Der Bij, and P. M. Zerwas. Qcd corrections to $\gamma\gamma$ decays of higgs particles in the intermediate mass range. *Physics Letters B*, 257, 1991.
- [103] M. E. Peskin and D. V. Schroeder. *An Introduction to Quantum Field Theory*. Westview Press, 1995.
- [104] R. Kleiss, W. J. Stirling, and S.D. Ellis. A new monte carlo treatment of multiparticle phase space at high energies. *Computer Physics Communications*, 40:359, 1986.
- [105] A. Denner. Techniques for the calculation of the electroweak radiative corrections at the one-loop level and results for w -physics at lep200. *Fortschritte der Physik*, 41:307–420, 1993.
- [106] Russel P. Kauffman, Satish V. Desai, and Dipesh Risal. Production of a Higgs boson plus two jets in hadronic collisions. *Phys.Rev.*, D55:4005–4015, 1997.

- [107] R. Kleiss and R. Pittau. Weight optimization multichannel monte carlo.
Computer Physics Communications, 83:141, 1994.